TÉCNICO LISBOA

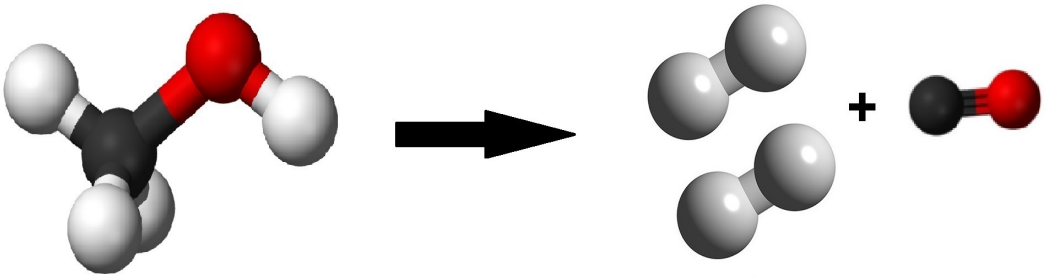

Use of methanol based syngas for waste heat recovery in vehicles

Shashank Sakleshpur Nagaraja

Thesis to obtain the Master of Science Degree in

Energy Engineering and Management

Supervisors : Prof. António Luís Nobre Moreira
Prof. Gonçalo Nuno Antunes Gonçalves
Prof. Grzegorz Przybyła

Examination Committee

President : Prof. Edgar Caetano Fernandes
Supervisor: Prof. António Luís Nobre Moreira
Member of the committee: Prof. Tiago Alexandre Abranches Teixeira Lopes Farias

July 2016

Acknowledgements

I would like to thank my supervisors, Prof. António Moreira, Dr. Gonçalo Gonçalves and Dr. Grzegorz Przybyła for their constant support during different phases of the thesis. The development of this project would not have been possible with out assistance and support from Prof. Francisco Lemos and Prof. Amelia Lemos. I am grateful to them.

I would also like to thank Mr. Sjur Haugen for sparking this idea and Mr. Knut Skårdalsmo for his technical support. I am eternally grateful to KIC InnoEnergy for financially supporting my stay for past two years. I am thankful to Dr. Krzysztof Pikoń, Dr. Lucyna Czarnowska and MSc. Magdalena Bogacka for their encouragement.

Last but not least, I would like to thank the research team on transports, energy and environment of IDMEC-IST and Vehicle and Propulsion Systems laboratory, my friends and flatmates, Daniele, Petar and Tejas for all the moral support provided.

Abstract

Electrification and hydrogen economy are touted as two alternatives to decarbonize transport sector. However, it is important to have a sustainable transition from oil and gas economy to these alternatives. Methanol, a liquid fuel with lowest carbon to hydrogen ratio can assist this transition. Due to the absence of carbon carbon bond in methanol, it is relatively easier to dissociate methanol to hydrogen and carbon monoxide by providing heat. Dissociated methanol has about 20 % higher energy content per unit mass than methanol. The present study exploits this property using the exhaust waste heat from an internal combustion engine and evaluates its feasibility on a vehicle under three real world driving conditions (highway, sub-urban and urban).

The fuel consumption is highest in case of urban driving conditions due to fluctuations in speed and power demand. Due to consistent speed and power, the fuel consumption is the lowest in highway conditions. Compared to pure methanol, use of M-TCR system in highway, sub-urban and urban driving conditions reduce fuel consumption per kilometer by 6.6%, 5.8% and 3.7% respectively. Approximate engine out emissions are also obtained from simulations. The reduction in HC emissions is about 41.2% for highway, 26.9% for sub-urban and 20.4% for urban driving conditions. However, CO emissions increase by about 70-80% and NOx emissions increase about three times in all the three driving conditions by using M-TCR system.

Overall, M-TCR system proves to be an efficient way to recover exhaust waste heat. Further investigations are required to check the implementation and economic tangibility of the system.

Keywords: Methanol, Dissociated Methanol, Thermo chemical recuperation, Engine duty cycle

Resumo

Duas das hipóteses para atingir a descarbonização do sector dos transportes são a electrificação e a economia do hidrogénio. É no entanto importante garantir uma transição sustentável de uma economia de gás e petróleo para estas alternativas. Uma das possibilidades de conseguir uma transição bem-sucedida é através do uso de metanol. Devido à ausência de ligações entre átomos de carbono é relativamente simples dissociar metanol em hidrogénio e monóxido de carbono fornecendo calor. A mistura de gases resultante tem um poder calorífico cerca de 20 % superior por unidade de massa. O presente estudo explora esta propriedade usando como fonte de calor os gases de escape de um motor de combustão interna num veículo automóvel em três condições de utilização reais (urbana, suburbana e via rápida).

O consumo de combustível é máximo em condições urbanas e mínimo para condução em via rápida. Comparado com o uso de metanol puro, este sistema de recuperação termoquímica de calor permite reduzir o consumo de combustível por quilómetro em 6.6 %, 5.8 % e 3.7 %, respectivamente para condições de via rápida, suburbana e urbana. Estimativas de emissões de poluentes foram obtidas por processos de simulação, tendo sido observadas reduções de emissões de HC de 41.2 % em condução em via rápida, 26.9 % em condições suburbanas e 20.4 % em condições urbanas. Em contrapartida, as emissões de CO aumentaram entre 70 e 80 % e as de NOx por um factor de 3.

Globalmente o sistema de recuperação termoquímica de calor demonstrou ser viável para recuperar energia dos gases de escape. Investigação adicional é necessária para demonstrar a validade técnica e económica do sistema proposto.

Palavras-chave: Metanol, Metanol dissociado, recuperação termoquímica, ciclo de utilização do motor

Contents

List of Figures

List of Tables

Nomenclature

AFR	Air-Fuel ratio
B	Bore in m
$BSCO$	Brake Specific Carbon monoxide emissions in g/kWh
$BSFC$	Brake Specific Fuel Consumption in g/kWh
$BSHC$	Brake Specific Hydrocarbon emissions in g/kWh
$BSNOx$	Brake Specific Nitrogen oxide emissions in g/kWh
CH_3OH or $MeOH$	Methanol
CO	Carbon monoxide
CO_2	Carbon dioxide
COV_{imep}	Coefficient of variation in indicated mean effective pressure
CR	Compression Ratio
ETL	Emissions to Liquid
H_2	Hydrogen
HC	Hydrocarbons
$HCPC$	Homogenous Charge Progressive Combustion
HHV	Higher Heating Value in kJ/kg
ICE	Internal Combustion Engine
ITE	Indicated thermal efficiency

L	Length of Connecting Rod in m
LHV	Lower Heating Value in kJ/kg
$\dot{m}_i$	Mass flow rate of ith species in g/s
MAP	Manifold Air Pressure
MPI	Multipoint Injection
Mpc	Fuel blend with pc % (by vol.) of methanol
$M-TCR$	Methanol Thermochemical Recuperator
NOx	Oxides of Nitrogen
R	Universal Gas Constant in J/molK
RPM	Rotations Per Minute
S	Stroke in m
SI	Spark-Ignition
T_{exh}	Exhaust gas temperature in K
V_c	Clearance Volume in m^3
V_s	Stroke Volume in m^3
WOT	Wide Open Throttle
x	Conversion ratio of methanol to syngas
θ	Crank Angle in degrees
λ	Excess air ratio
ϕ	Equivalence ratio

1 Introduction

1.1 Problem Description

The abundant availability of fossil raw materials such as crude oil, natural gas, brown coal (lignite) and coal has given rise to our enormous prosperity. Fossil raw materials satisfy our energy needs and they provide a wide spectrum of chemicals that enrich our lives. The overall primary energy consumption of the world in 2015 is illustrated in Fig. 1.1 [1].

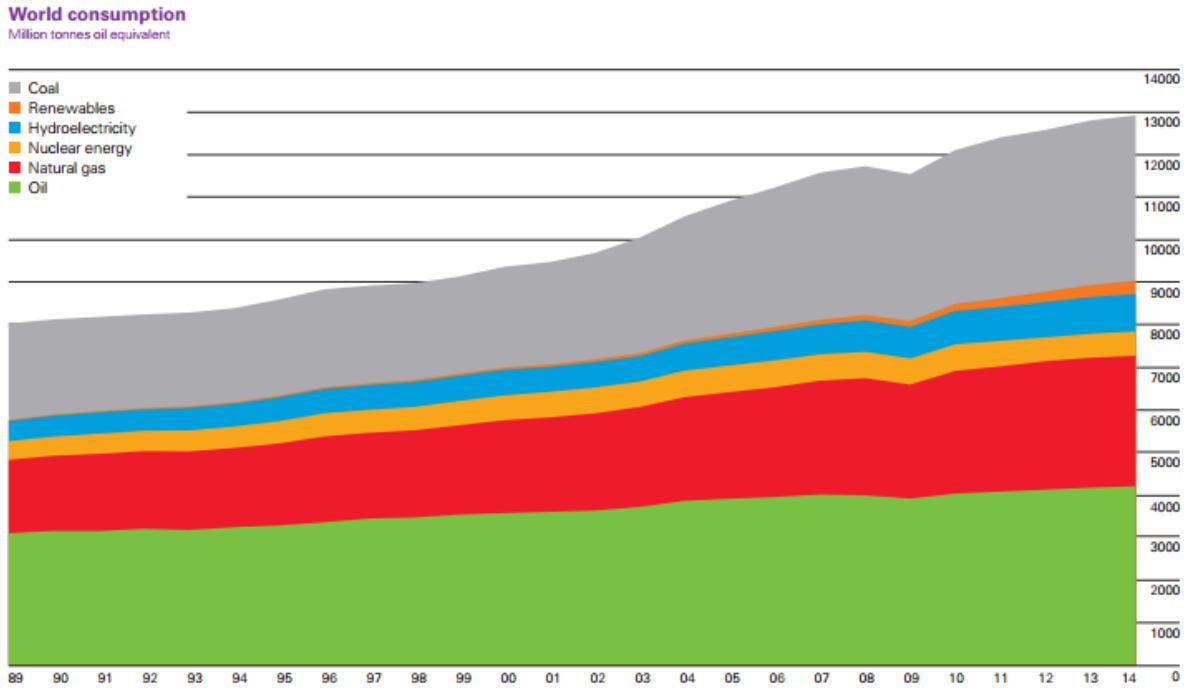

Figure 1.1: Growth of world overall primary energy consumption
Source: BP Statistical review of World energy 2015

It is clear that fossil fuels still influence the energy market to a greater extent. In the transportation domain, gasoline and diesel continue to dominate the global market. Crude oil required to produce these fuels are concentrated in certain regions. Total world proved oil reserves reached 1700.1 billion barrels at the end of 2014, sufficient to meet 52.5 years of global production. OPEC countries continue to hold the majority of the world's reserves, accounting for 71.6 % of the global total [1]. Hence, to have energy and economic security in the transportation sector, domestically produced fuels should be given prominence [2]. Added to this, climate change prevention policies are driving the society towards renewable, low green house gas (GHG) emitting fuels. In the US, the Energy Independence and Security Act of 2007 has mandated

that a total of 36 billion US gallons of ethanol be used in the fuel pool by 2022 [3], and in the European Union (EU) the Renewable Energy Directive (RED) seeks to establish a minimum proportion of renewable energy in the fuel pool of 10 % by 2020 [4]. Due to these policies, bioethanol and biodiesel have been introduced into the fuel pool in significant quantities. The use of these alternative fuels has been possible without a quantum change in either the transport energy distribution infrastructure or the technology and, therefore, the cost of the vehicles in which they are used. In these respects, liquid biofuels are superior to electrification or to the use of molecular hydrogen as alternative energy carriers [5]. Furthermore, pledges made during 2015 United Nations Climate Change Conference (COP21) promise to give new impetus to the move towards a lower-carbon and more efficient energy system [6].

Another light alcohol fuel that has the potential to improve energy security and offer prospects of carbon neutral transportation is methanol. Methanol is a colorless, water soluble liquid with a mild alcoholic odour. Containing only one carbon atom, methanol is the simplest of all alcohols. During the world war era, synthetic methanol produced from coal was blended with gasoline as a fuel. Methanol-gasoline blends were used by Volkswagen and had shown significant improvement in cars performance. During 1990s, different technological advances were achieved and this reduced the emission problems and at the same time, decreased interest in methanol based fuels. Today, methanol is mainly used as a primary feedstock for the chemical industry with an approximate 70 million ton market per year . This clearly shows it has all the necessary infrastructure in place [7].

Methanol is a hydrocarbon which can be produced from numerous sources like syn-gas, oxidative conversion of methane and reductive hydrogenative conversion of carbon dioxide (CO_2). The chemical recycling of excess CO_2 would also help to mitigate the climate changes caused by use of fossil fuels [8]. The figure below explains the concept of 'Methanol-Economy' by Nobel laureate Dr. George Olah.

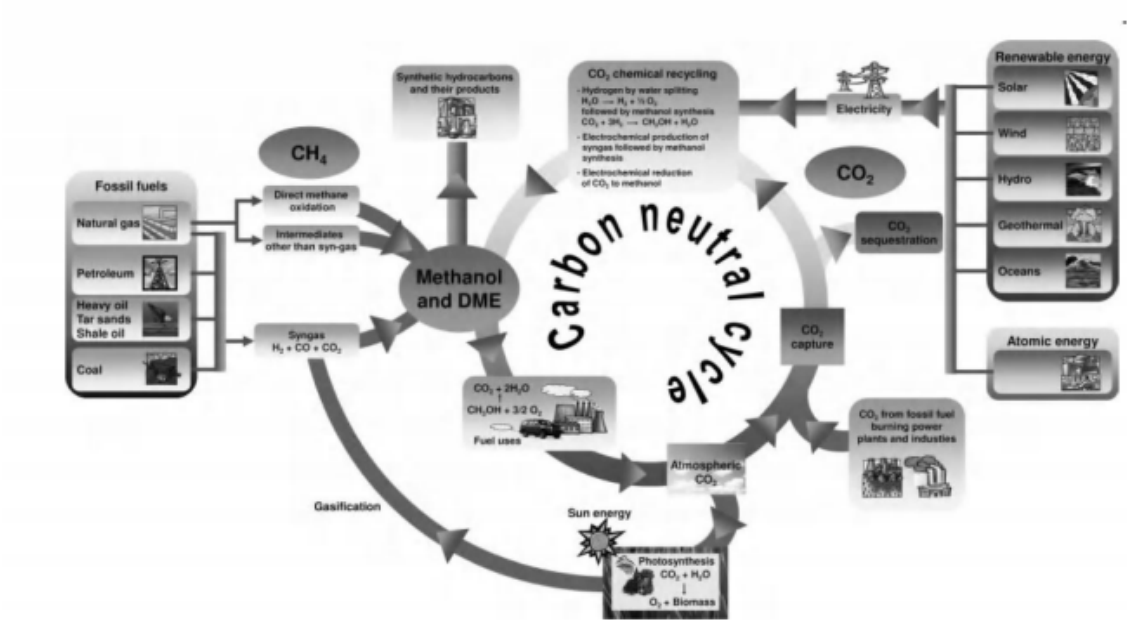

Figure 1.2: Methanol economy [7]

The properties of methanol, ethanol and gasoline are provided in Table 1.1 [9].

Table 1.1: Properties of Methanol, Ethanol and Gasoline

Property	Gasoline	Methanol	Ethanol
Chemical formula	Various	CH_3OH	C_2H_5OH
Oxygen content by mass (%)	0	50	34.8
Density at NTP (kg/l)	0.74	0.79	0.79
Lower heating value (MJ/kg)	42.9	20.09	26.95
Volumetric energy content (MJ/l)	31.7	15.9	21.3
Stoichiometric air to fuel ratio (kg/kg)	14.7	6.5	9
Energy per unit mass of air (MJ/kg)	2.95	3.12	3.01
Research octane number (RON)	95	109	109
Motor octane number (MON)	85	88.6	89.7
Sensitivity (RON–MON)	10	20.4	19.3
Boiling point at 1 bar (°C)	25–215	65	79
Heat of vaporization (kJ/kg)	180–350	1100	838
Reid vapour pressure (psi)	7	4.6	2.3
Mole ratio of products to reactants[a]	0.937	1.061	1.065
Flammability limits in air (λ)	0.26–1.60	0.23–1.81	0.28–1.91
Laminar flame speed at NTP, $\lambda = 1$(cm/s)	28	42	40
Adiabatic flame temperature (°C)	2002	1870	1920
Specific CO_2 emissions (g/MJ)	73.95	68.44	70.99

[a] Includes atmospheric nitrogen. NA: not available. NTP: normal temperature (293 K) and pressure (101325 Pa).

Carbon dioxide, a significant greenhouse gas, is considered a harmful pollutant of our atmosphere and a major source for human-caused global warming. So far, however, besides the proposed collection and sequestration of excess CO_2, a costly and only temporary solution, which in seismically active areas could cause devastating releases of CO_2 in case of earthquakes or other earth movements, no new technology emerged for its disposal. Deep ocean storage is no longer considered feasible because it greatly increases the problem of ocean acidification. In the recent years, extensive work has been carried out at Loker Hydrocarbon Research Institute on chemical recycling of CO_2 to methanol (MeOH). This practical, feasible approach, not only offers a solution to the environmental problem of carbon dioxide increase in our atmosphere and associated global warming, but also renders our fuels renewable and environmentally carbon neutral.

Carbon Recycling International Inc. (CRI) incorporated in 2006, began operation of first commercial scale plant, the George Olah Plant in 2011 based on this technology . CRI's Emission to Liquid (ETL) technology enables cost-effective conversion of renewable energy to liquid fuel on small scale. ETL consists of a system of electrolytic cracking and catalytic synthesis, leading to a low pressure and low temperature electrochemical production process.

Added to this, scientists from Stanford University, SLAC National Accelerator Laboratory and the Technical University of Denmark combined theory and experimentation to identify a new nickel-gallium catalyst that converts hydrogen and carbon dioxide into methanol with fewer side-products than the conventional catalyst [10]. All these discoveries have created a conducive atmosphere for production of methanol. Therefore, it is the right time to look beyond conventional fuels and align ourselves with discovering new techniques to adopt methanol as a practical alternative fuel.

An unique advantage offered by methanol is thermo-chemical recuperation. Methanol can be decomposed to form hydrogen (H_2) and carbon monoxide (CO). The overall reaction is shown in equation 1.1 [11]. This mixture of gases is called a syngas (H_2 + CO). The heat content of syngas is 20.7 % more per unit mass than methanol. Even though ethanol can be converted to syngas, the C-C bond present requires higher dissociation energy.

$$CH_3OH \rightarrow 2H_2 \ + \ CO \qquad \Delta H^0_{298} \ = \ 90.7 \ kJ/mol \tag{1.1}$$

In an internal combustion engine, about 70 % of total energy is lost as low grade waste heat in coolant and high grade waste heat in exhaust gases. This fact is well illustrated in Fig 1.3. This energy can be used for splitting methanol in to H_2 and CO.

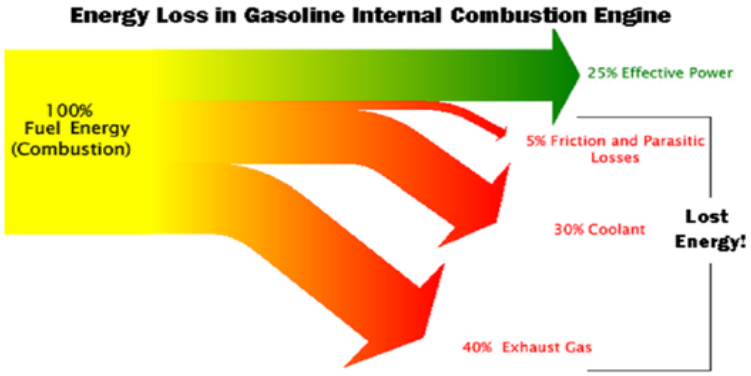

Figure 1.3: Typical energy split in IC engines [12]

The present study is aimed at computationally evaluating the concept of a vehicle with methanol/ syngas as fuel with an onboard methanol splitter, henceforth called methanol thermo chemical recuperator (M-TCR). This study attempts to provide an overview about a fuel that has potential to supplant gasoline in the future. Methanol has an advantage of having the lowest carbon to hydrogen ratio for any liquid fuel. This helps in low carbon emissions. Furthermore, the increase in energy content of the fuel by splitting of methanol using exhaust waste heat increases overall efficiency of the engine. Hence, methanol can be seen as an unique and prominent answer to the conundrum of fuel crisis, low carbon emissions and increasing overall engine efficiency. Fig 1.4 shows the rudimentary schematic of the concept. This will be later modified by changing the location of the components in order to obtain better overall efficiency of the system.

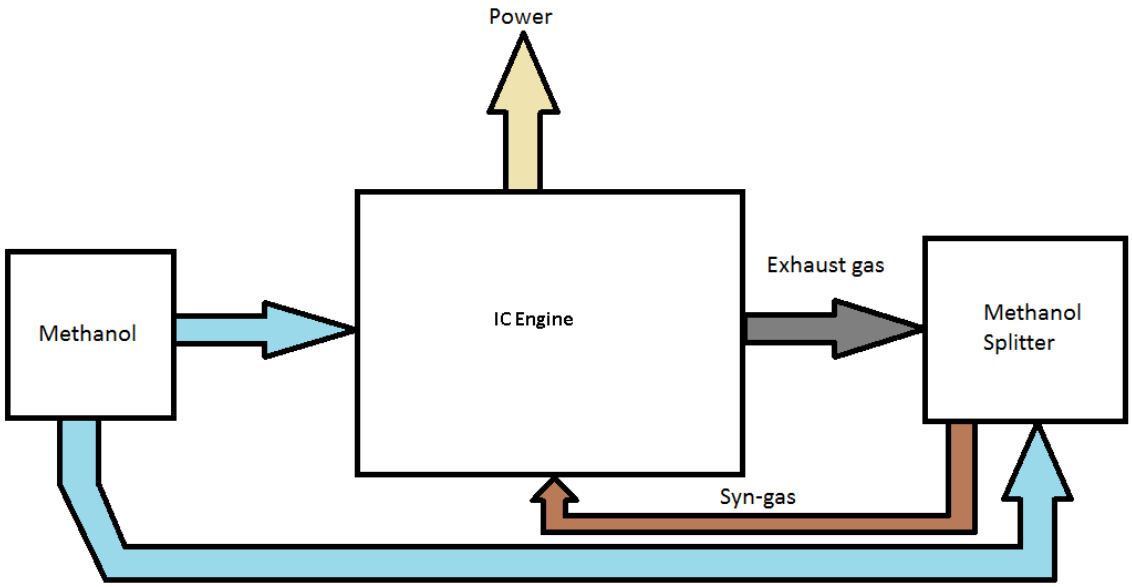

Figure 1.4: Schematic diagram of the idea

1.2 Objectives

The following are the objectives of the present study:

1. **Evaluate the feasibility of the proposed concept by performing simulations using various tools.**
   To check the feasibility of the concept, various blocks have to be assembled together to build the whole system. This system consists of two blocks, namely the engine and M-TCR. It is important to rightly choose the tools required to build these blocks and check the feasibility of the concept using these tools.

2. **Check the utility of the proposed concept by testing it under different driving conditions.**
   Utility is important for any research. This study is aimed at automotive sector. Hence, the proposed concept is evaluated under three different driving conditions namely urban, sub-urban and highway.

3. **Scope for future research is to be highlighted.**
   This study is the first step in evaluating the concept. It is important to look at prospective research areas and the possibilities.

1.3 Outline

The structure of the thesis is presented in this section.

Chapter 1. Introduction
This chapter elaborates the problem in hand and explains the possible ways of overcoming this. The importance of methanol and its significance in reducing the CO_2 emissions and closing the carbon cycle artificially is illustrated. Finally, the concept of using methanol as a reactant for thermo chemical recuperation in M-TCR is introduced and objectives of the present study are defined.

Chapter 2. Literature Review
This chapter aims at showcasing the previous works related to the area of the present study. The first section explains the available techniques for waste heat recovery in an ICE and previous studies on these techniques. The second section addresses the studies performed with dissociated methanol as fuel and the last section explains the possibility of simulating of combustion engines and previous research in this domain. Finally, a summary of literature is provided and research gap is identified.

Chapter 3. Methodology
This chapter explains the the importance and requirement of different components needed to build the whole system. The tools required to build these blocks are identified and an overview of the implementation of these tools is provided. Finally, the procedure used to evaluate the feasibility of the proposed concept is illustrated.

Chapter 4. Simulation
Different equations behind each of the tools used in the study are shown in this chapter. An insight into different models used on AVL Boost for various processes taking place inside an engine are described. The assumptions made in building M-TCR are stated. The division of an engine drive cycle into three states is explained and the decision process is demonstrated using a flow chart.

Chapter 5. Results and Discussions
This chapter provides a description of results obtained on virtual engine test bench and on-road vehicle under different driving conditions with and without M-TCR. An evaluation and possible implications of the results is provided.

Chapter 6. Scope for future research
Various possibilities for future research is described in this chapter.

Chapter 7. Conclusions
Conclusions are drawn from the available results.

2 Literature Review

In the present study, the literature reviewed is divided into three sections, namely:

1. Waste heat recovery
2. Dissociated methanol as a fuel in IC engines
3. Simulation of IC engines

A brief overview of each study is provided.

2.1 Waste heat recovery

In internal combustion engines, enormous amount of heat is lost in the form of waste heat through the exhaust gas. In an ICE about 70 % of energy is rejected to the environment in the form of heat out of which 27.7 % is lost as thermal energy through exhaust [13]. There are numerous techniques to recover this waste heat. Some of these techniques are discussed.

Thermoelectric energy conversion

Thermoelectric Generators (TEG) are one of the most promising devices for low grade heat recovery. The thermoelectric generator extracts waste heat from the exhaust that will generate DC current to recharge the battery. This improves fuel efficiency by as much as 10% [14]. The primary challenge of using TEG is its low thermal efficiency. To overcome this drawback, development of new materials with higher thermoelectric conversion efficiency is necessary [15].

Organic Rankine Cycle

A Rankine cycle is a closed-loop system used to transform waste heat into mechanical or electrical power. If the selected working fluid is organic in nature, researchers often refer to this system as an Organic Rankine Cycle (ORC). ORC system exhibits great flexibility, high safety and low maintenance requirements in recovering this grade of waste heat [16]. Conversion of low grade waste heat to electricity can be achieved by integrating an ORC into the energy system [17].

Patel and Doyle (1976) used the exhaust heat of a Mack 676 diesel engine [18]. Flurinol-50 was the chosen working fluid as it maintains minimum temperature difference between the exhaust gas and the working fluid. At peak power condition, an additional 36 horse power was produced without the need of supplementary fuel.

Hung et al. (1997) compared the efficiencies of ORCs using different working fluids such as benzene, ammonia, R11, R12, Rl34a and R113 [19]. It was concluded that isentropic fluids [1] are most suitable for recovering low temperature waste heat.

In another study by Chen et al. (2010), a review of the organic Rankine cycle and supercritical Rankine cycle is presented [20]. A discussion of the 35 screened working fluids was provided. It was concluded that there is no single fluid that meets all the requirements of ORC. However, it was mentioned that isentropic fluids with relatively high critical temperatures, are favoured for ORC.

Briggs et al. (2010) conducted a study on a waste heat recovery in a diesel engine at Oak Ridge National Laboratory [21]. This lab demonstration was designed to maximize the peak brake thermal efficiency of the engine, and the combined system with ORC achieved an efficiency of 45 %. Valentino et al. (2013) used these results to calibrate a model and used this model to predict the steady-state power output, thermal efficiency, and state point temperatures of the ORC as a function of refrigerant flow rate and engine speed/load for a spark ignition engine based on experimental exhaust flow data [22]. The maximum predicted net power output of the ORC was about 11.5 kW for the S.I. engine at high speed and load where as for light loads in the range of 2-4 bmep and engine speeds of 2000 rpm and lower, the predicted net power was in the range of 1 kW or less, calling into question its practicality for light-duty vehicles.

Turbocharger

A turbocharger is combination of a compressor with a gas turbine where heat and pressure of the exhaust gases are used to increase engine power by compressing the air that goes into the engine. The exhaust gas drives the turbine which in turn runs the compressor increasing the mass of air entering the combustion chamber.

Early development of exhaust-driven turbocharger was recorded by Dr. Alfred J. Buchi (1942) [23]. The main challenges with turbochargers are turbo lag and heated bearings. Park et al. studied the mechanism of turbocharger response delay and found that its primary reason was due to weight of the system [24]. They also concluded that the secondary factor is a decreased effective turbine energy caused by a shift in the operating point, resulting from the primary factor.

To overcome challenges associated with turbochargers, several concepts like Variable geometry turbine [25], two-stage turbocharger [26] and HCPC turbocharged engine [27] have been proposed. However, these techniques are beyond the scope of present study.

[1] An "isentropic" fluid shows a vertical saturation vapor curve. It remains very close to the saturated vapor state after an hypothetical isentropic expansion.

Turbo-compounding

Turbo-compound engine employs a turbine to recover heat from exhaust and directly provides the recovered energy to the crankshaft using gear-train [28]. Such engines were predominantly used for piston aero engines [29]. This concept is indirectly employed in Formula 1 cars now.

Thermo-Chemical Recuperation

Thermochemical recuperation (TCR) is currently receiving renewed interest as a possible means for increasing the efficiency of internal combustion (IC) engines. The basic concept involves using exhaust heat to promote on-board reforming of hydrocarbon fuels into syngas (a mixture of carbon monoxide and hydrogen) [30]. The reforming reactions are endothermic. The low grade exhaust waste heat can be utilized to obtain chemical energy. Several TCR studies focusing on gas turbine applications have been published [31] [32]. A study on theoretical potential of TCR was carried out by Chakravarthy et al [30]. It was found that for a stoichiometric mixture of methanol and air, TCR can increase the estimated ideal engine second law efficiency by about 3 % for constant pressure reforming and over 5 % for constant volume reforming. For ethanol and isooctane, the estimated second law efficiency increases for constant volume reforming are 9 and 11 %, respectively. In the next section, a deeper insight into use of dissociated methanol as fuel is provided.

2.2 Dissociated Methanol as a fuel in IC Engine

As discussed earlier, thermo-chemical recuperation can be an attractive technique for waste heat recovery. For on-board TCR, methanol is suggested as the original fuel can be converted directly to syngas by adding heat at relatively low temperatures in the presence of a catalyst.

Methanol is an efficient hydrogen carrier. If decomposed, 1 mole of methanol produces 2 moles of molecular hydrogen and 1 mole of carbon monoxide. 2 moles of hydrogen and 1 mole of carbon monoxide stand for approximately 76 % and 44 % energy content of one mole of methanol respectively, calculated on the lower heating value basis. Therefore, the energy content in the produced gas is 20 % greater than in liquid methanol per unit mass [33]. California Clean fuel program in 1980s motivated researchers to work on methanol and dissociated methanol as a fuel.

Sjostrom (1982) at the Royal Institute of Technology (KTH), reported experiments with a Volvo B21 engine and a reactor equipped with a nickel catalyst [34]. The methanol feed to the reactor was mixed with recirculated exhaust gas in order to suppress the coke deposition on the catalyst. At 500 ^{o}C, 10 % exhaust gas recirculation was needed in order to thermodynamically avoid carbon precipitation. The methanol conversion in the reactor was reported to be 57-90%. This means that the performance was not optimized. A maximum relative efficiency gain over methanol with 12-19 % was reported.

Finegold (1984) conducted experiments on a General Motors 2.5 L., in-line, four-cylinder engine rated at 65 kW fueled with on-board generated syngas [35]. The compression ratio was increased

from stock value of 8.3 to 14. The engine dynamometer test results with dissociated methanol demonstrated improvements in brake thermal efficiency about 30 % to 100% compared to gasoline . It was also found that the exhaust temperature is always almost high enough for dissociation to occur, but at lower power outputs, there is only enough exhaust energy for partial dissociation of the methanol depending on engine speed and torque.

Since the reformed gas is hydrogen rich it has the potential to increase the engines brake thermal efficiency and reduce exhaust emission compared to liquid methanol. To explore this possibility a series of dynamometer engine tests were conducted by Adams (1984) to compare the performance of a 100% dissociated methanol fueled engine to a liquid methanol fueled engine [36]. The combustion characteristics of the dissociated methanol are comparable to those of hydrogen. There was a reduction of exhaust emissions and improvements in brake thermal efficiency at low speed and low load but there were backfires and pre-ignition at mid and high speeds.

A study by König et al. (1985) on use of dissociated methanol as a fuel was performed at Volkswagen [37]. Syngas was obtained by a combined process of cracking and partial oxidation. This approach was taken as the main objective was to run the engine ultra lean but the temperature for complete dissociation could not be obtained at such running conditions. A precious metal catalyst was used for cracking of methanol. Engine tests employing such a catalyst gave up to 10 % better energy consumption and very favorable exhaust emissions as compared to engines on pure methanol.

In another study by Yamaguchi et al. (1985), a dissociated methanol gas fueled spark ignition engine along with a cold starter and an exhaust dissociator was developed [33]. The cold starter reformed the rich alcohol fuel mixture into dissociated methanol gas through a bubbling process at a cold start and during warmup. This starter allowed to start the engine at ambient temperatures as low as - 15 ^{o}C, while resulting in reduced undesirable emissions. The engine fueled with liquid and dissociated methanol had a thermal efficiency better by about 20 percent than that fueled with gasoline, and gave exhaust emission levels similar to those of gasoline engines.

2.3 Simulation of IC Engine

The advent of high-speed digital computers and advances in computational methods has made analysis of complex physical processes feasible. The huge amount of results that are obtained by simulation studies are rather very difficult to be obtained experimentally. Advances in computational algorithms have helped researchers to even simulate the combustion process happening within the cylinder.

Kodah et al. (2000) worked on engine simulation for the prediction of pressure within a spark ignition engine [38]. Combustion modeling was carried using the Wiebe function approach,

which is an exponential function in the form $y = 1 - exp\{-ax^m\}$ to calculate the rate of fuel burned. The Eichelberge equation was used to calculate the heat-transfer rate between the cylinder gases and combustion chamber walls. The modified Mallard and Le Chatelier equation was used to calculate the laminar flame speed. The propagating flame surface was considered to be spherical as assumed in many earlier studies. The effects of the many operating conditions, such as compression ratio, engine speed, and spark timing were studied.

Alla (2002) worked on computer simulation of four stroke spark ignition engine [39]. In this study, discussion about general introduction to computer simulation and zero dimensional model of spark ignition engine was carried out. The thermodynamic model was developed based on the first law of thermodynamics and ideal gas law. An arbitrary heat release formula was used to predict the cylinder pressure, which in turn was used to and the indicated work. Combustion modeling was carried out using the Wiebe function. The heat transfer from the combustion mixture to cylinder wall was calculated using empirical correlation. The parameters which can affect the performance of four stroke spark ignition engines, such as equivalence ratio, spark timing, heat release rate, compression ratio, compression index and expansion index were studied.

Al-Baghdadi (2006) developed a model for simulating the performance parameters of spark ignition engines fueled with a range of fuels (gasoline, ethanol, or hydrogen) and their mixtures [40]. For modeling, the combustion chamber was generally divided into burned and unburned zones separated by a flame front. The pressure was assumed to be uniform throughout the cylinder charge. The instantaneous heat interaction between the cylinder content (burned and unburned zones)and its walls was calculated by using the following semi-empirical expression for a 4-stroke engine. The instantaneous energy flows into the crevices were calculated by using the following semi-empirical expression of Gatowski et al. (1984) for a spark ignition engine [41].

Pourkhesalian et al. (2010) developed the computer code for simulating spark ignited engine using alternative fuels and results were validated with experimental data [42]. The engine model is a quasi-dimensional two-zone model including ordinary differential equations for describing dynamical behavior during the intake, compression, power and exhaust strokes. The engine model uses the Woschni correlation to estimate engine heat transfer.

Presently many researchers use commercially available software like GT Power, Ricardo Wave, Ansys ICE for simulation of combustion engines. AVL Boost, one of such softwares is persistently used for studies involving alcohol fuels. A study by Iliev (2015) analyzed Gasoline, Ethanol and Methanol blends using AVL Boost [43]. He also investigated the performance of ethanol gasoline blends [44]. Yashwanth et al. (2014) performed simulation studies to determine the effective octane number in an engine fueled with ethanol-gasoline blends [45]. Similarly, Trimbake and Malkhede (2016) studied port duel fuel injection engines with ethanol-gasoline blends using AVL Boost [46]. Furthermore, the author of this dissertation has validated AVL simulation results with experimental data for gasoline-iso-butanol blends [47]. From all these studies, it is

very clear that AVL Boost in as effective tool to study alcohol fuels.

Based on these state of the art studies, AVL Boost was used as a tool for the present study.

2.4 Summary

Some of the notable features found during the literature review are listed below:

- Diminishing crude oil reserves and concern for environment has alarmed the researchers to find alternative renewable fuels which could effectively supplant gasoline and can be domestically produced with reduced cost per unit energy.
- Second generation biofuels are considered as a better option to be used as alternative fuels.
- Waste heat recovery is an important technique employed to increase the overall efficiency of the engine. Thermochemical recuperation (TCR) is currently receiving renewed interest as a possible means for increasing the efficiency of ICE by waste heat recovery.
- Use of quasi one-dimensional simulation models for thermodynamic analysis were found to be sufficiently accurate. Many authors use the Wiebe two zone model for combustion analysis, the Woschni's model for heat transfer assessment and the Zeldovich mechanism for estimating NOx emissions.
- Methanol has been historically used as fuel in IC engines. However, use of dissociated methanol is more beneficial to obtain higher overall efficiency.
- The engine fueled with liquid and dissociated methanol had a thermal efficiency better by about 20 percent than that fueled with gasoline, and gave exhaust emission levels similar or better to those of gasoline engines.

2.5 Research Gap

The following gaps were found during literature survey:

- The analysis of engine parameters using methanol and syngas blends for different engine operating conditions.
- The analysis of engine parameters using methanol and syngas blends for different ratio of blending.
- Effect of different drive cycles on methanol and syngas fueled SI engine.
- Use of simulation tools like AVL Boost for analyzing performance and emission characteristics of such an engine.

The present study attempts to bridge this research gap by analyzing a fuel that may help us during the sustainable transition to the 'Hydrogen economy'.

3 Methodology

3.1 Concept Evolution

This section is aimed at describing the concept. The initial idea is shown in Fig. 3.1.

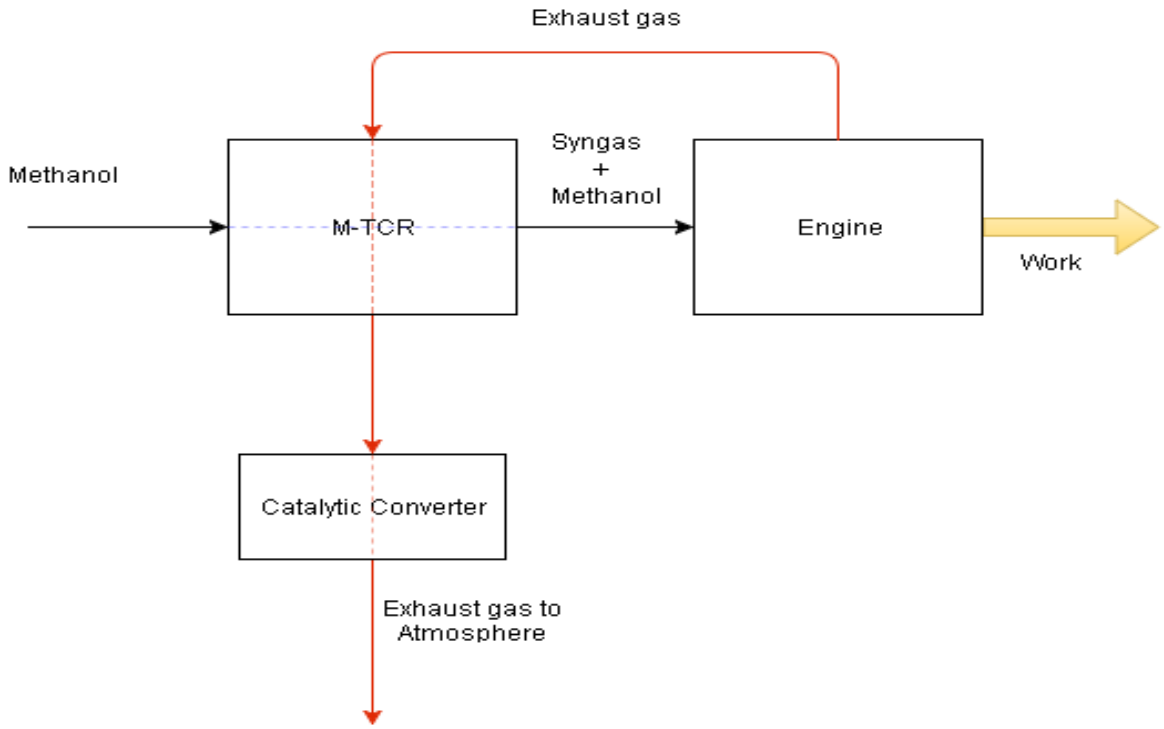

Figure 3.1: Schematic diagram of the initial concept

The fuel coming out of M-TCR is a mixture of syngas and methanol vapour at a temperature of about 300 ^{o} C. This temperature is set based on the fact that the exhaust gas cannot go below 300 ^{o} C due to the catalytic converter light off temperature [48]. However, this high temperature reduces the overall efficiency of the engine. Hence, addition of a intercooler between M-TCR and engine was considered.

Concept 1: Intercooler

The overall setup after the addition of intercooler is shown in the following Fig. 3.2.

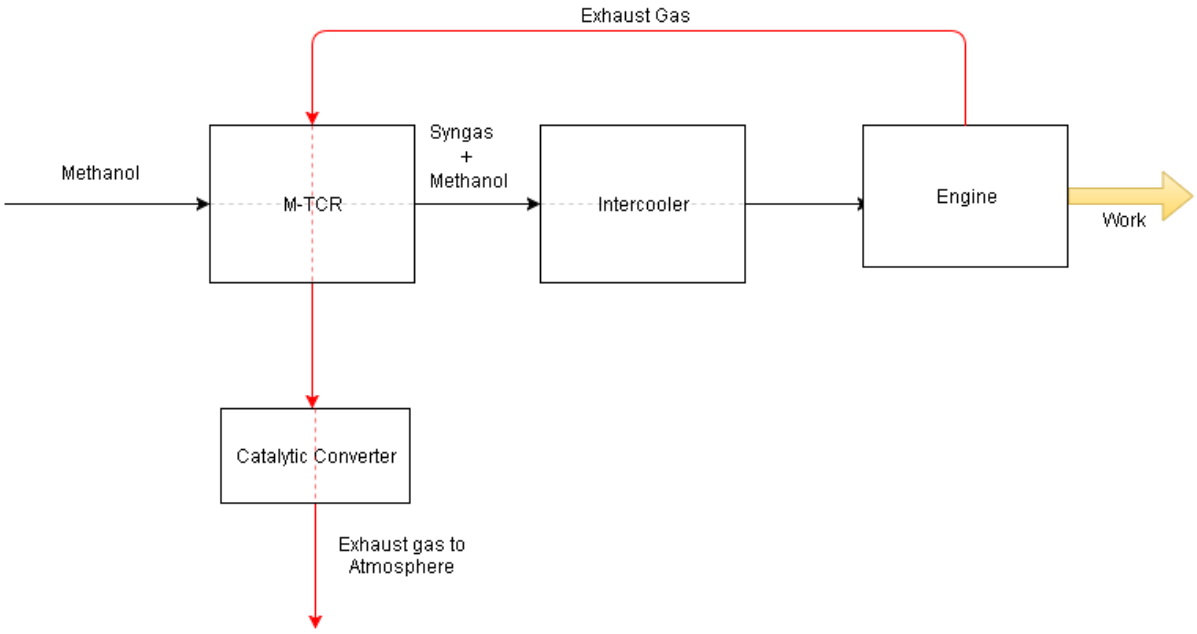

Figure 3.2: Schematic diagram of the system with intercooler

Brake specific fuel consumption (BSFC) is considered to be an indirect measure of overall efficiency as it provides the value of fuel consumed to produce unit energy. In Fig.3.3, a comparison of BSFC of cases with and without intercooler is provided. It is assumed that intercooler cools the fuel to room temperature of 25 ^{o}C.

The percentage reduction in BSFC by addition of intercooler is 1 % and this does not make sense economically. Eventhough, hot intake charge increases the probability of knocking, the minimum octane number of the fuels considered in the study are higher than 110 and this effect is negligible. Therefore, it was decided not to add the intercooler.

Figure 3.3: Comparison of BSFC between the cases with and without intercooler

Concept 2: Methanol pre-vaporizer after the catalytic converter

The amount of heat recoverable in M-TCR is limited due to the catalytic converter light off temperature. It was found that considerable amount of waste heat was used in the phase change process. The numerical calculation is shown in APPENDIX. Therefore, it was decided to pre-vaporize methanol and a separate phase change heat exchanger was placed after the catalytic converter. The new setup is shown in Fig. 3.4.

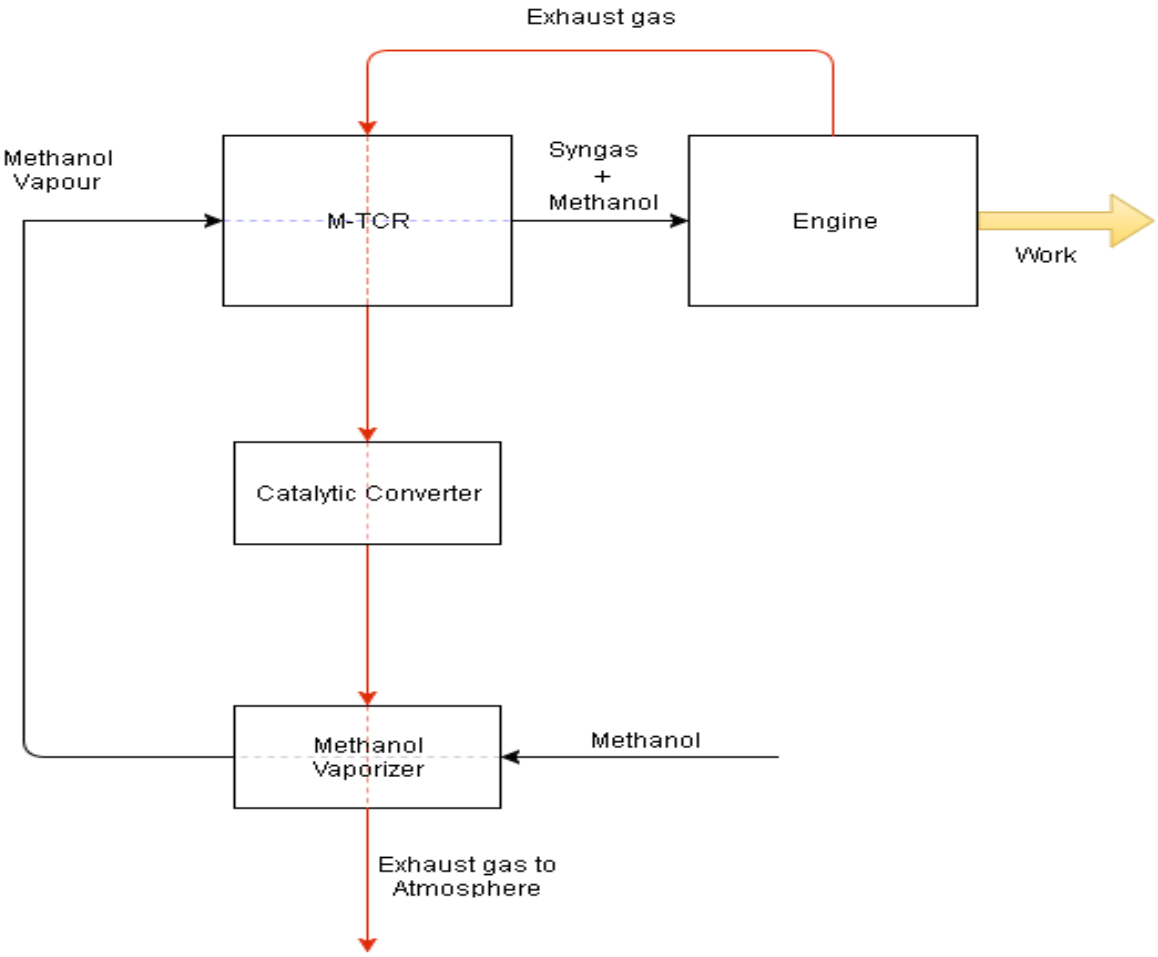

Figure 3.4: Schematic diagram of the system with pre-vaporizer

To compare the system with and without pre-vaporizer, a constant stream of exhaust gas at 1000 K and a mass flowrate of 1 g/s of methanol was provided to M-TCR. Initial temperature of M-TCR was 300 K. Conversion ratio is defined as the amount of methanol converted in syngas on mass basis. The conversion ratio of systems with and with out pre-vaporizer is shown in Fig. 3.5.

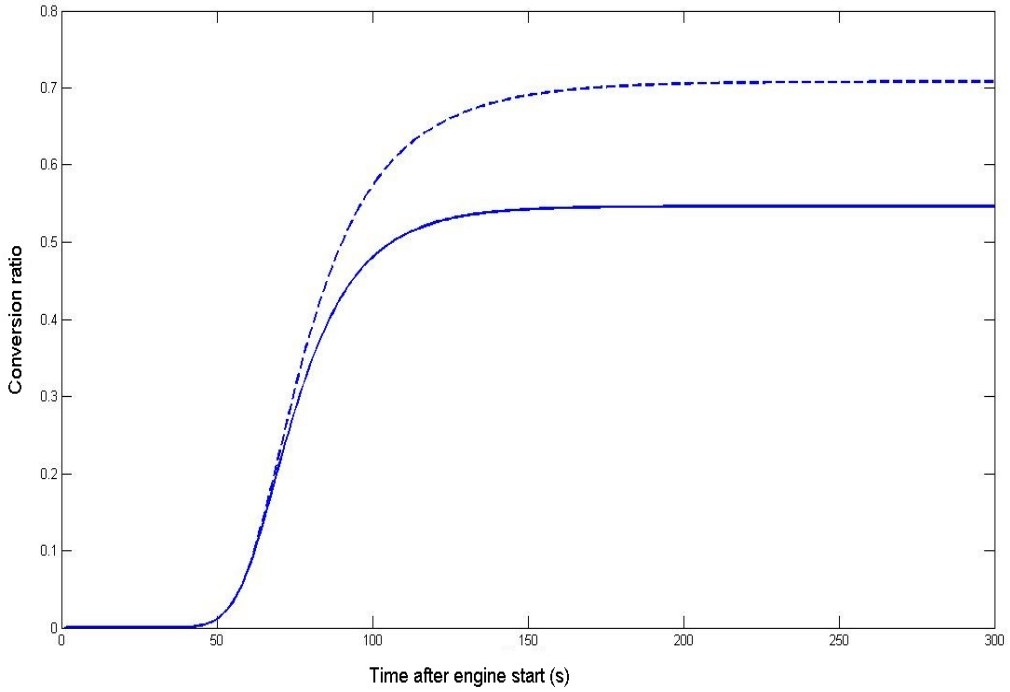

Figure 3.5: Comparison between conversion ratios of the two systems (**Dashed line**: With pre-vaporizer, **Solid line**: Without pre-vaporizer)

This change increases conversion ratios by about 18 % as all the heat is utilized for the reaction. This is a substantial positive change and hence, it was decided to carry out further investigation on the setup shown in Fig. 3.4.

As a consequence of this setup, the fuel is always in gaseous form and this displaces a small amount of intake air. Therefore, the volumetric efficiency of the engine is relatively lower than the engine running on liquid fuels. This has an effect on the brake power developed in the engine. The overall reduction in brake power is approximately about 13 % estimated based on the amount of fuel going in for unit volume of charge.

The next section is dedicated to discuss the methodology employed in this study.

3.2 Procedure

The fundamental concept of this study is based on the endothermic reaction of methanol into a mixture of hydrogen and carbon monoxide. The reaction has been earlier illustrated. The comparison of lower heating values is provided in Table 3.1.

Table 3.1: Comparison of combustion properties of two fuels used in the study

Fuel	**Lower Heating value(kJ/kg)**	**Octane Rating (RON)**	**Laminar flame speed (m/s)(ϕ =1)**	**Source**
Methanol	19930	109	0.42	[9] [49]
Syngas	24063	> 130 (H_2), 106 (CO)	2 (H_2), 0.16 (CO)	[50] [51] [52]

The exhaust waste heat can be used to provide the heat required for the endothermic reaction. This increases the overall LHV of the fuel as shown in Table 3.1. This is the basic idea of the whole concept. Utility of any concept is vital. It was decided to study the effect of this system on a vehicle fueled with methanol/syngas blend with onboard reactor.

Firstly, a fuel-air standard Otto cycle simulation is run on MATLAB with methanol as fuel and the exhaust gas temperature is obtained. When the temperature is found to be sufficient, feasibility of this concept is checked by doing an analysis on a virtual engine test bench built on AVL Boost. The chapter on **Simulation** provides a detailed understanding of engine simulations. After the feasibility is verified, engine maps of BSFC, exhaust gas temperature, emissions of CO, HC and NOx are obtained for different fuel blends from AVL BOOST. In-detail description of this step is provided in **APPENDIX**.

In the next step, M-TCR model is built based on first law of thermodynamics with certain assumptions discussed in the forthcoming chapters. The engine duty cycles for different driving conditions were obtained from previous studies. A tool is built on MATLAB integrating the engine maps and the M-TCR model.

Depending on the type of duty cycle, the engine spends significant amount of time under idle (no load) and fuel cut-off conditions. Hence, it is necessary to consider these states while building the tool. The decision process used to determine the states are explained in the next chapter. The tool reads the torque and engine speed value and determines the domain it is operating in and directly provides results in the idle and fuel cut-off domain. However, if it is under load, the tool reads the conversion ratio from M-TCR and decides the blend to be used and provides the results for the chosen blend from the engine map for the required torque and speed demand obtained from engine duty cycle data. The following are the results obtained:

- BSFC in g/kWh
- Emissions of CO, HC and NOx in g/s
- Exhaust gas temperature in K
- Mass of fuel input in g/s

Power integrator tool is used to compare the performance of a vehicle with and without M-TCR fueled with methanol for certain engine duty cycles obtained from real-world driving. This comparison demonstrates the practicality of this concept. The results obtained from this investigation and further modifications required for optimization of the system are discussed in the successive chapters. Fig. 3.6 provides an overview of how the tool developed using MATLAB works.

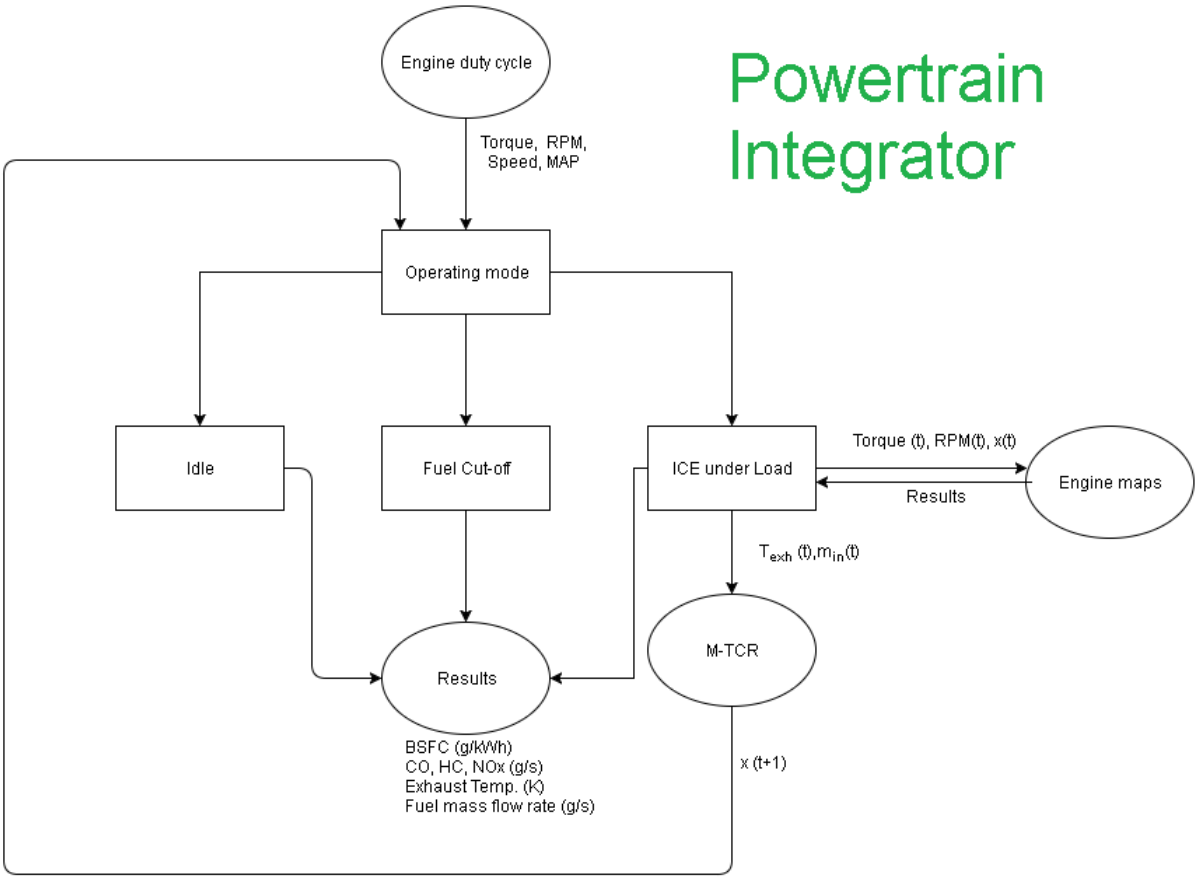

Figure 3.6: Powertrain Integrator schematic

After having an overview of the methodology used in this study, it is necessary to understand the notion behind each block that make the tool complete and robust. This discussion is provided in the next chapter.

4 Simulation

The present investigation is based on the fact that there is enough exhaust heat to dissociate methanol into syngas. In order to check this feasibility, an air-fuel standard Otto cycle simulation is performed in MATLAB and for further investigations, a 1 D simulation is carried out on AVL Boost.

4.1 Fuel-Air Standard Cycle

Standard Otto cycle simulations enable us to determine the approximate exhaust gas temperature. For the endothermic dissociation of methanol, a temperature of around 300 - 400 ^{o}C is required in the reformer. Therefore, an exhaust gas temperature above this range is required for this concept to be viable.

Otto cycle consists of adiabatic compression, isochoric heat addition, adiabatic expansion and isochoric heat rejection. P-V diagram of a standard Otto cycle is shown in Fig. 4.1.

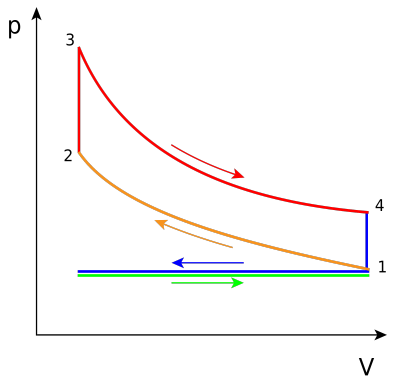

Figure 4.1: Standard Otto Cycle

MATLAB, a commercial software provides a numerical computing environment with a fourth generation programming language. This software is used for Otto cycle simulation.

The compression and expansion processes are discretized into 180 points each. Temperature and Pressure are determined at each point. Volume in the cylinder at any instant is given by the following equation [53]

$$V = V_c\Big(1 + \frac{1}{2}(CR\ -\ 1)\big[R + 1 - cos\theta\ -\ (R^2\ -\ sin^2\theta)^{\frac{1}{2}}\big]\Big) \tag{4.1}$$

where
V is the instantaneous volume and R is the ratio of Connecting Rod Length to Crank Radius

Gas properties are calculated at each point using JANAF tables [54]. The results of Otto cycle calculations are shown in Fig 4.2.

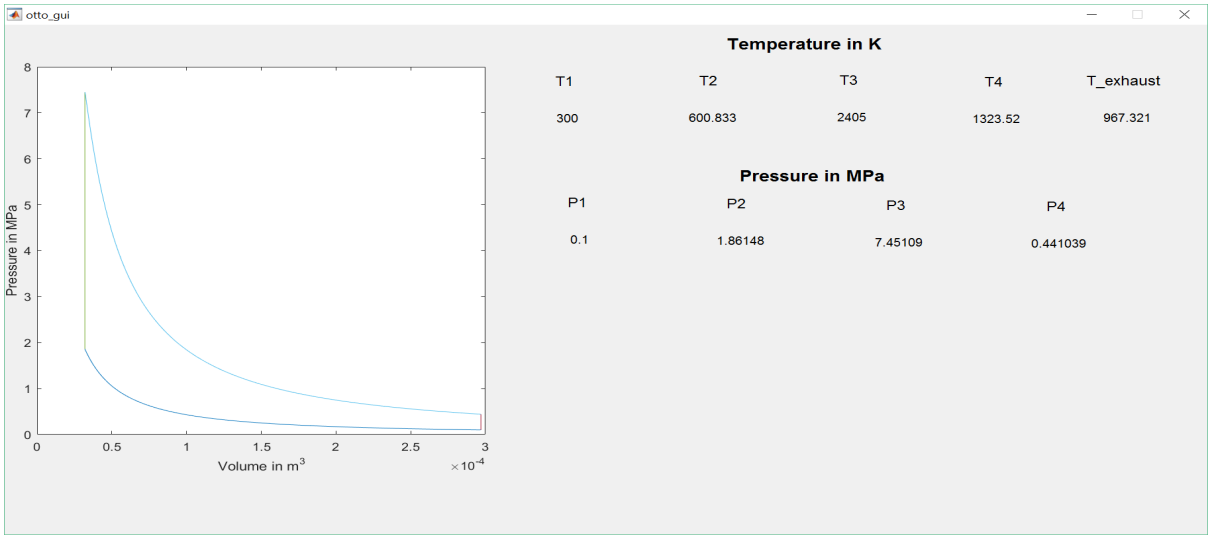

Figure 4.2: Otto Cycle Simulation Results

The theoretical exhaust temperature obtained using standard cycle shows the feasibility of dissociation and hence, a study using AVL Boost is carried out to compare methanol and dissociated methanol as fuel.

4.2 AVL Boost

In the present study, AVL Boost is used for the simulation. AVL Boost is a package of computer codes which enables the user to model and simulate the various processes of an Internal Combustion Engine.

The specifications of the engine used for this study is shown in Table 4.1.

Table 4.1: Engine Specifications

Engine Parameters	**Value**
Bore	86 mm
Stroke	86 mm
Compression Ratio	10.5
Lngth of connecting rod	143.5 mm
Spark timing	18 deg BTDC
Displacement	2.0 L
No. of cylinders	4
No. of strokes	4
Injection type	Port fuel injection
No. of valves per cylinder	2
No. of spark plugs per cylinder	1

The pre-processing steps of AVL Boost enables the user to model a 1-Dimensional engine test bench setup using the predefined elements provided in the software toolbox. The various elements are joined by the desired connectors to establish the complete engine model using pipelines.

The various configurations and parameters are set for each element. The system boundary conditions are specified. It is important to make a correct estimate of the boundary conditions as it directly affects the accuracy of the results. MPI modification is suitably incorporated into the computational model and heat of vaporization of methanol is neglected as the fuel is always in the gaseous state. Atmospheric conditions are specified as system boundary conditions.

In Fig 4.3, E1 represents the engine C1, C2, C3, C4 represent the four cylinders of the engine. MP1 to MP14 represent the measuring points, PL1, PL2 represent the plenum. SB1, SB2 are for the system boundary and the flow pipes are numbered 1 to 30. CL1 represents the intake air cleaner and R1 to R9 represent flow restrictions.

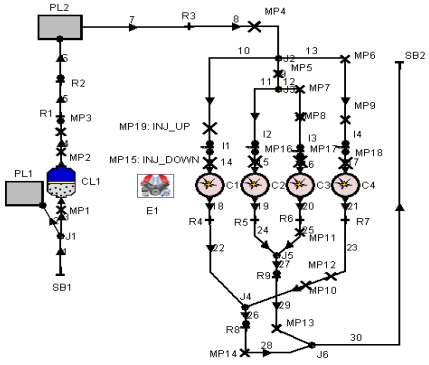

Figure 4.3: AVL Engine Testbench

Combustion

For the current study the Wiebe two zone model is selected for the combustion analysis from several options given by AVL Boost. This model divides the combustion chamber into unburned and burned gas regions [53]. The first law of thermodynamics is applied to each of the zones to predict the rate of fuel consumed with respect to crank angle. The following equations govern the Wiebe two zone model [55]:

$$\frac{dm_b u_b}{d\alpha} = -p_c \frac{dV_b}{d\alpha} + \frac{dQ_f}{d\alpha} - \sum \frac{dQ_{Wb}}{d\alpha} + h_u \frac{dm_b}{d\alpha} - h_{BB,b} \frac{dm_{BB,b}}{d\alpha} \tag{4.2}$$

$$\frac{dm_u u_u}{d\alpha} = -p_c \frac{dV_u}{d\alpha} - \sum \frac{dQ_{Wu}}{d\alpha} - h_u \frac{dm_b}{d\alpha} - h_{BB,u} \frac{dm_{BB,u}}{d\alpha} \tag{4.3}$$

where

$dm_b u_b$	Change of the internal energy in the burned zone of the cylinder
u_b	Specific internal energy (burned zone)
m_b	Mass in the burned zone
$dm_u u_u$	Change of the internal energy in the unburned zone of the cylinder
u_u	Specific internal energy (unburned zone)
m_u	Mass in the unburned zone
p_c	Cylinder Pressure
V_i	Volume of ith zone (i= b for burned and i= u for unburned zone)
$p_c \frac{dV_b}{d\alpha}$	Piston work with respect to burned zone
$p_c \frac{dV_u}{d\alpha}$	Piston work with respect to unburned zone
Q_f	Fuel Energy
Q_w	Wall Heat Loss
α	Crank angle
h_{BB}	Enthalpy of blow-by
$\frac{dQ_f}{d\alpha}$	Fuel heat input
$\frac{dQ_{Wb}}{d\alpha}$	Wall heat losses in the burned zone
$\frac{dQ_{Wu}}{d\alpha}$	Wall heat losses in the unburned zone
$h_u \frac{dm_b}{d\alpha}$	Enthalpy flow from the unburned to the burned zone
$h_{BB,b} \frac{dm_{BB,b}}{d\alpha}$	Enthalpy due to blow by in burned zone
$h_{BB,u} \frac{dm_{BB,u}}{d\alpha}$	Enthalpy due to blow by in unburned zone.

Mass Fraction Burned

To represent the mass fraction burned, the Wiebe function is chosen. The Wiebe function for mass fraction burned is shown by the equation below:

$$x_b \;=\; 1 \;-\; exp\Big[-a\Big(\frac{\theta \;-\; \theta_o}{\Delta\theta}\Big)^{m+1}\Big] \tag{4.4}$$

where

x_b	Mass fraction burned
θ_o	Start of Combustion
$\Delta\theta$	Burn Duration

a and m are constant factors depending on the fuel (a is called efficiency factor and m is called shape factor)

For this study, a complete combustion is assumed. Values of 'a' and 'm' are chosen to be 6.9 and 3 respectively [56] [57]. The shape factor affects ignition delay and initial flame development. However, the values are subject to further analysis and provides scope for future research.

In-cylinder Heat Transfer

The heat transfer to the walls of the combustion chamber is calculated from :

$$Q_{wi} \;=\; hA_i(T_c \;-\; T_{wi}) \tag{4.5}$$

where

Q_{wi}	Wall heat flow
A_i	Surface area
h	Heat transfer coefficient
T_c	Temperature of the gas in the cylinder
T_{wi}	Wall temperature

Woschni model is selected to determine the heat transfer coefficient [58].

Emissions

AVL Boost predicts NOx generated by combustion based on the model by Pattas and Hafner which incorporates the well known Zeldovich mechanism [59]. The reactions of Zeldovich mechanism is shown in Table 4.2.

Table 4.2: Reactions according to Zeldovich mechanism

	Stoichiometry	Rate $k_i = k_{0,i} \cdot T^a \cdot e^{\left(\frac{-TA_i}{T}\right)}$	k_0 [cm^3/mol s]	a [-]	T_A [K]
R1	N2 + O = NO + N	$r_1 = k_1 \cdot c_{N2} \cdot c_O$	4.93E13	0.0472	38048.01
R2	O2 +N = NO + O	$r_2 = k_2 \cdot c_{O2} \cdot c_N$	1.48E08	1.5	2859.01
R3	N +OH = NO + H	$r_3 = k_3 \cdot c_{OH} \cdot c_N$	4.22E13	0.0	0.0
R4	N2O + O = NO + NO	$r_4 = k_4 \cdot c_{N2O} \cdot c_O$	4.58E13	0.0	12130.6
R5	O2 + N2 = N2O + O	$r_5 = k_5 \cdot c_{O2} \cdot c_{N2}$	2.25E10	0.825	50569.7
R6	OH + N2 = N2O + H	$r_6 = k_2 \cdot c_{OH} \cdot c_{N2}$	9.14E07	1.148	36190.66

The rate of NOx production is estimated by using the following equation:

$$r_{NO} = C_{PPM} C_{KM} (2.0)(1 - \alpha^2) \frac{r_1}{1 + \alpha K_2} \frac{r_4}{1 + \alpha K_4} \tag{4.6}$$

$$\alpha = \frac{c_{NO,actual}}{c_{NO,equilibrium}} \frac{1}{C_{PPM}} \tag{4.7}$$

$$K_2 = \frac{r_1}{r_2 + r_3} \tag{4.8}$$

$$K_4 = \frac{r_4}{r_5 + r_6} \tag{4.9}$$

where

C_{PPM}	Post processing multiplier
C_{KM}	Kinetic multiplier
c_i	Molar concentration of ith species
r_i	Rate of ith reaction of Zeldovich mechanism

The amount of CO emissions is predicted by AVL Boost using the following equation which is taken from a model presented by Onorati et al [60].

$$r_{CO} = C_{constant}(1 - \alpha)(r_1 + r_2) \tag{4.10}$$

$$\alpha = \frac{c_{CO,actual}}{c_{CO,equilibrium}} \tag{4.11}$$

where

c_i	Molar concentration of ith species
r_i	Rate of ith reaction of the Onorati model

One of the main sources of unburned hydrocarbons is charge that escapes from the flame in the crevices provided by the piston ring grooves [61]. The process of formation of unburned hydrocarbons in the crevices is described by assuming that, the pressure in the cylinder and in the crevices is the same and that the temperature of the mass in the crevice volumes is equal to the piston temperature [62].

The mass in the crevices at any time period is given by the following equation:

$$m_{crevice} = \frac{pV_{crevice}M}{RT_{piston}} \tag{4.12}$$

where

$m_{crevice}$	Mass of unburned charge in the crevice
p	Cylinder pressure
$V_{crevice}$	Total crevice volume
M	Unburned charge molecular weight
R	Gas constant
T_{piston}	Temperature of the piston

To complete the entire system, a quasi steady, stirred reactor model is created in MATLAB. An overview of this model will be given in the next section.

4.3 M-TCR Simulation

Assumptions

Most of the computational models are based on assumptions. M-TCR is fundamentally a completely stirred chemical reactor. The following are the assumptions made for M-TCR model:

- The reactor is assumed to be quasi steady. The mass flow rate of methanol changes discretely at every time step. Based on this assumption, the reactor forecasts the conversion ratio for the next time step. This assumption is made to simplify the kinetic model and must be carefully considered by the system designer. Whenever there is a change of the logical state, the fuel mass flow rate changes drastically. In such situation, use of conversion ratio from the previous time step might not yield precise results.
- Reactions take place in a closed vessel. There is no spatial inhomogeneity in parameters such as temperature and pressure.
- A reacting system is in quasi-steady state (QSS), or quasistationary, with respect to certain species, which means that the rates of change of their concentrations are negligibly small compared to the overall rate of reaction, during some relevant time interval [63]. Also, a single step reaction is assumed.
- There are no heat losses to the surrounding. The heat transfer occurs only between alumina matrix containing the catalyst and the exhaust gases.

This study aims at examining the feasibility of methanol/syngas blends as fuel in a vehicle with on-board syngas generation using M-TCR . Hence, detailed model of the reactor is out of scope for this study. Rather, a computational model of the reactor with detailed chemical kinetics can be interesting for future investigations.

4.3.1 Governing equations

Mass Balance

$$m_{in}x \;=\; K_o e^{\frac{-E_a}{RT}} \left(\frac{P(1-x)}{1+2x}\right) W \tag{4.13}$$

where

K_o	Equilibrium constant
E_a	Activation energy in kJ/mol
T	Temperature in K
W	Weight of catalyst in kg
P	Absolute pressure of the reactor in Pa

Energy Balance

$$\begin{aligned} m_{in}x\Delta h_{f,methanol} \;-\; m_{in}x\Delta h_{f,CO} \;-2m_{in}x\Delta h_{f,H_2} \;=\; m_{in}(1-x)C_{p,methanol}\Delta T \;+ \\ +\; 2m_{in}xC_{p,H_2}\Delta T \;+\; m_{in}xC_{p,CO}\Delta T \;+\; m_{exhaust}xC_{p,exhaust}\Delta T \end{aligned} \tag{4.14}$$

where

$\Delta h_{f,j}$	Specific enthalpy of formation of jth species
ΔT	Temperature difference between inlet and outlet of respective streams
x	Conversion ratio of methanol to syngas

4.3.2 Computational Model

The schematic diagram of the M-TCR is shown in Fig. 4.4. The cold stream is marked in blue and hot stream is marked in red. Minimum temperature difference at pinch point is assumed to be 20 K.

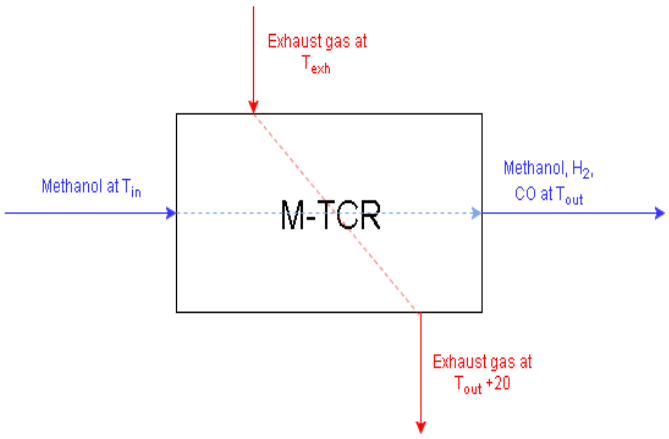

Figure 4.4: Schematic diagram of the M-TCR

It is observed from previous studies that a catalyst increases the conversion ratio of methanol

to syngas considerably at lower temperatures [64] [65]. Hence, a precious metal based catalyst data obtained from HyDragon is used in this study [66]. A thermodynamic model is built using this data with the help of Chemical Engineering Department at IST. Results from this model is compared with experimental results obtained by HyDragon and is shown in Fig 4.5.

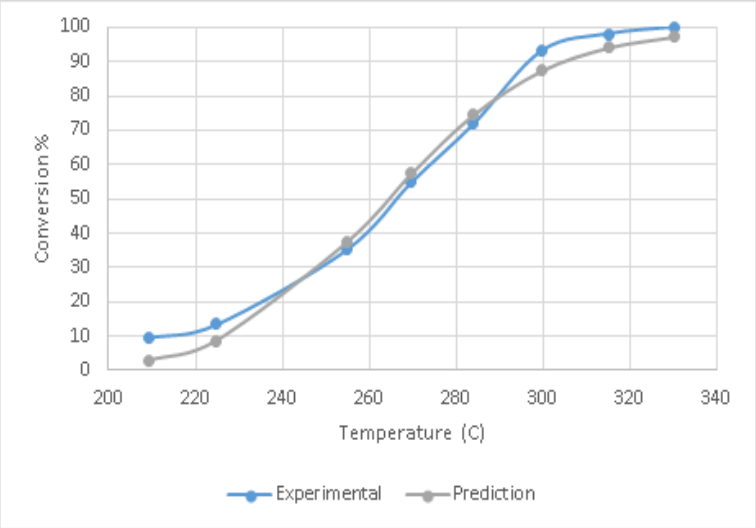

Figure 4.5: Comparison between experimental data and computational results for a space velocity of 5900 ml/h $g_{catalyst}$ of methanol

It is very important to account for the thermal inertia of the M-TCR matrix. Therefore, an alumina matrix with a weight of 0.5 kg is considered for this study. The following sequence is considered for the energy exhange in M-TCR.

1. The matrix is at a given temperature.
2. The reaction of methanol to syngas occurs which absorbs heat from the matrix and the temperature of the matrix drops.
3. Now, there is a difference of temperature between exhaust gas and matrix which acts as a driving force. Heat transfer occurs from exhaust gas to matrix and the matrix temperature rises.

This energy balance occurs at every time step and it is assumed that there is no spacial temperature inhomogeneity with in the matrix. It should be noted that usually the thermal conductivity of the matrix is low and this fact should be considered by the designer.

4.4 Powertrain Integrator

Powertrain integrator is built in MATLAB to integrate engine duty cycle, maps obtained from AVL Boost and M-TCR model. Any vehicle spends significant amount of time at idle and fuel cut-off condition during any drive cycle. Therefore, it is considered important to differentiate the data received from the engine duty cycle into three domains. The engine duty cycle consists

of torque, engine speed, vehicle speed and manifold air pressure. The tool reads the engine duty cycle data and then follows the sequence below.

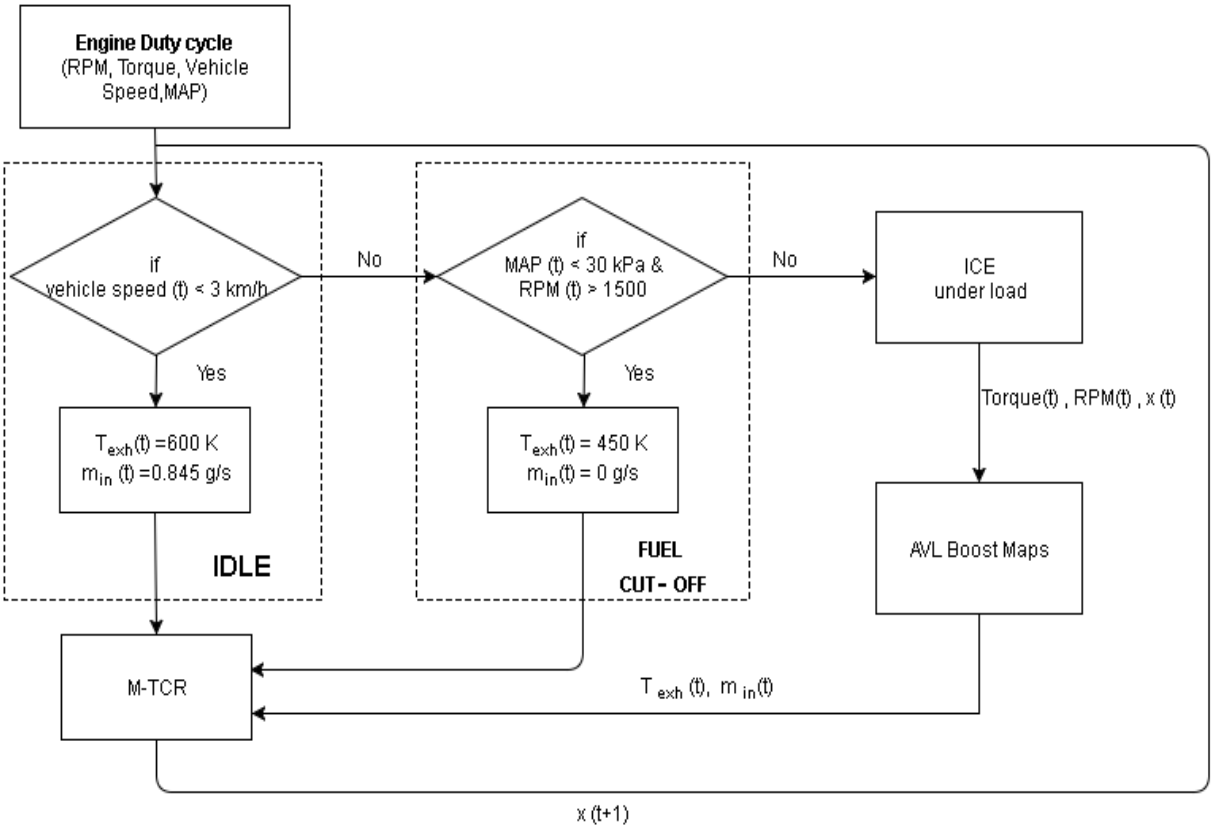

Figure 4.6: MATLAB Tool flowchart

This process continues until the termination time determined by the user or until the end of the engine duty cycle is reached. The values for exhaust temperature and fuel mass flow in case of idle conditions is obtained from previous literature [53] [67]. In case of fuel cut-off, the engine has no fuel and it is assumed that the air attains the average temperature of the cylinder walls [68] . After understanding the processes behind the tool, next chapter is dedicated to analyse and discuss the results obtained using this tool.

5 Results and Discussions

In the present investigation, the results are obtained on a virtual engine test bench and for three engine duty cycles representing an actual vehicle run. Based on these facts, the results are divided into two broad sections namely, engine simulation results and engine duty cycle results.

5.1 Engine Simulation Results

The concept of using methanol as a fuel and a reactant for thermo-chemical recuperation(TCR) is tangible theoretically and it is seen from Table 3.1 that there is an increase of 20.7 % in the energy content per unit mass by dissociating methanol using low grade waste heat. However, to check its feasibility on a engine, simulations are carried out using different blends of methanol and syngas (0, 25, 50, 75, 100 % by volume of methanol represented by M0, M25, M50, M75 ans M100 respectively) on AVL Boost. Engine performance and emissions maps are built at constant throttle positions. The procedure used for obtaining engine maps is explained in APPENDIX.

Engine Maps

Engine performance and emission maps are generated using a virtual engine test bench on AVL Boost. In this subsection, the maps obtained for different blends are illustrated.

BSFC

BSFC maps obtained for different blends are shown in Fig. 5.1 - 5.3. The dashed red lines correspond to different throttle positions and are shown for reference only. Therefore, they are not included in the legend. The focus here is on the iso-BSFC lines which get denser at lower loads [53]. In all cases, the lowest value of BSFC is seen around the region of peak load with the values increasing with decrease in load. This implies that the overall efficiency of the engine decreases with decrease in load at a given RPM. Similar results were obtained by Brusstar et al. for neat alcohol fuels, Vancoillie et al. for methanol and Shah et al. for syngas [69] [49] [70].

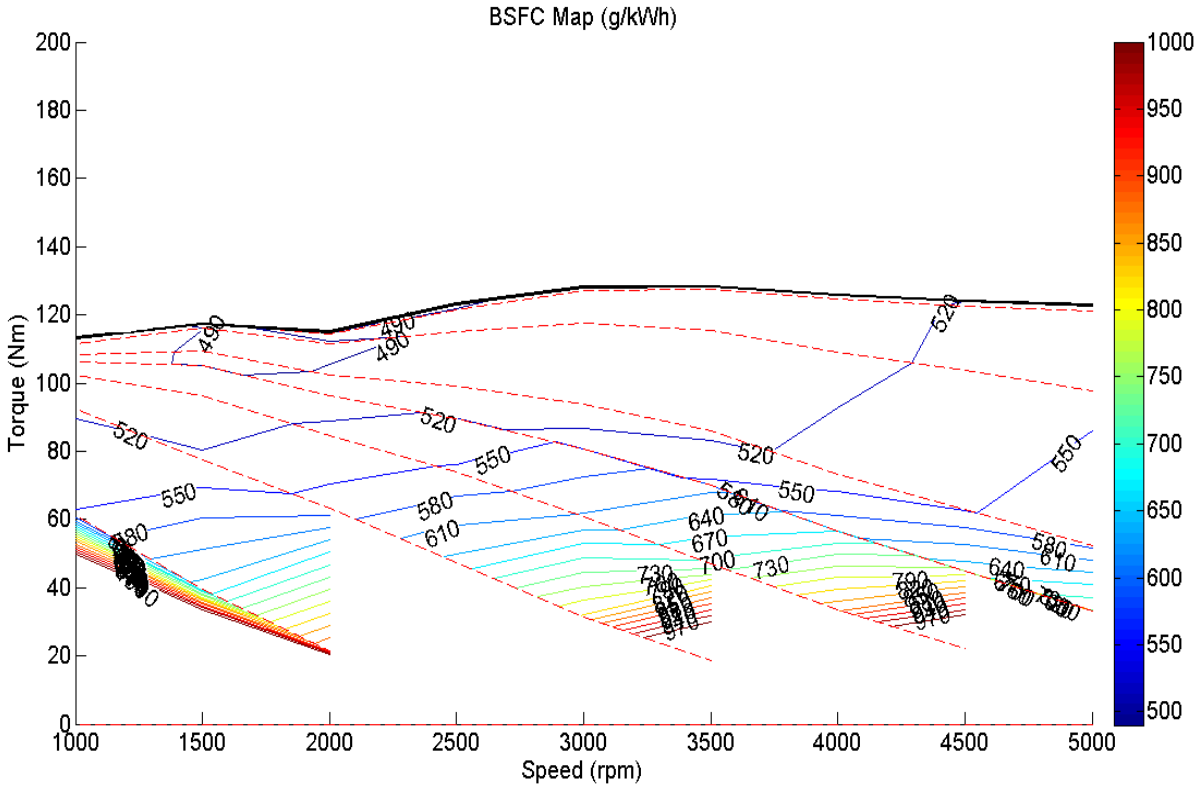

Figure 5.1: BSFC map for M0

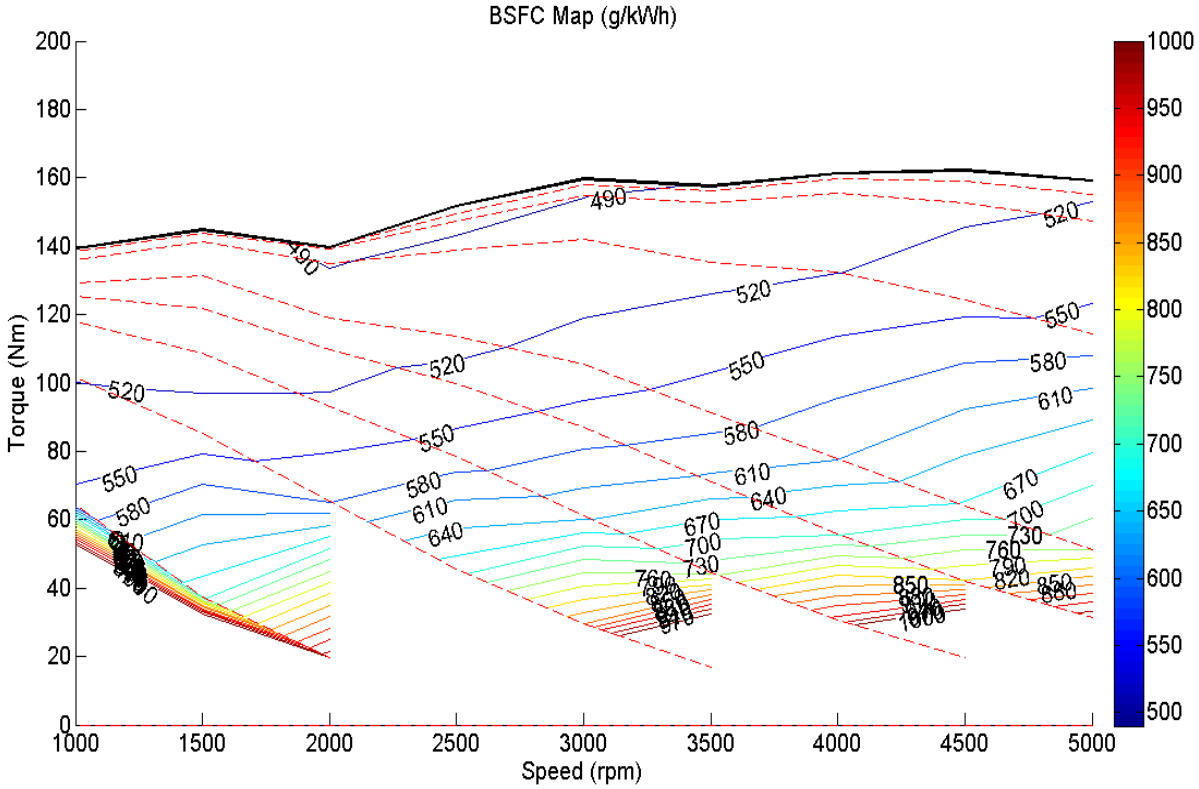

Figure 5.2: BSFC map for M50

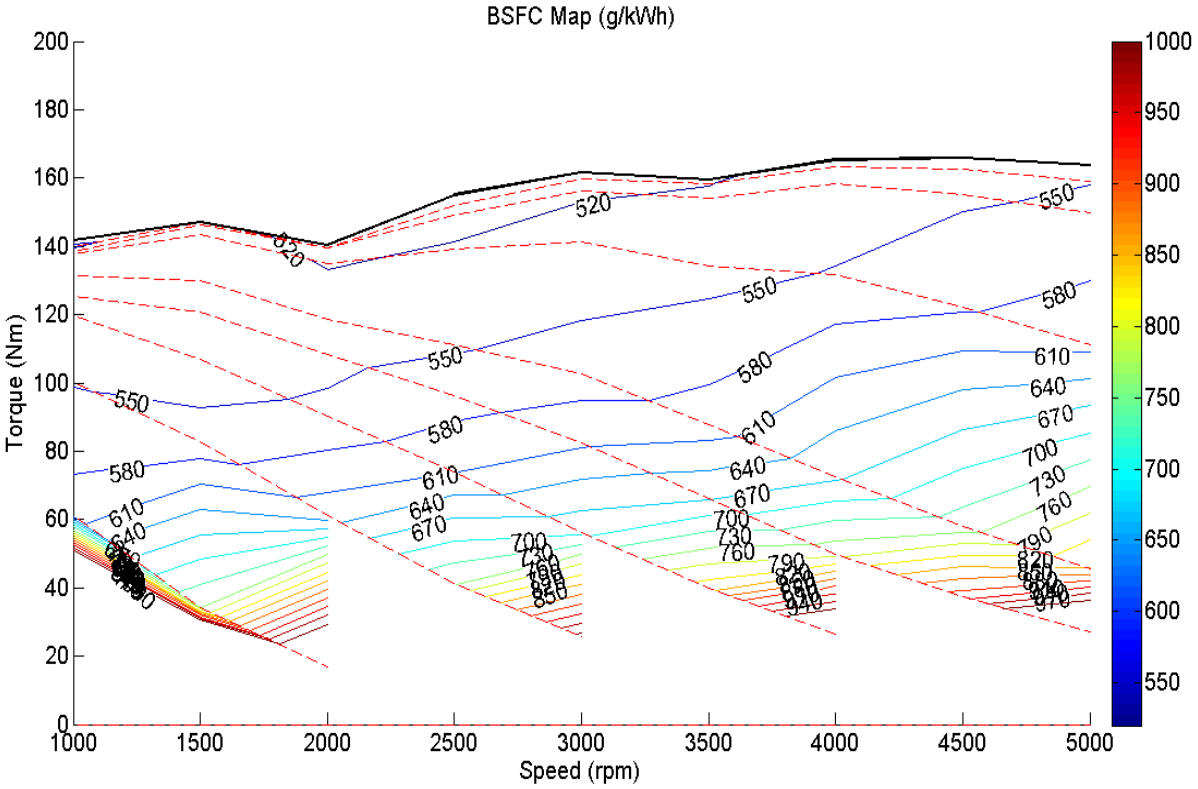

Figure 5.3: BSFC map for M100

Exhaust Gas Temperature

Exhaust gas temperature is an important parameter required for this study as the heat in exhaust is used to dissociate methanol. The change of exhaust gas temperature is more pronounced with the increase in RPM. Even though the exhaust gas temperature increases with increase in load, it is more sensitive to increase in engine speed. These results are in line with previous experimental results on Audi engine by Vancoillie et al. at University of Gent [71]. Isothermal lines for different fuel blends are illustrated in Fig. 5.4 - 5.6.

Mass flow of Fuel

Another important parameter for the M-TCR model is the fuel mass flow rate. Fuel mass flow rate increases with increase in load and speed. This fact is reinforced for both methanol and isooctane by Ebersole and Manning [72]. It is very obvious that in an SI engine with constant AFR, as the mass of air flow per second increases, the amount of fuel injected also increases proportionally. Comparison between different fuel blends at constant speed and at constant load will be explained later. Fig. 5.7- Fig. 5.9 illustrates the fuel flow map for different speed and torque conditions.

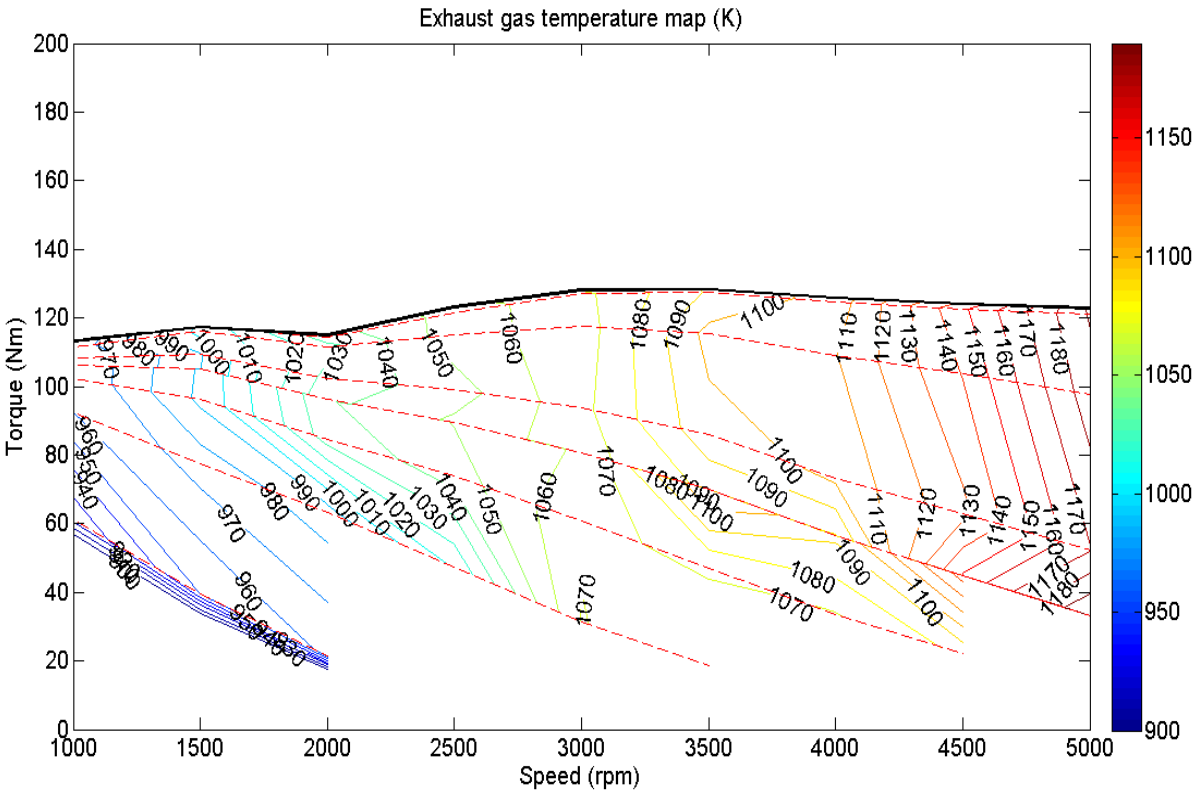

Figure 5.4: Exhaust gas temperature map for M0

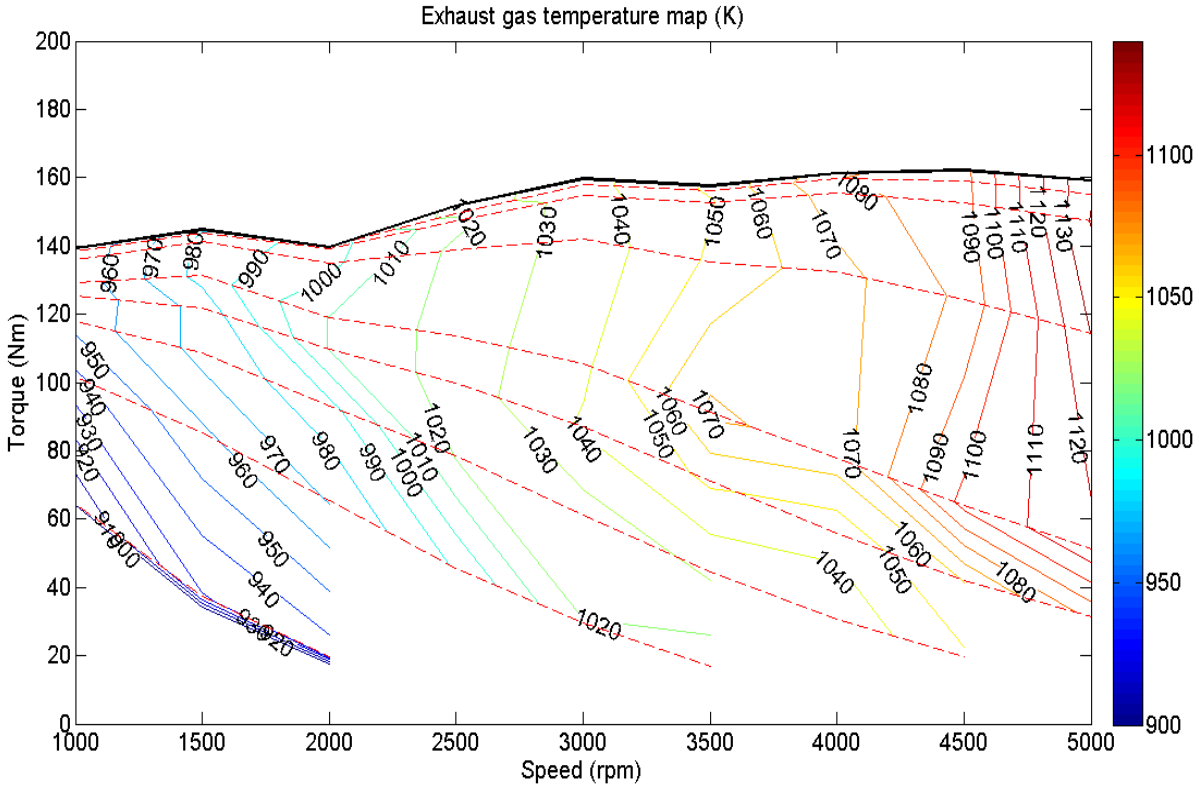

Figure 5.5: Exhaust gas temperature map for M50

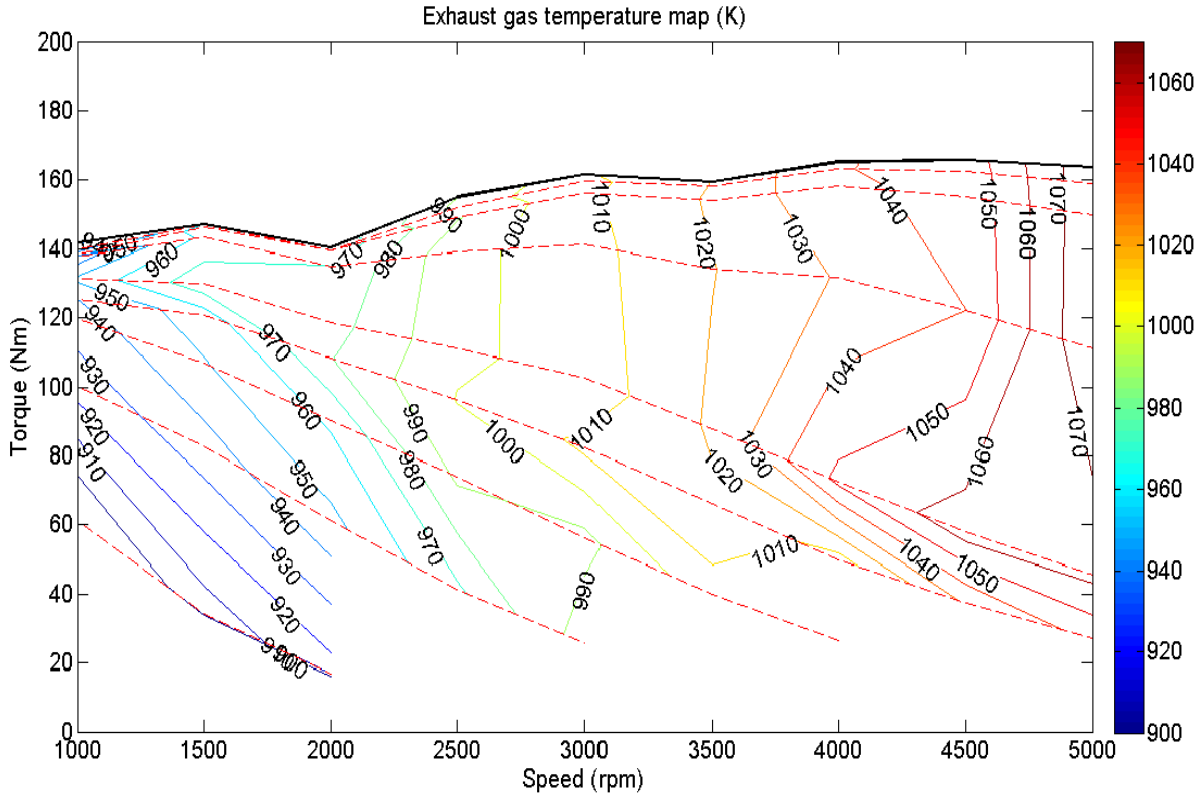

Figure 5.6: Exhaust gas temperature map for M100

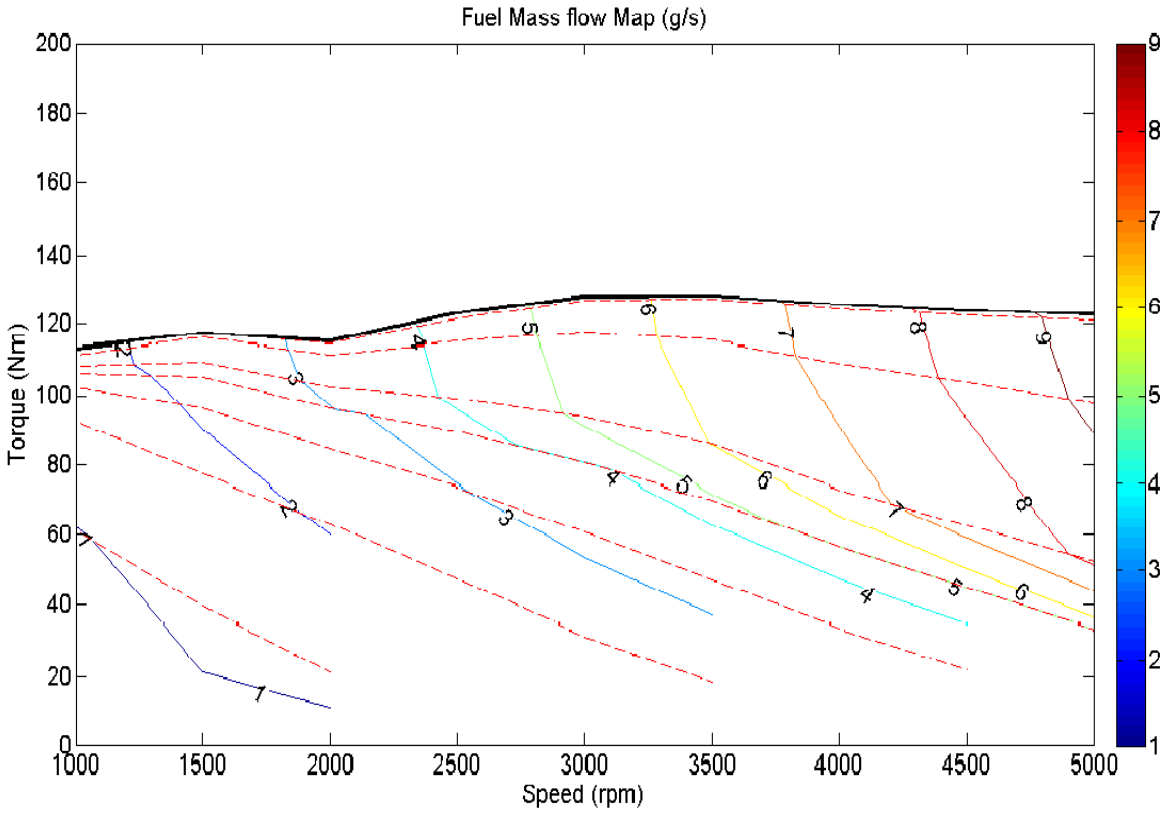

Figure 5.7: Fuel consumption per second for M0 blend

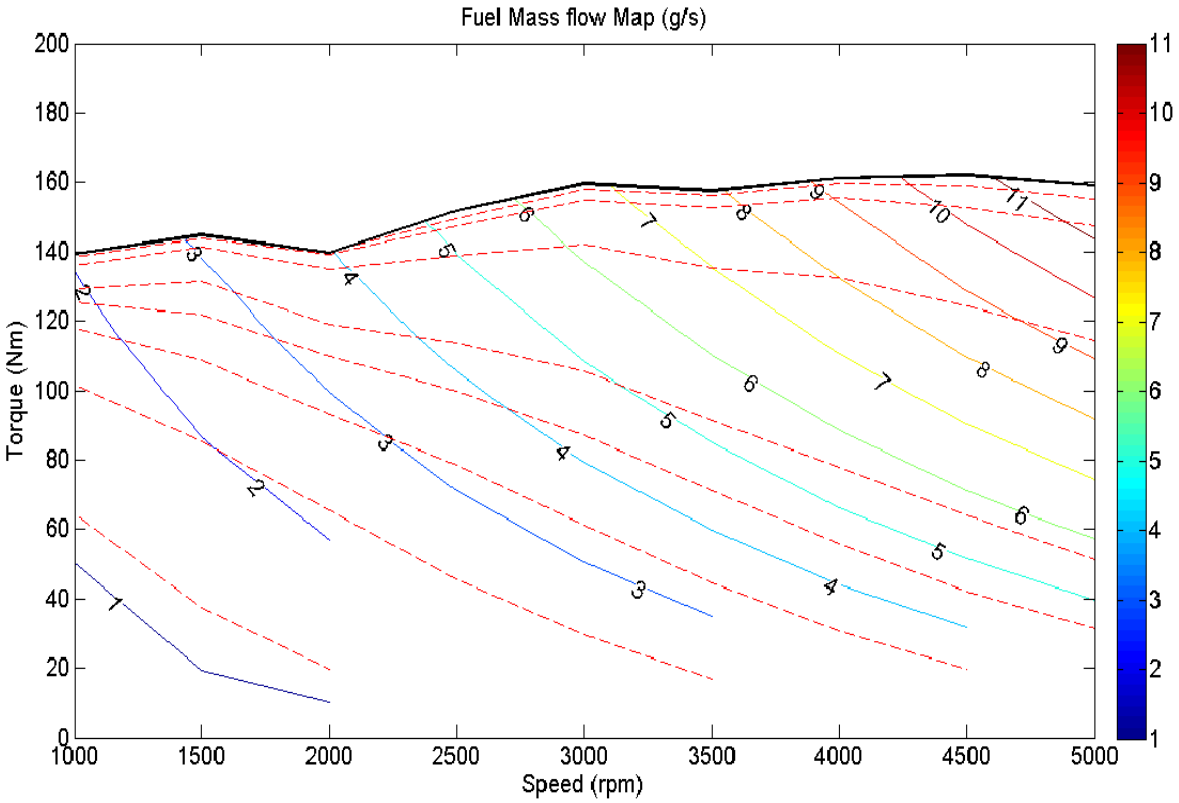

Figure 5.8: Fuel consumption per second for M50 blend

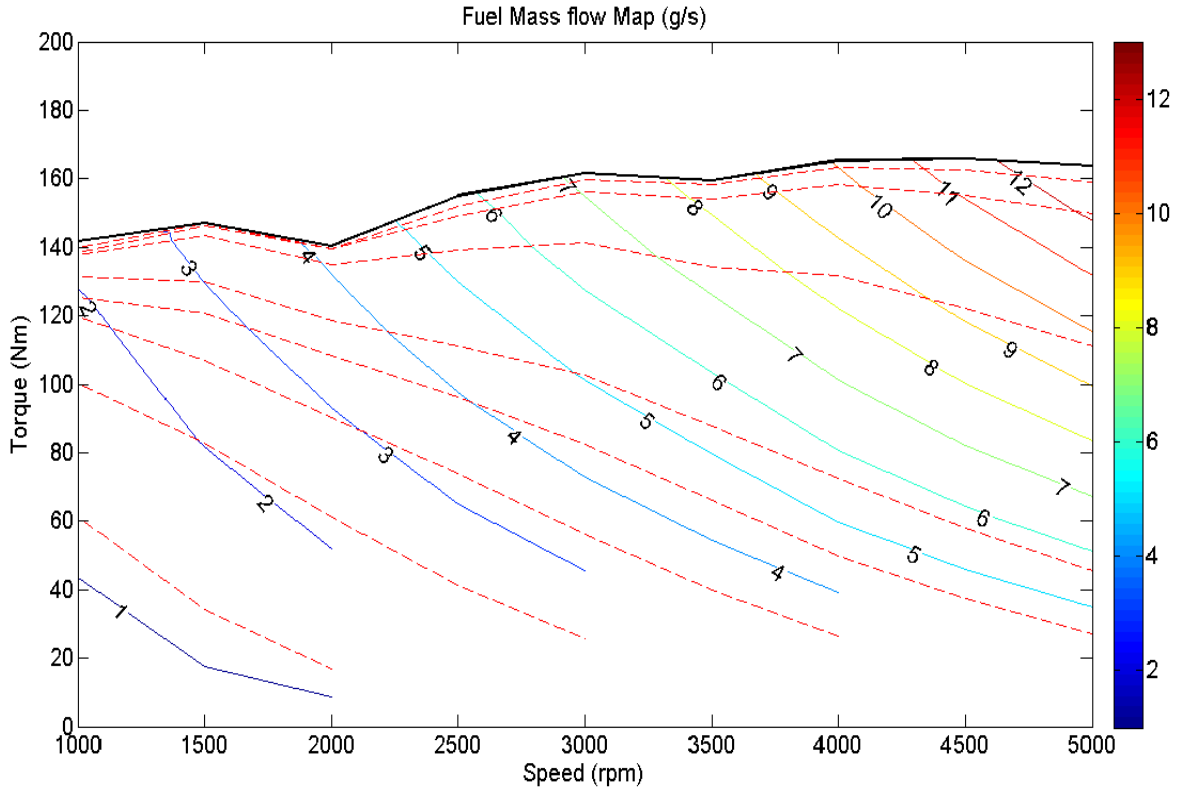

Figure 5.9: Fuel consumption per second for M100 blend

Emission maps

The mass flow rate of CO emissions increases with increase in speed due to higher number of cycles per second. There is a slight increase in the mass flow rate of CO emissions with increase in load due to the increase of the amount of fuel burned. However, if the brake specific CO emissions is considered, the value remains almost constant as the engine is operated at fixed stoichiometric ratio. Similar trend was obtained by researchers earlier [72]. CO emission maps are considered in this study as the tests will be further carried out on a vehicle. Fig. 5.10- 5.12 illustrate the CO emission maps. The mass flow rate of HC emissions increase with increase in speed and load. Fig. 5.13-5.15 show HC emission maps. The mass flow rate of NOx emissions increase with respect to speed and load. Fig. 5.16-5.18 illustrate NOx emission maps. NOx maps are generated for the purposes of calculating emissions on a vehicle under different traffic conditions which will be studied in the next section.

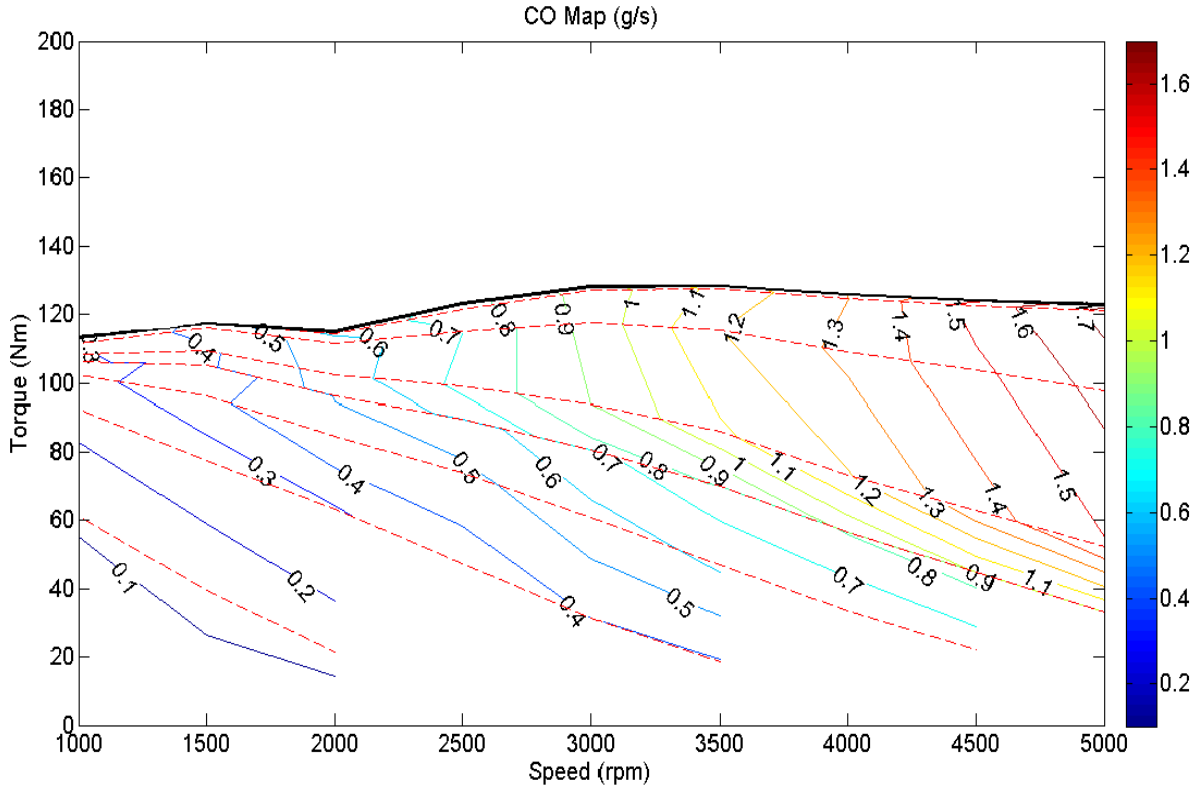

Figure 5.10: CO emission map for M0

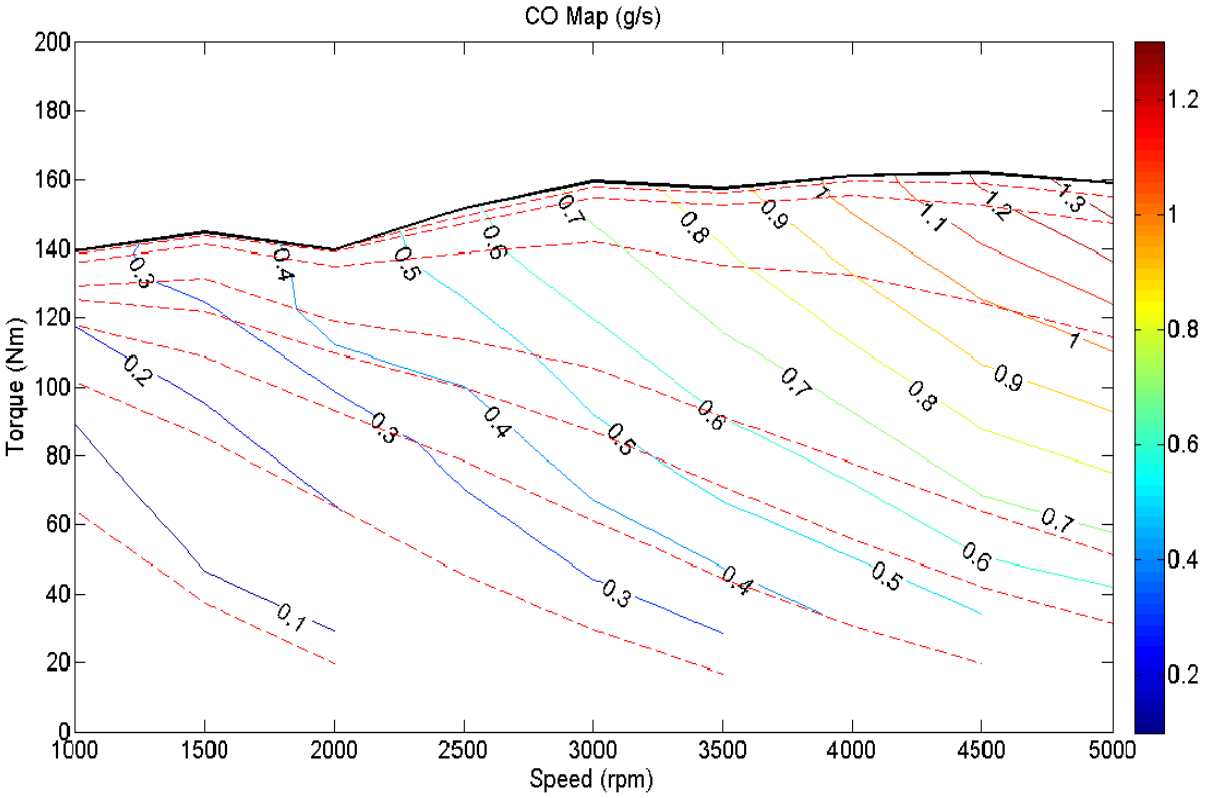

Figure 5.11: CO emission map for M50

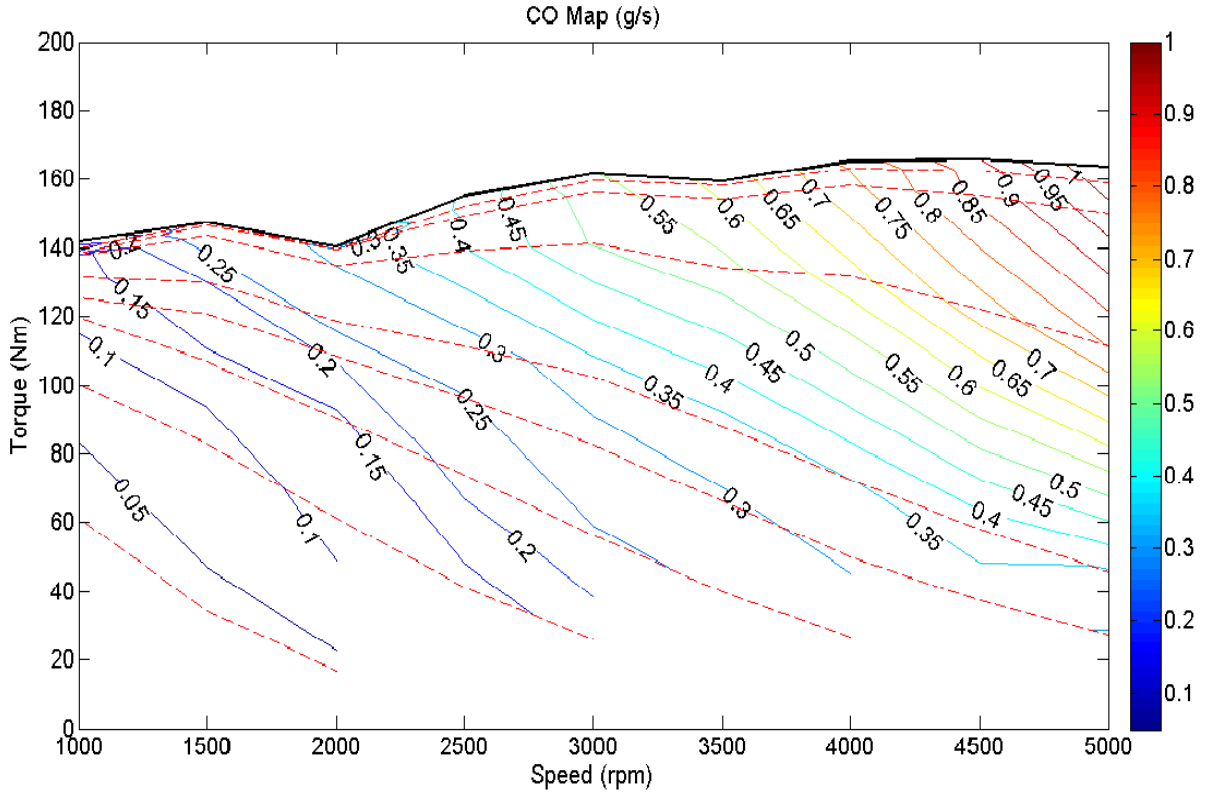

Figure 5.12: CO emission map for M100

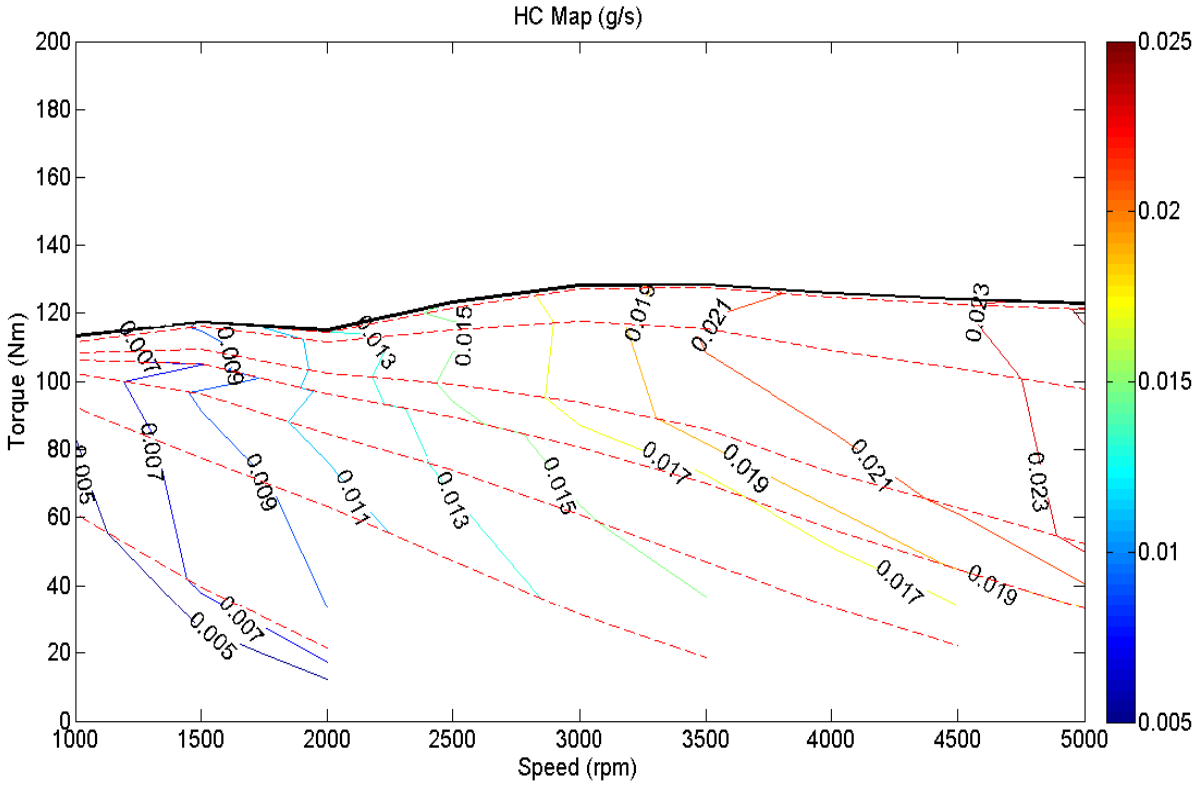

Figure 5.13: HC emission map for M0

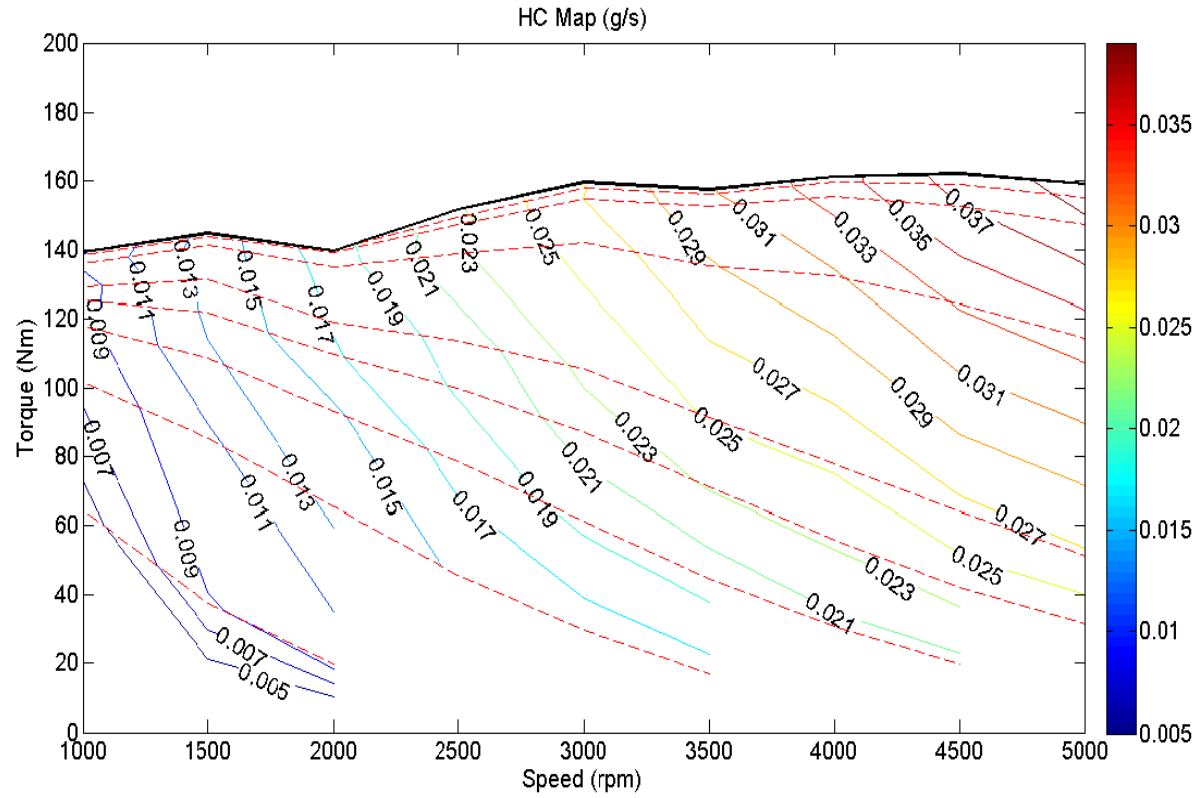

Figure 5.14: HC emission map for M50

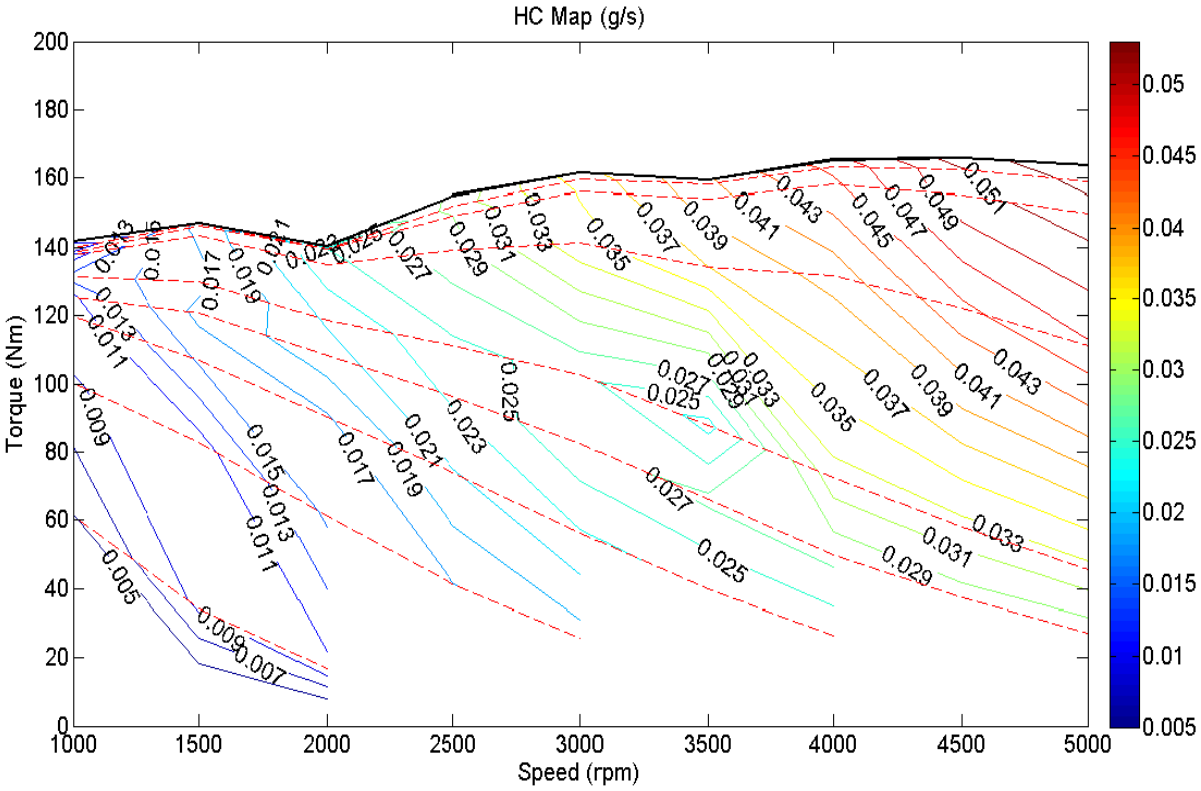

Figure 5.15: HC emission map for M100

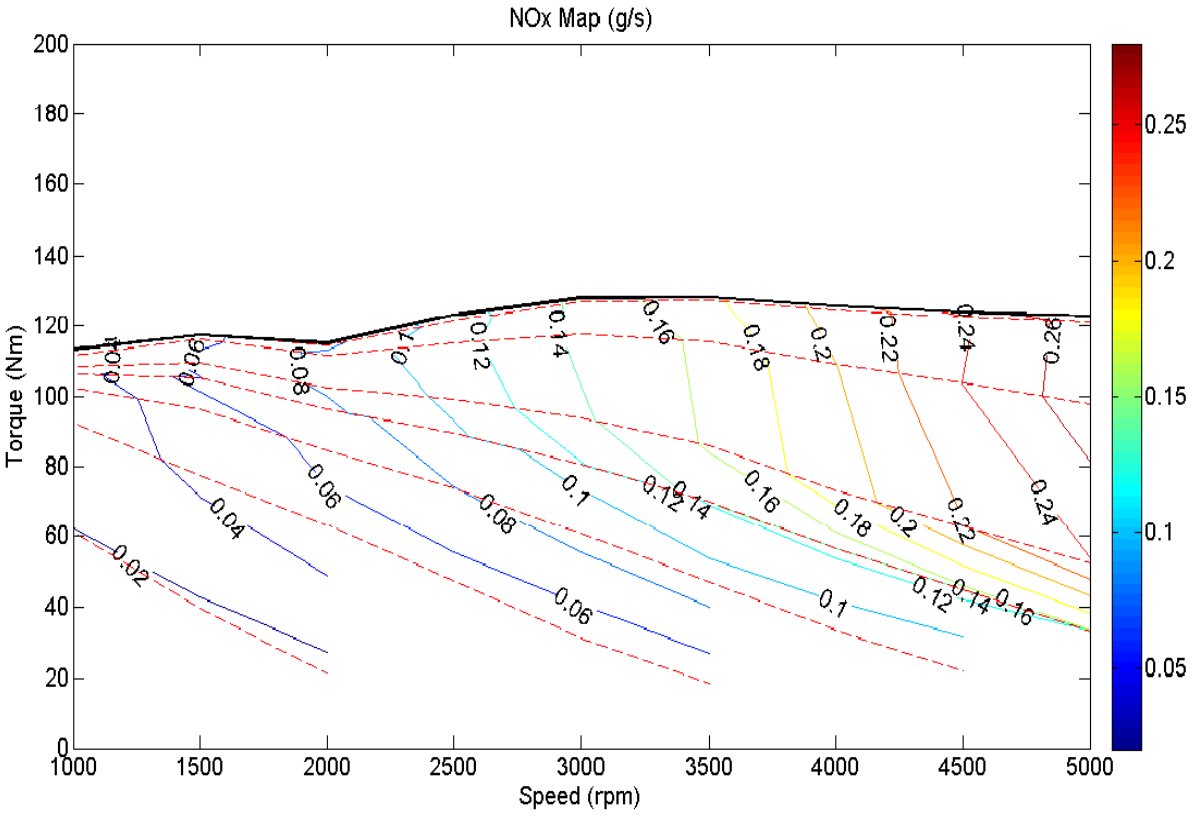

Figure 5.16: NOx emission map for M0

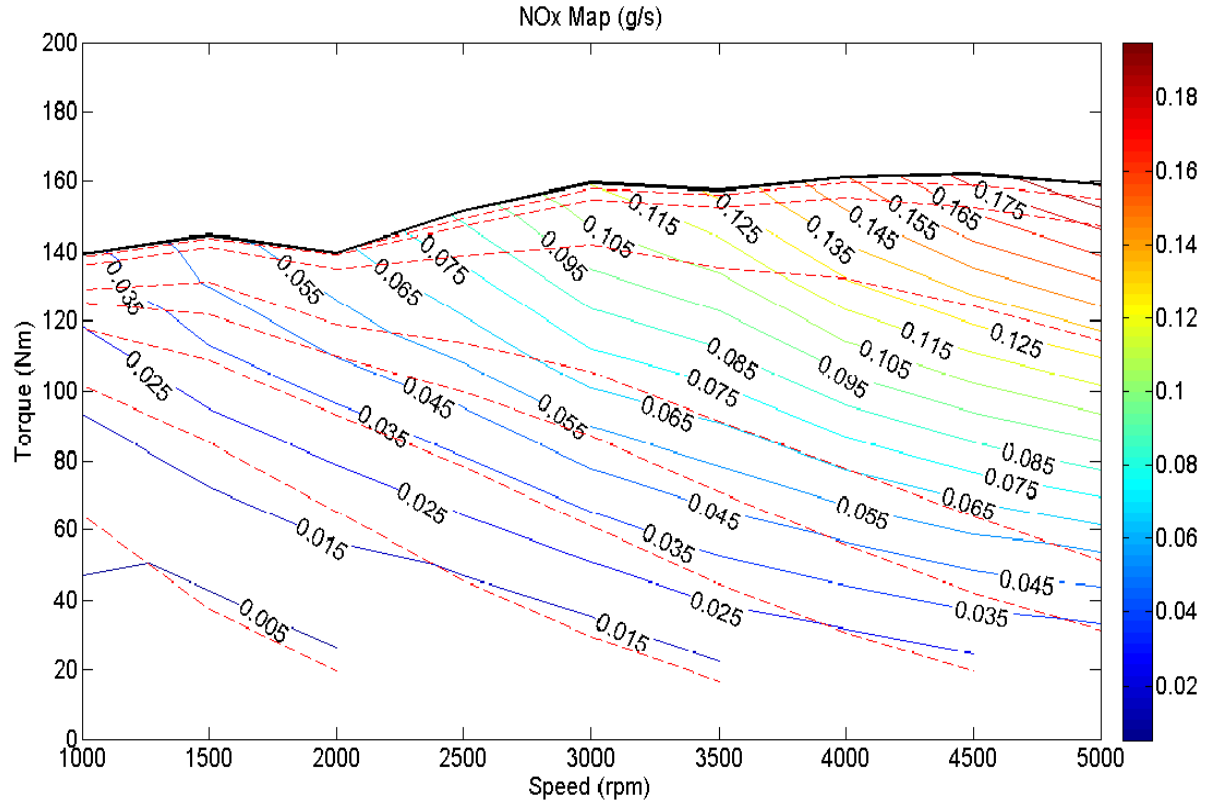

Figure 5.17: NOx emission map for M50

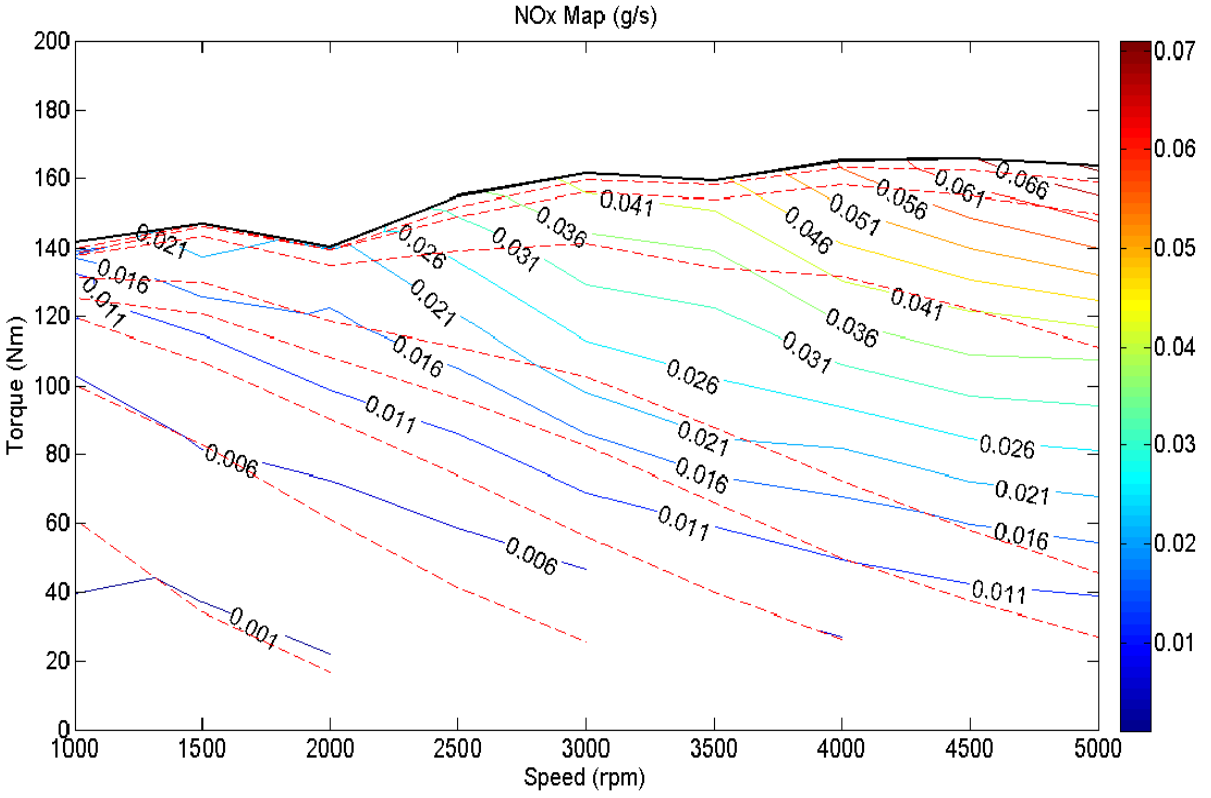

Figure 5.18: NOx emission map for M100

It is interesting to obtain results from these maps for the cases of constant load and constant speed to compare the blends under study.

Constant Torque

The tests are carried out on a virtual engine test bench for different engine speeds at a constant torque of 60 Nm.

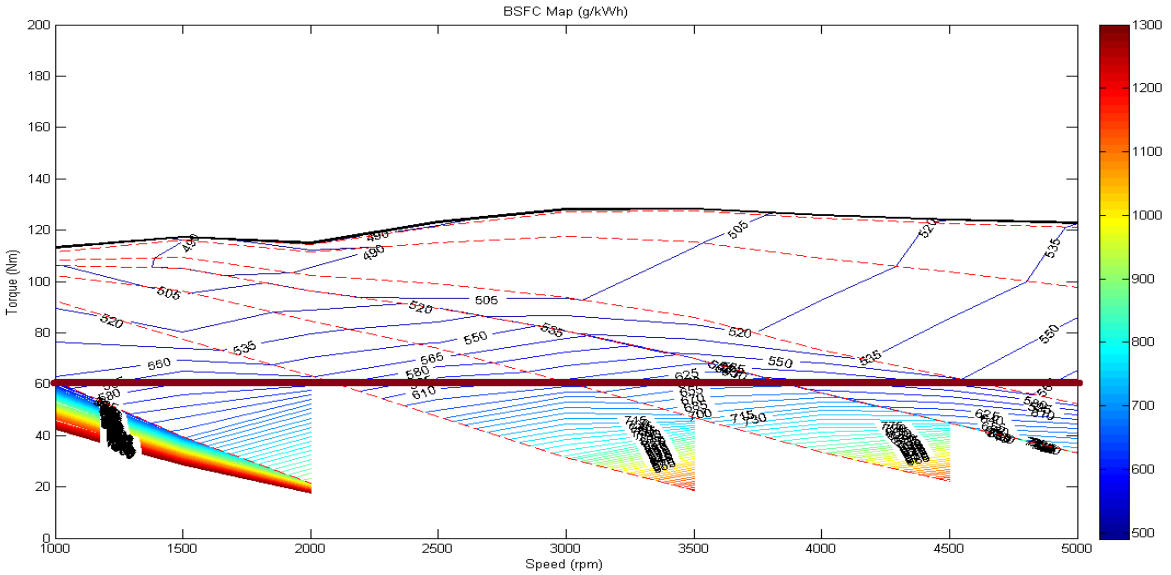

Figure 5.19: Constant Torque of 60 Nm on a BSFC map

The value of torque chosen is based on mean torque requirement during a two-way trip between two cities involving urban, sub-urban and highway driving conditions [67]. The results are shown in figures below.

BSFC

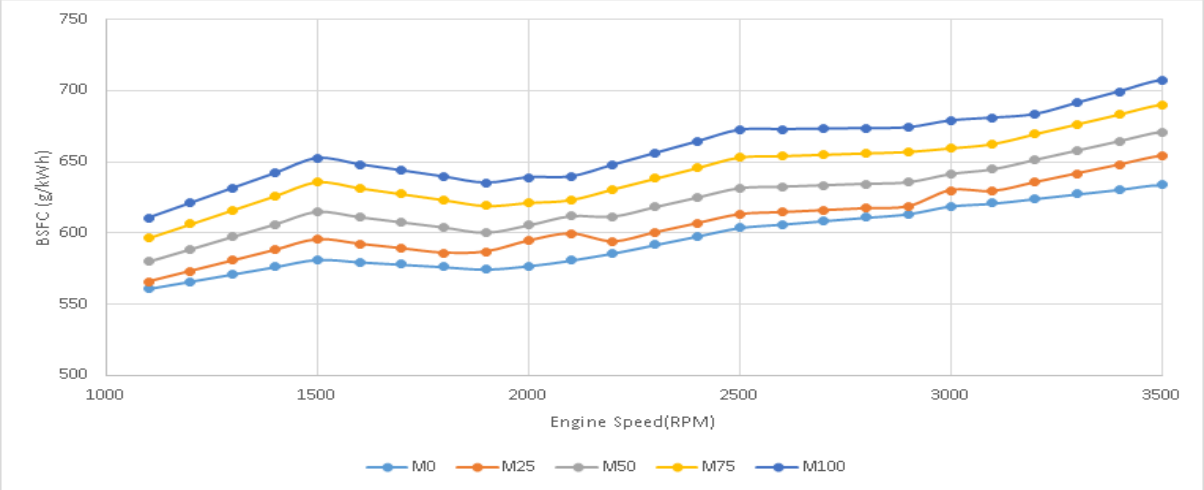

Figure 5.20: BSFC of different blends at torque of 60 Nm

It is clearly seen that with the increase in concentration of syngas, the BSFC decreases. Higher the rate of conversion obtained in M-TCR, lower is the fuel consumption of the vehicle per unit energy output. The two plausible reasons for this effect is the higher heat content of the fuel and the ratio of operating load to the full load at that engine speed for the chosen fuel composition. This ratio is higher for M0 than M100. It is a known fact that part load efficiency increases with increase in load. According to O.A. Kutlar et al., indicated thermal efficiency varies between 20 % to 40 % in this range of part load [73]. These results were corroborated by another study on gaseous fuels by Bauer and Forest. In their investigation, the researchers found a substantial decrease in BSFC values between 35 % and 50 % of peak load [74]. This effect is also seen in the present study.

CO emissions

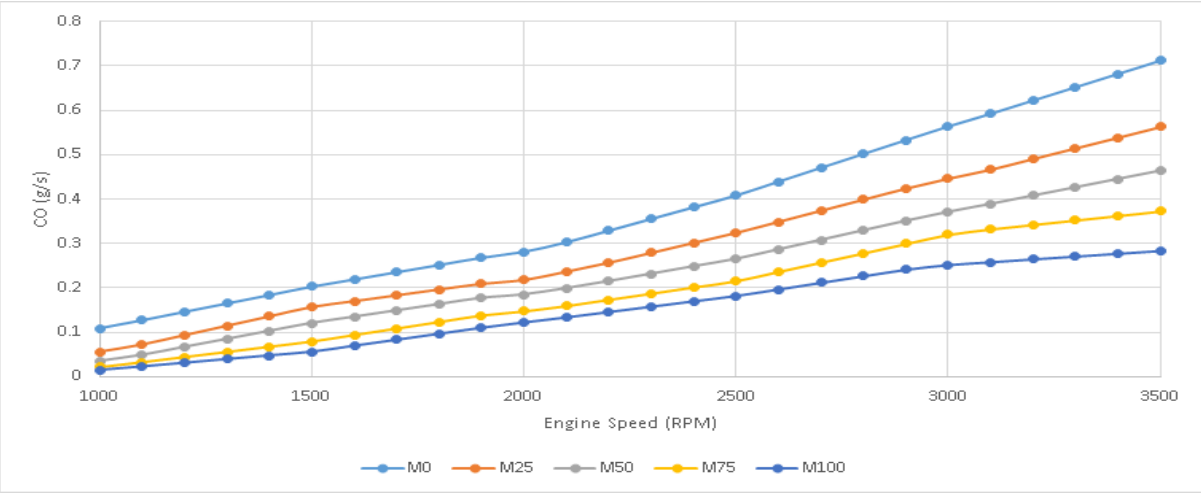

Figure 5.21: CO emissions of different blends at torque of 60 Nm

CO emissions is a strong function of equivalence ratio [75]. Since the engine is running at stoichiometric conditions, there is slight increase in CO emissions awith increase in engine speed due to insufficient mixing time leading to incomplete combustion and higher engine cycles per second. Furthermore, unburned CO from dissociated methanol adds more CO to the exhaust gas stream. So, the two sources of CO in the present study are [76]:
- Unburned CO emissions from dissociated methanol
- Incomplete combustion of methanol .

With the increase in concentration of CO in the fuel, the first effect becomes highly significant and the second effect decreases in importance. This was also seen in previous studies [77]. The researchers also state that when the concentration of H_2 is higher, there is a possibility of creation of local oxygen starvation around CO due to higher stoichiometric air-fuel ratio of hydrogen and methanol. Added to this, hydrogen has significantly higher laminar flame speed [52]. This may lead to differences in flame propagation across different fuels leaving CO oxygen starved and leading to an increase in CO emissions which is clearly seen in Fig. 5.21.

HC emissions

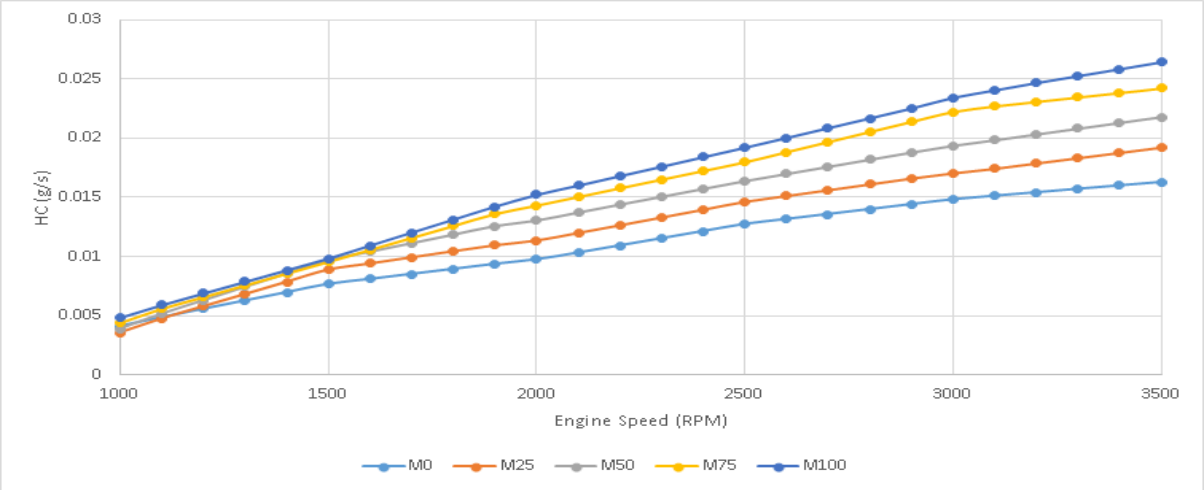

Figure 5.22: HC emissions of different blends at torque of 60 Nm

Similar to CO emissions, HC emissions increase at higher speeds due to lack of sufficient time for complete combustion and higher engine cycles per second. With increase in concentration of syngas, amount of H-C bonds decrease leading to lower unburned hydrocarbon emissions. Similar trend was observed by Yamaguchi et al. and König et al. [33] [37] .

NOx emissions

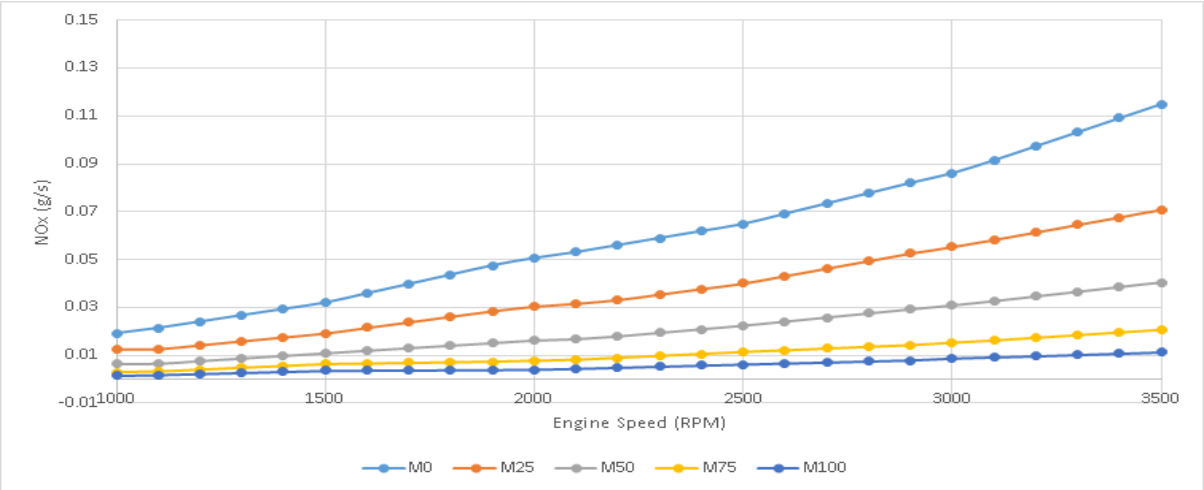

Figure 5.23: NOx emissions of different blends at torque of 60 Nm

Nitrogen oxide (NOx) emissions come primarily from two sources, fuel NOx formation and thermal NOx formation. Prompt NOx formation is responsible for a smaller fraction of NOx emissions. Since the fuels under consideration does not contain any nitrogen, possibility of fuel NOx is completely eliminated. Thermal NOx emissions are mainly affected by the equivalence ratio, peak temperature, ignition timing and oxygen concentration in the fuel [78]. In the present study, equivalence ratio, ignition timing and oxygen concentration are unchanged. Hence, the variable that affects the NOx emissions to a great extent is the peak temperature of each Otto

cycle. Therefore, it is important to look at adiabatic flame temperature of H_2, CO and MeOH. Table 5.1 compares the adiabatic flame temperatures of the three fuels in air at stoichiometric condition.

Table 5.1: Adiabatic Flame Temperature of the three fuels studied

Fuel	Adiabatic Flame Temperature (K)	Source
MeOH	2222	[79]
CO	2250	[80]
H_2	2377	[81]

From the above table, it is clear that at higher concentration of H_2, NOx emissions are higher. This fact has been reinforced by previous experimental studies by the author in methane-hydrogen blends [82]. Similar trend was seen in another study by Hoekstra et al. [83].

The results obtained from different constant loads can be summarized from Fig. 5.24.

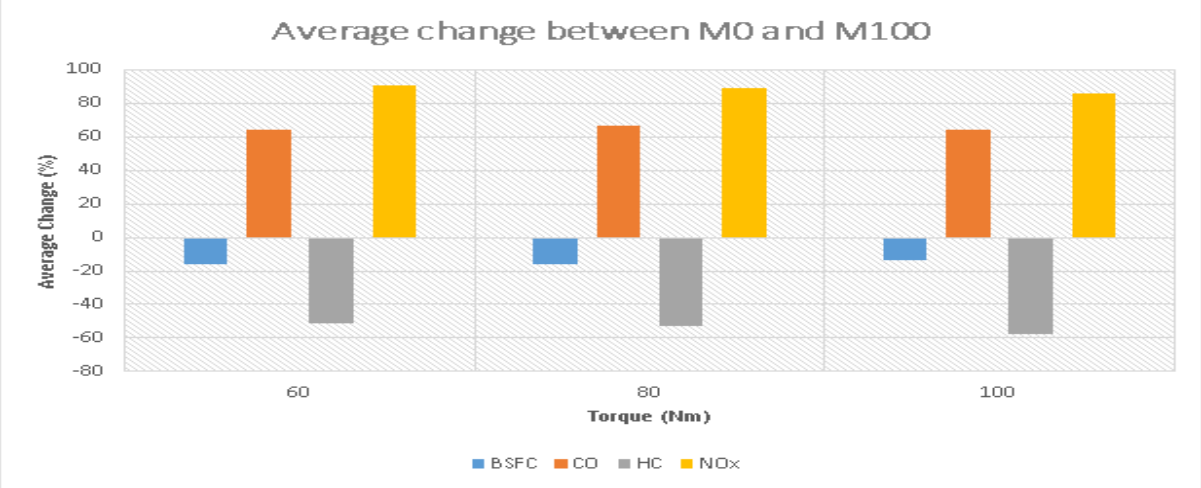

Figure 5.24: Average change of BSFC and emission of CO, HC and NOx emissions between M0 and M100 for different torque levels

A positive number implies that M0 has higher numerical value than M100 and vice versa. With the increase in load from 60 Nm to 100 Nm, the change in BSFC among two blends decreases from 16 % to 14 %. The change is not very substantial. This value is lower than the expected value of about 20 % possibly due to the assumptions made during definition of heat release rate in AVL Boost. AVL Boost has physical and chemical properties of fuel but not the heat release data. This is input based on previous literature for methanol and same data is used for syngas. This simplifies the problem to a great extent due to lack of experimental data of methanol-syngas blends. When such studies are performed experimentally, there is a possibility of obtaining lower BSFC than simulation results and is beyond the scope of present study. A trend similar to 60 Nm load is obtained even at higher loads for CO, HC and NOx emissions.

This system can be further optimized. A variable compression ratio engine with methanol as a fuel and TCR reactant provides scope for future research in this domain. The octane rating of syngas is higher than methanol and hence, a higher CR engine can be used. This study is restricted to a constant CR engine and further focus will be streamlined to check feasibility of the proposed concept.

Constant Speed

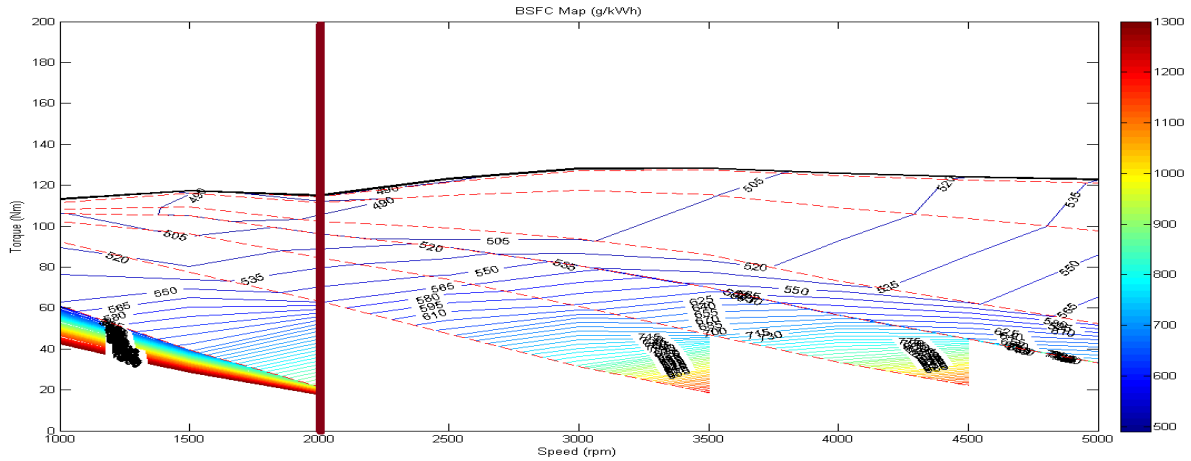

Figure 5.25: Constant speed of 2000 rpm illustrated on a BSFC map

Another set of tests are carried out on virtual engine test bench at constant engine speed of 2000, 3000 and 4000 RPM. These tests are to show the utility in the power generation sector. It is interesting to analyze the Brake specific (BS) exhaust emissions for conditions of constant speed. Emission results obtained from the tests obtained at 2000 RPM are shown in Fig. 5.26-5.28

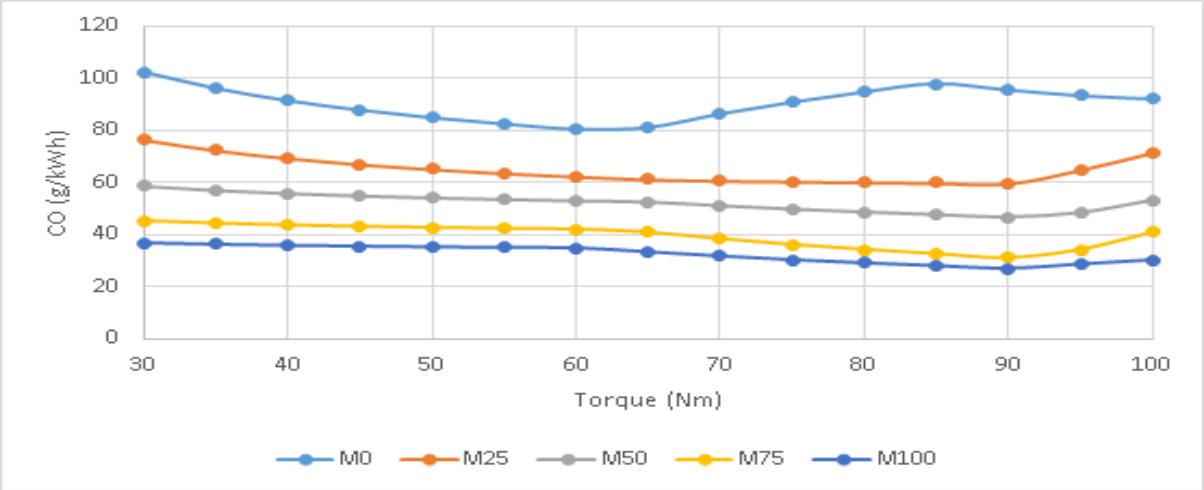

Figure 5.26: Brake specific CO emissions for constant speed of 2000 RPM

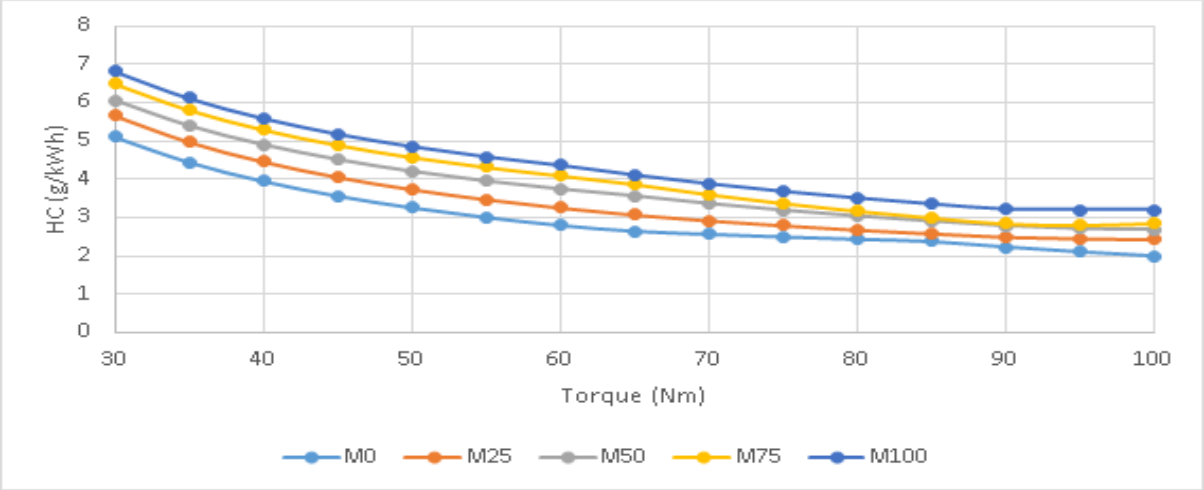

Figure 5.27: Brake specific HC emissions for constant speed of 2000 RPM

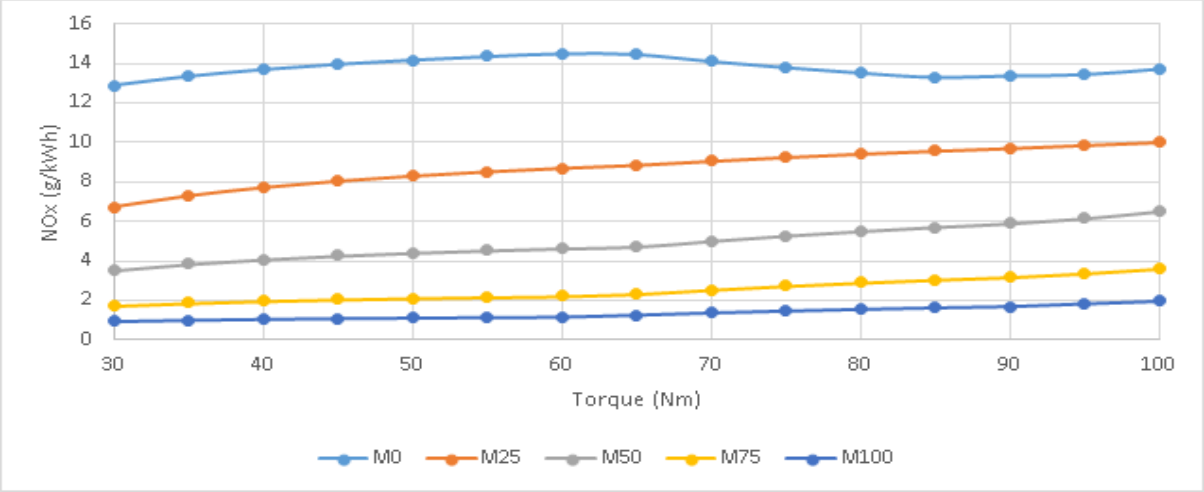

Figure 5.28: Brake specific NOx emissions for constant speed of 2000 RPM

CO emissions

At constant speed, BSCO emissions remain almost constant with increase in load. As mentioned earlier, CO emissions is a strong function of AFR and since it is constant for the tests performed, BSCO emissions also remain constant.

HC emissions

BSHC emissions decrease with increase in load at constant speed. Higher loads are likely to affect several of the HC formation mechanisms, the in-cylinder mixing of unburned hydrocarbons which escape combustion with the bulk gases, and the fraction of the in-cylinder HC which escape into the exhaust [53].

NOx emissions

BSNOx emissions remain almost constant. However, it is important to note that with increase in load, overall NOx emissions increase . This is in agreement with results obtained by Heywood et al. [84] . The results obtained from different constant speed cases is summarized in Fig. 5.29.

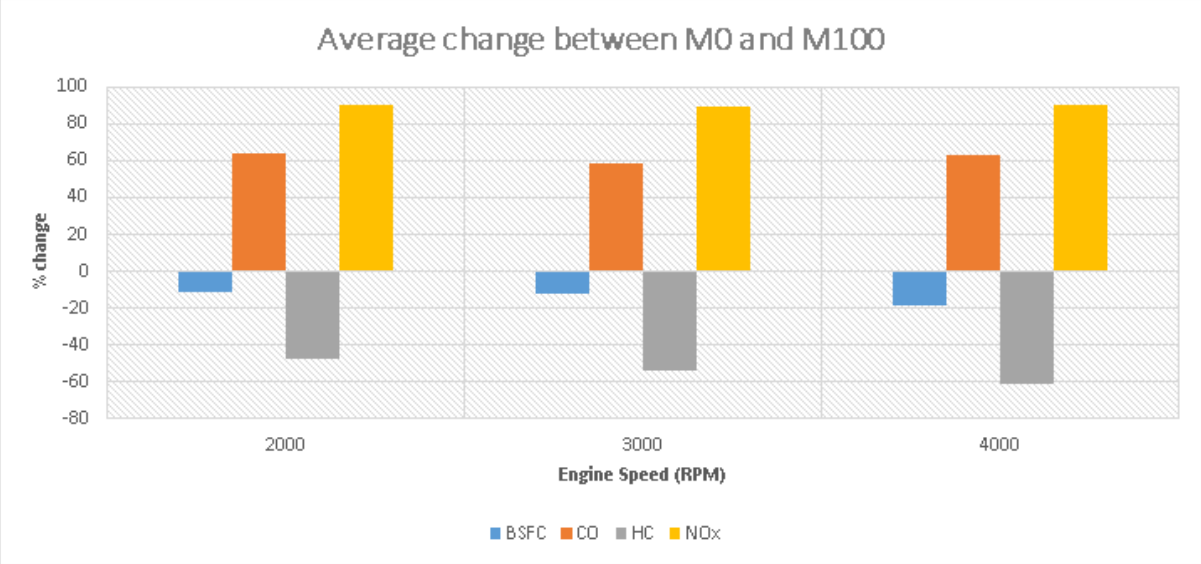

Figure 5.29: Average change of BSFC and emission of CO, HC and NOx emissions between M0 and M100 for different engine speeds

The decrease in BSFC between M0 and M100 varies from 12 % to 18 % for the cases studied. The increase in CO and NOx emissions is about 61 % and 90 % respectively. Furthermore, the decrease in HC emissions is approximately 54 %. CO and NOx emissions can be decreased by running engine lean. This leads to higher efficiency and lower emissions. Therefore, lean burn engines with M-TCR provide scope for future research.

The maps discussed above are used to obtain results for on-road driving under different traffic and road conditions which will be discussed in the succeeding section.

5.2 Engine duty cycle results

Engine duty cycles for three driving conditions are analyzed. The three conditions and their characteristics are provided in Table 5.2 [67].

Table 5.2: Average speed and power of the vehicle during three driving conditions under study

Cycle	Distance (km)	Avg. Speed (km/h)	Avg. Power (kW)
Highway	9.65	98.96	23.22
Sub-Urban	24.08	43.32	10.99
Urban	8.69	24.06	8.63

From the above table, it is clear that the power required and speed achieved are the highest in

highway conditions followed by sub-urban and urban driving conditions. Characteristics of the three driving cycles used in the study are discussed in this section.

Highway driving conditions

Highway conditions are typically characterized by constant vehicle speed as shown in Fig. 5.30. Added to this, the engine speed is high and load is constant either at high level or at low level. The engine operates in fuel cut-off mode approximately half the time in the cycle considered. Therefore, the overall fuel consumption is the lowest among the three cycles. It can also be deduced from the number of plateau in the graph, the engine operates at almost constant load and has maximum efficiency.

Sub-urban driving conditions

In sub-urban conditions, the engine is mostly under load, seldom under idle conditions. Time spent under fuel cut-off condition is significant. The average engine speed is 43.32 km/h. Due to the frequent change in power requirement and engine speed conditions, the efficiency of the engine is lower than highway conditions. Nevertheless, the engine spends less time idling compared to urban drive cycle and is more efficient than the vehicle under urban driving conditions.

Urban driving conditions

The engine spends more time in idling compared to other two cycles. The average speed of the vehicle is relatively lower due to the traffic and road conditions in the urban environment. There is plethora of fluctuations in power demand and engine speed leading to lower engine efficiency. The engine operates lesser time in fuel cut-off mode compared to other two driving conditions. Due to these effects, the fuel consumption of the vehicle is relatively higher.

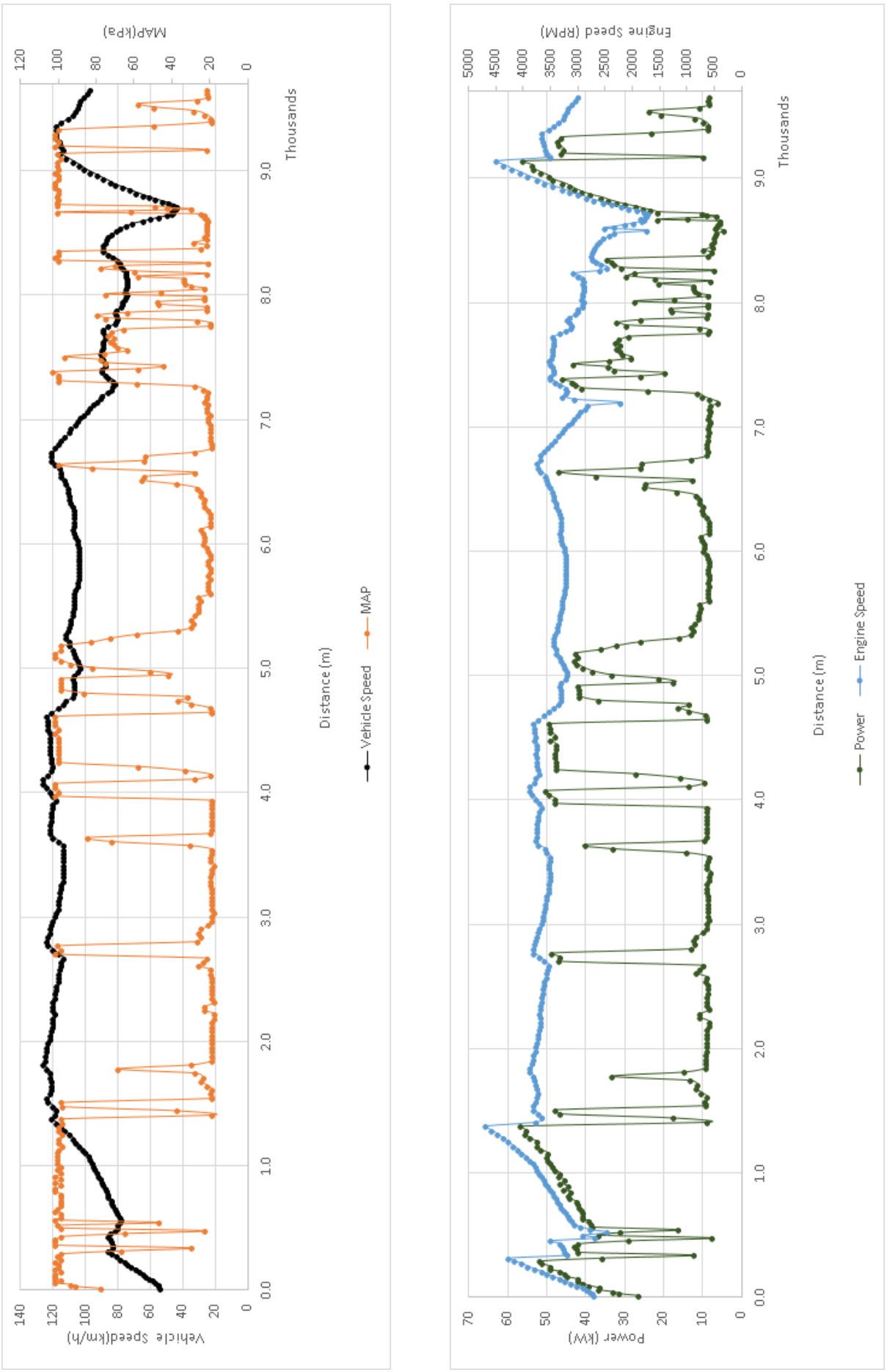

Figure 5.30: Characteristics of the highway driving conditions

Figure 5.31: Characteristics of the sub-urban driving conditions

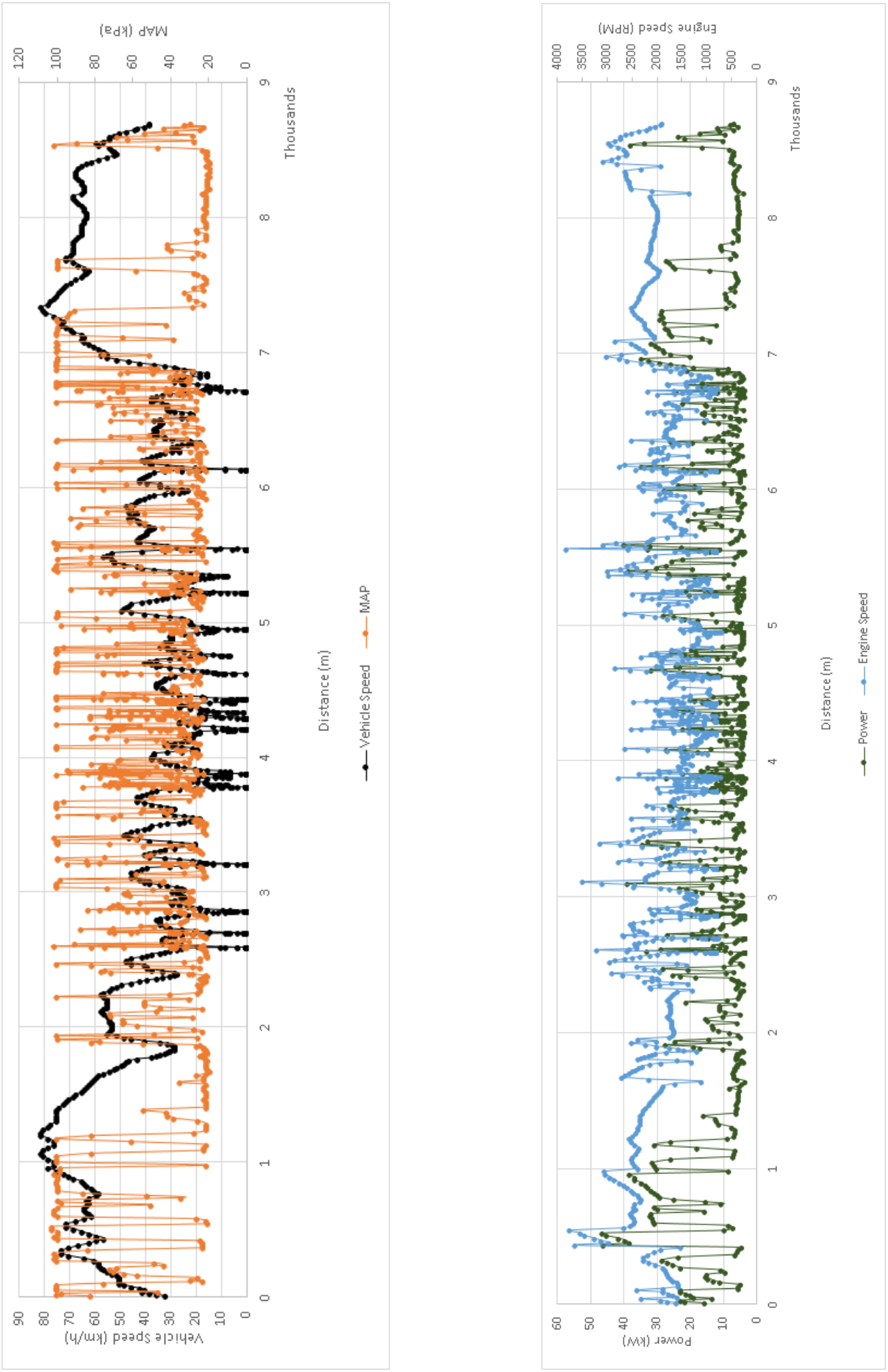

Figure 5.32: Characteristics of the urban driving conditions

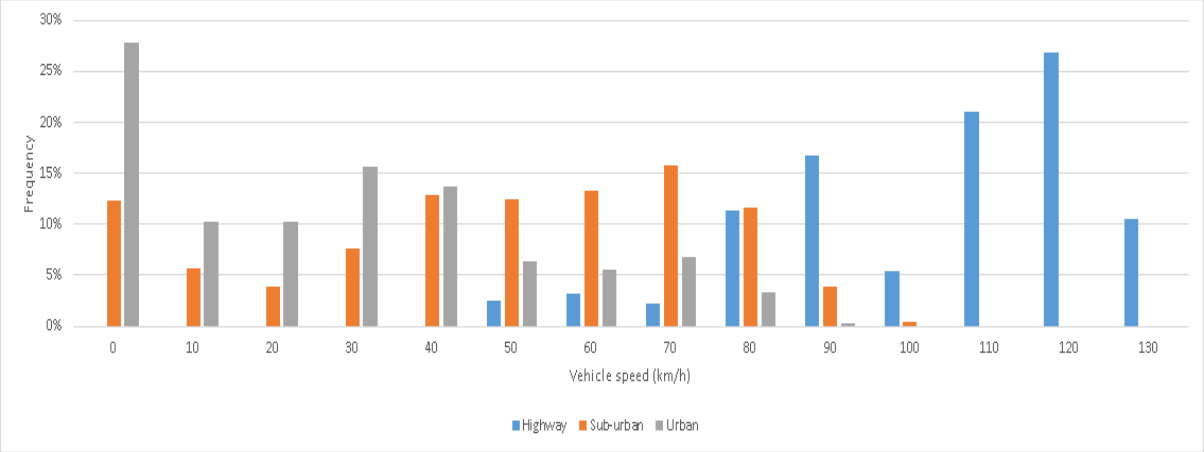

Figure 5.33: Histogram of vehicle speed for the three driving conditions considered

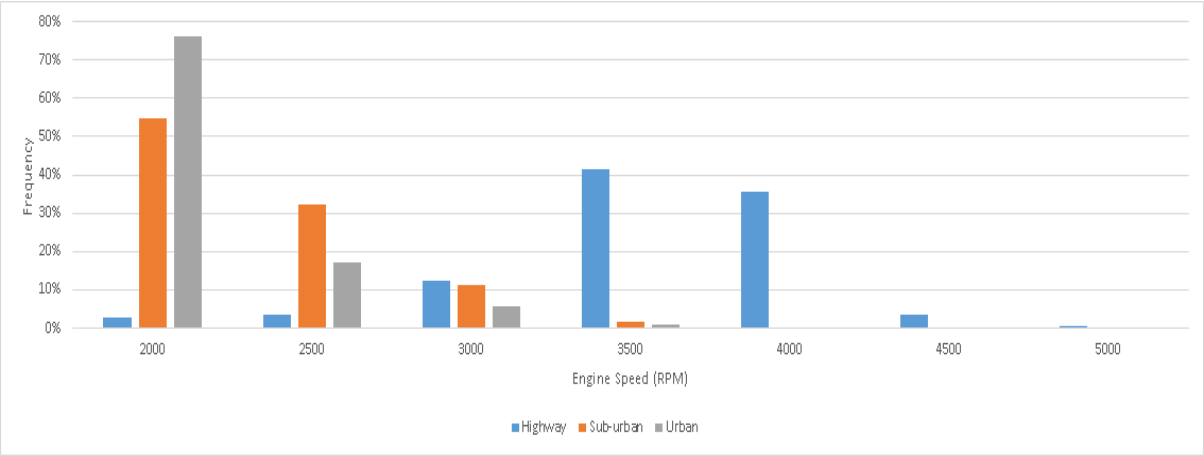

Figure 5.34: Histogram of engine speed for the three driving conditions considered

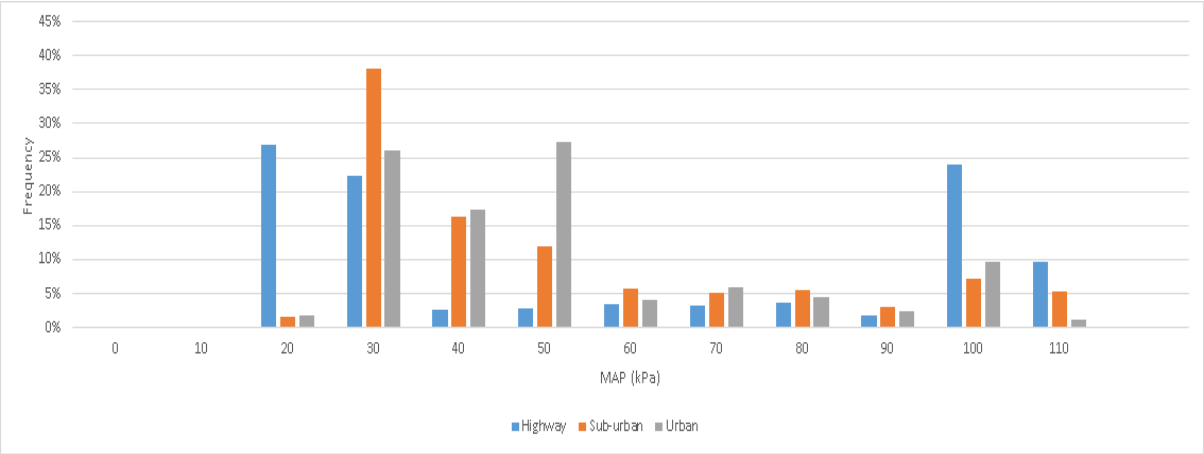

Figure 5.35: Histogram of MAP for the three driving conditions considered

From Fig. 5.33, it is observed that the vehicle is at higher speed at highway conditions and

the speed under these conditions is never below 40 km/h. On the contrary, the vehicle is at a speed less than 40 km/h for more than 75 % of the time in urban driving conditions. Similar observations can be made in engine speed. During urban driving, engine operates at lower RPM most of the duration whereas in highway conditions, the engine operates at higher RPM for londer duration. It is interesting to note that MAP never goes below 10 kPa in all three driving conditions. From these histograms, it can be obeserved that the three cycles considered for the study are contrasting and therefore, these driving conditions test the robustness of M-TCR system.

An analysis of the behaviour of M-TCR system under different driving conditions is shown in following figures. Only the part of the whole cycle where the traits of these cycles are significantly different from other two are shown. It is found that the matrix temperature plays a significant role on the conversion ratio and it is important to maintain high temperature. The exhaust temperature is at 450 K in fuel cut-off mode and at 600 K in idling mode. These assumptions were explained earlier. When the exhaust gas temperature is lower than the matrix, the exhaust gas is bypassed and the reduction of matrix temperature is negligible. This system is pragamtic and provides a scope for future studies. However, when this bypass valve is absent, the drop in matrix temperature is noticeable and decreases the conversion ratio of methanol to syngas. Hence, all the further tests were carried out on a M-TCR system with exhaust bypass system.

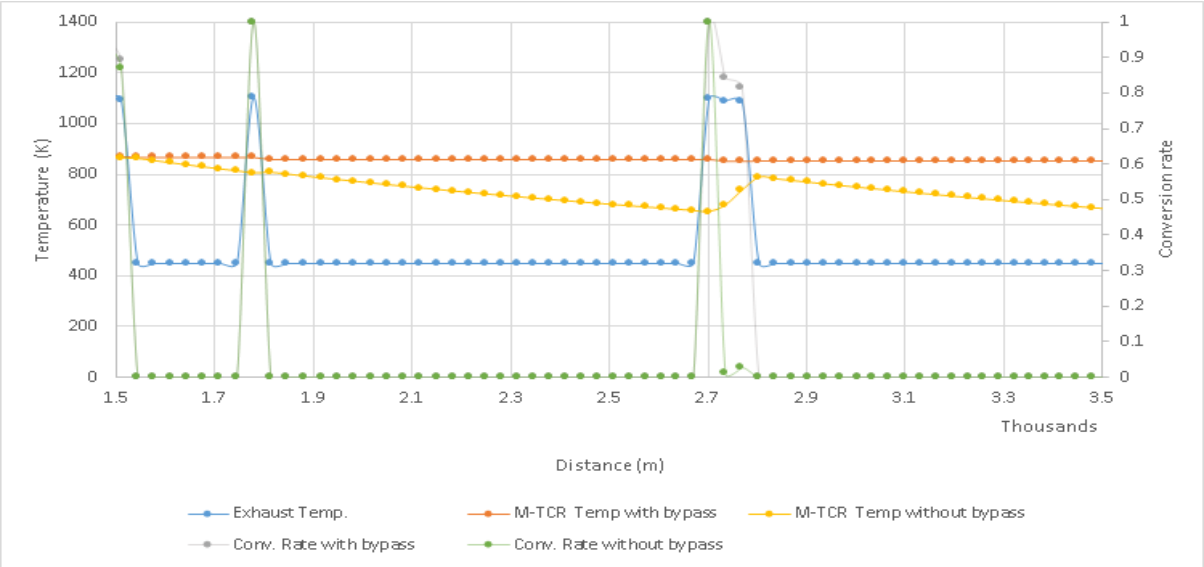

Figure 5.36: M-TCR system characteristics in highway conditions

Highway driving conditions

Under highway conditions, the vehicle spends about half of the time in fuel cut-off condition represented by the plateau in the exhaust temperature profile in Fig. 5.36. M-TCR has a stabilized temperature profile. During fuel cut-off, methanol is converted to syngas and there is only no heat transfer between the M-TCR matrix and exhaust gas due to bypass valve. Therefore, the drop in matrix temperature is almost negligible practically. It is also seen that

whenever the engine is under load, the M-TCR matrix temperature tends to follow the exhaust gas profile.

Sub-urban driving conditions

Under sub-urban conditions, the engine speed is generally under 3500 RPM. The engine spends significant amount of time in fuel cut-off mode like in highway driving condition. The M-TCR matrix temperature has a lower mean value than highway conditions. The engine fluctuates between fuel cut-off condition and loaded condition more frequently leading to varying conversion ratios and lower mean conversion ratio than highway conditions. It can also be observed that the conversion ratio is very sensitive to M-TCR matrix temperature and a slight drop in matrix temperature results in substantial drop in conversion ratio and vice versa.

Urban driving conditions

There are higher fluctuations of exhaust gas temperature compared to other two driving conditions. This leads to frequent change in M-TCR matrix temperature and in turn the methanol to syngas conversion ratio. Average exhaust temperature is comparable to the other two conditions. However, the M-TCR matrix average temperature is the lowest among the three cases considered. Therefore, the mean conversion ratio is lesser than suburban and highway driving conditions. The increase in overall efficiency due to waste heat recovery is the lowest in case of urban driving conditions.

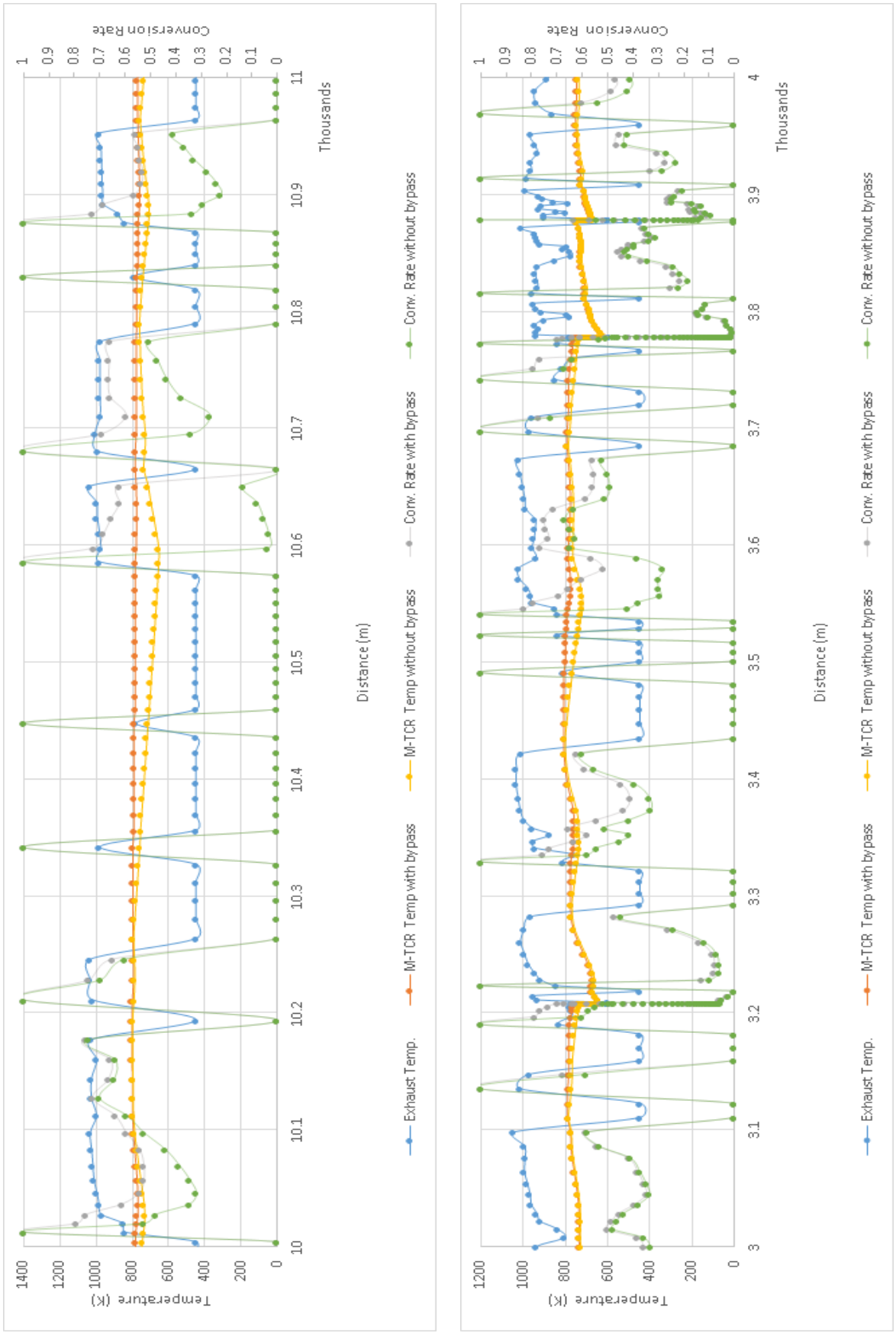

(a) (b)

Figure 5.37: M-TCR system characteristics in (a)Sub-urban (b) Urban conditions

To analyse the behaviour of the system in these three conditions, methanol is used as fuel with an onboard generator in a fictional vehicle and the results are shown Fig. 5.38- Fig. 5.41. The emissions provided are engine-out emissions and will require exhaust gas after-treatment to meet emission regulations.

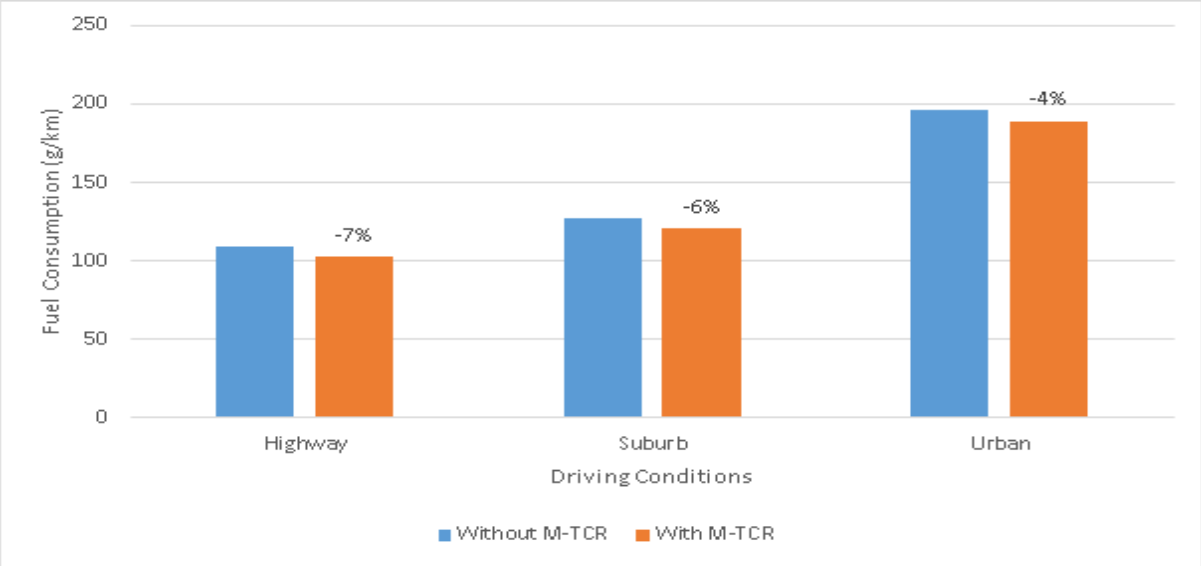

Figure 5.38: Fuel consumption for three driving conditions with and without M-TCR (The number on the bar graphs denote the % change)

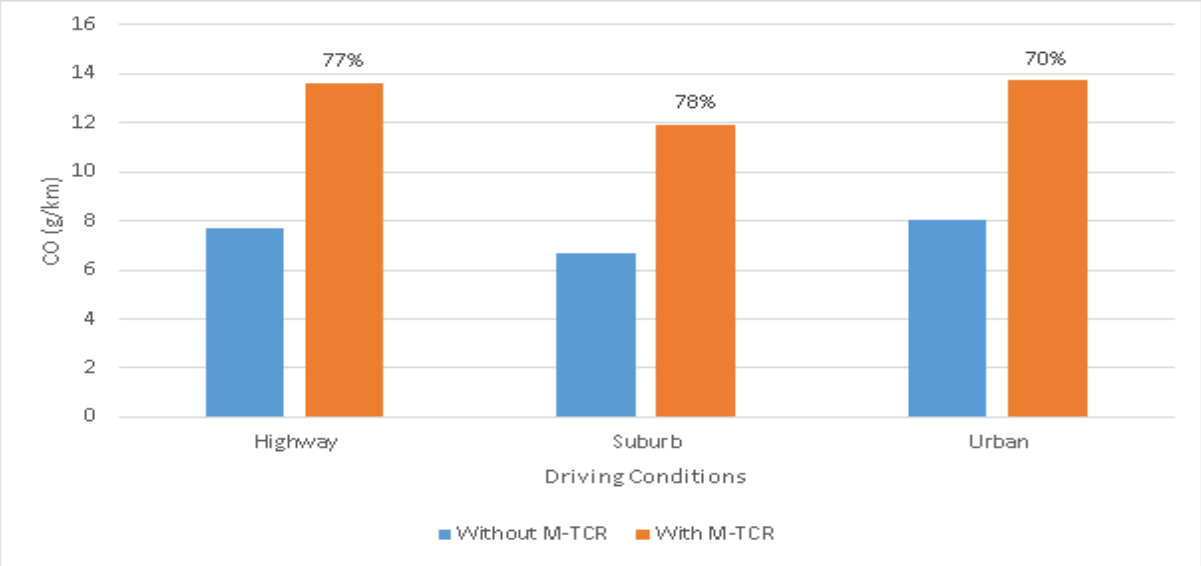

Figure 5.39: CO emissions for three driving conditions with and without M-TCR (The number on the bar graphs denote the % change)

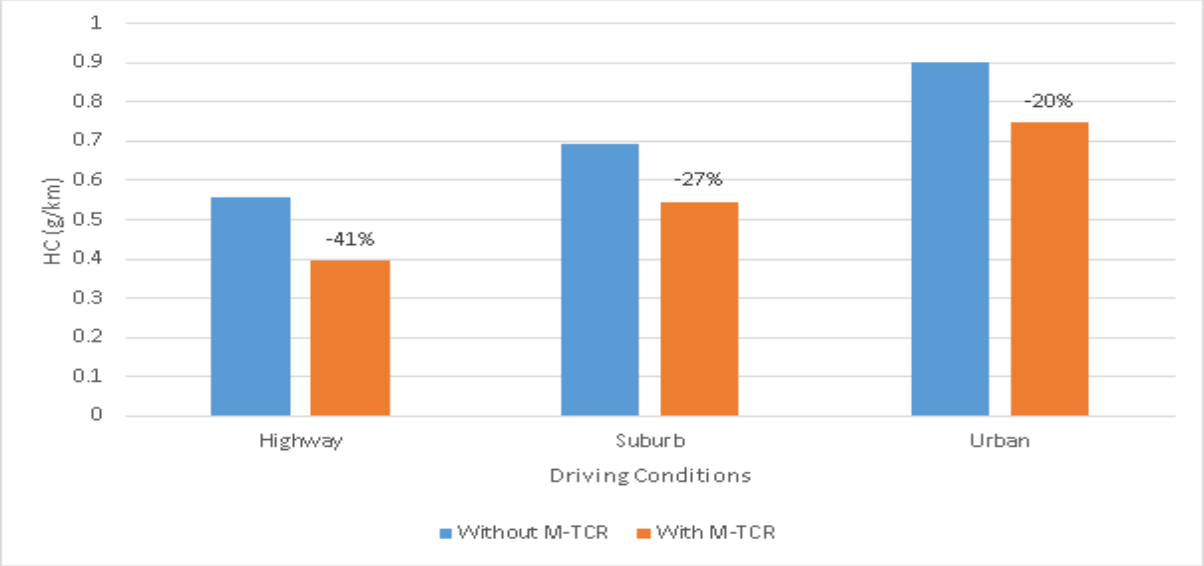

Figure 5.40: HC emissions for three driving conditions with and without M-TCR (The number on the bar graphs denote the % change)

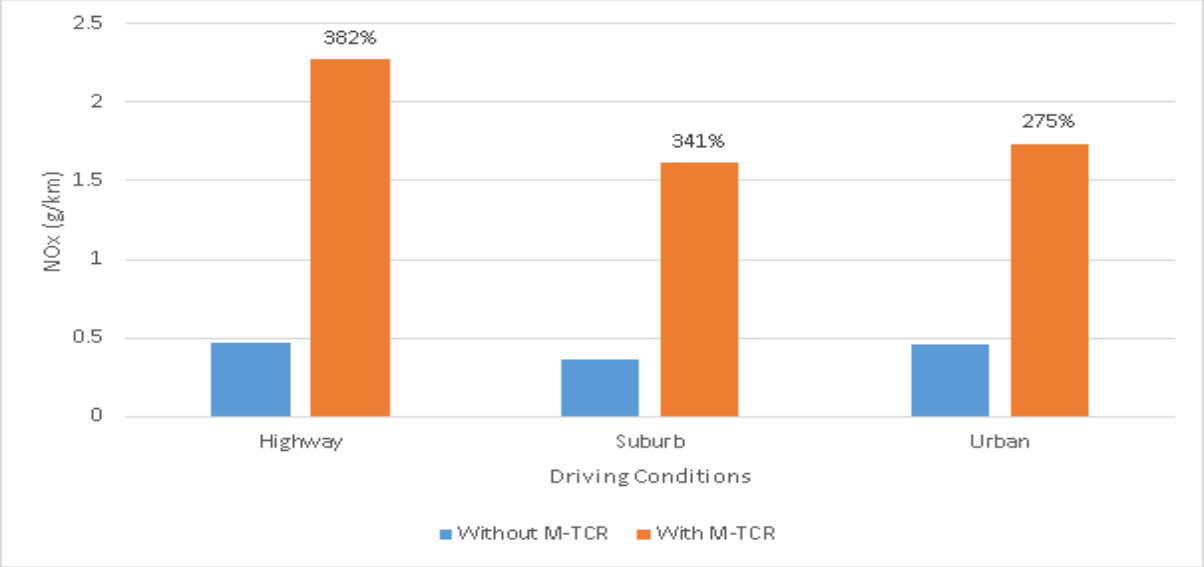

Figure 5.41: NOx emissions for three driving conditions with and without M-TCR (The number on the bar graphs denote the % change)

From the above figures, it is clear that M-TCR system increases energy efficiency. The fuel savings is about 7 g/km in each driving conditions which roughly translates to 139.51 kJ/km of energy savings. CO emissions are higher with M-TCR as the engine is running at stoichiometric conditions and the amount of CO in the fuel is higher in the vehicle with M-TCR. So, higher CO in case of vehicle with M-TCR is analogous to higher unburned hydrocarbons in case of engine running on gasoline under stoichimetric conditions. More detailed explanation has been previously provided in the case of engine simulations. HC emissions are lower in case of vehicle with M-TCR due to lower H-C bonds in the fuel compared to the vehicle running on pure methanol. NOx emissions are higher due to higher combustion temperatures in case of vehicle with M-TCR. Even though engine-out exhaust gas emissions are higher in case of vehicle with

onboard M-TCR, this can be easily treated using three way catalysts. Average BSFC for the whole and average conversion ratio under three driving conditions is provided in Table 5.3. Average BSFC is calculated from the total fuel consumed and overall power demand of the whole cycle.

Table 5.3: Average BSFC and average conversion ratio under different driving conditions

Driving conditions	Avg. BSFC (g/kWh)	Avg. Conversion Rate (%)
Highway	437	77
Sub-urban	475	59
Urban	527	45

The average conversion ratio is calculated by the ratio of mass of syngas used to the mass of fuel used in each driving condition. The average BSFC is the highest and the conversion ratio is the lowest in case of urban driving conditions and vice versa in highway conditions. This effect is due to different conversion ratios and driving conditions. The conversion is higher in highway condition and the driving is more consistent. Hence, these two effects add up in reducing the fuel consumed per unit energy. The vehicle spends considerable amount of time in idle conditions where the fuel consumption per unit energy is very high. On the other hand, the vehicle spends a lot of time in fuel cut-off mode in highway conditions, leading to a lesser fuel consumption per unit energy. Fluctuation between these modes changes the matrix temperature leading to different conversion ratios. A histogram of % of time spent in the three operating modes for different driving conditions is provided in the figure below.

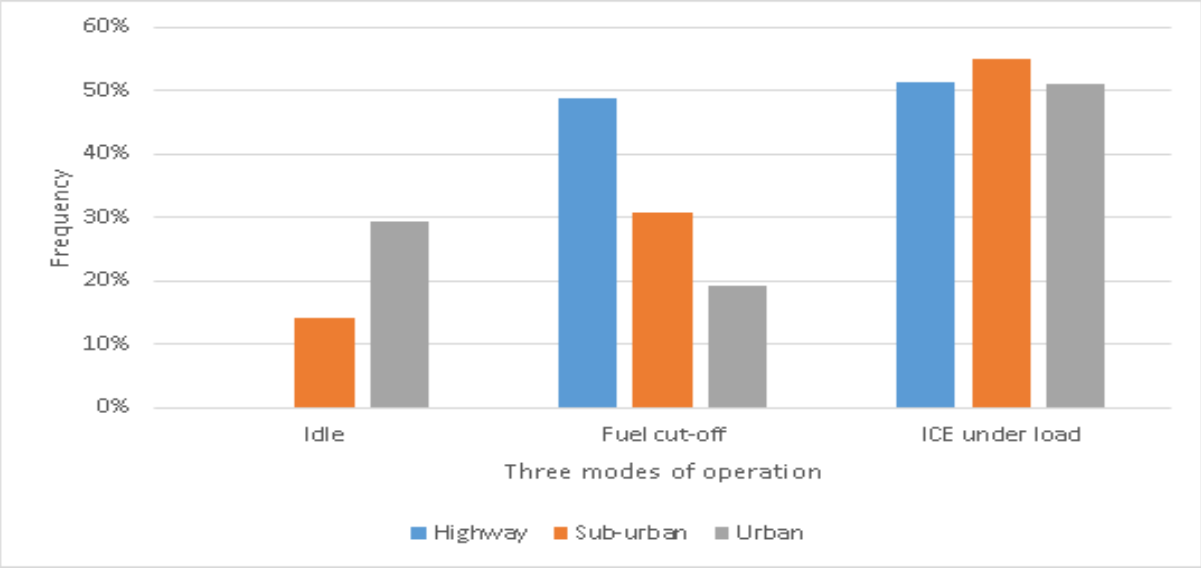

Figure 5.42: Percentage of time spent in three modes of operation for three driving conditions

From this figure, it is clear that the efficiency of the system drops significantly when the engine operates in idle mode. Similarly, fuel consumption is lower when there is increase in the time spent on fuel cut-off mode.

After observing different results and providing arguments for such a behaviour, it is important to derive significant conclusions. In this chapter, the results obtained from engine simulation and engine duty cycles obtained from real world driving scenarios were presented and discussed. Various topics which need further research has also been highlighted. These topics are discussed in the next chapter. The conclusions from these results are discussed in the successive chapter.

6

Scope for Future Research

Variable Compression Ratio Engine

There is a potential to optimize this system for higher efficiency. It is a well known fact that hydrogen has higher laminar flame speed and wide flammability limits compared to other fuels [85]. Added to this, the presence of CO increases the knock resistance of the engine [86]. The octane rating of the three fuels used in the study are shown in Table 6.1. All these properties allows us to increase the compression ratio of the engine. Hence, the compression ratio of the engine is increased from 10.5 to 12.5 on the virtual test bench and the simulation is carried out. The results comparing the BSFC of engine (CR=12.5) fueled with syngas and engine (CR=10.5) fueled with methanol at WOT conditions is illustrated in Fig. 6.1.

Table 6.1: Octane rating of the fuels used in the study

Fuel	Octane Rating	Source
Hydrogen	> 130	[50]
Carbon monoxide	106	[51]
Methanol	109	[9]

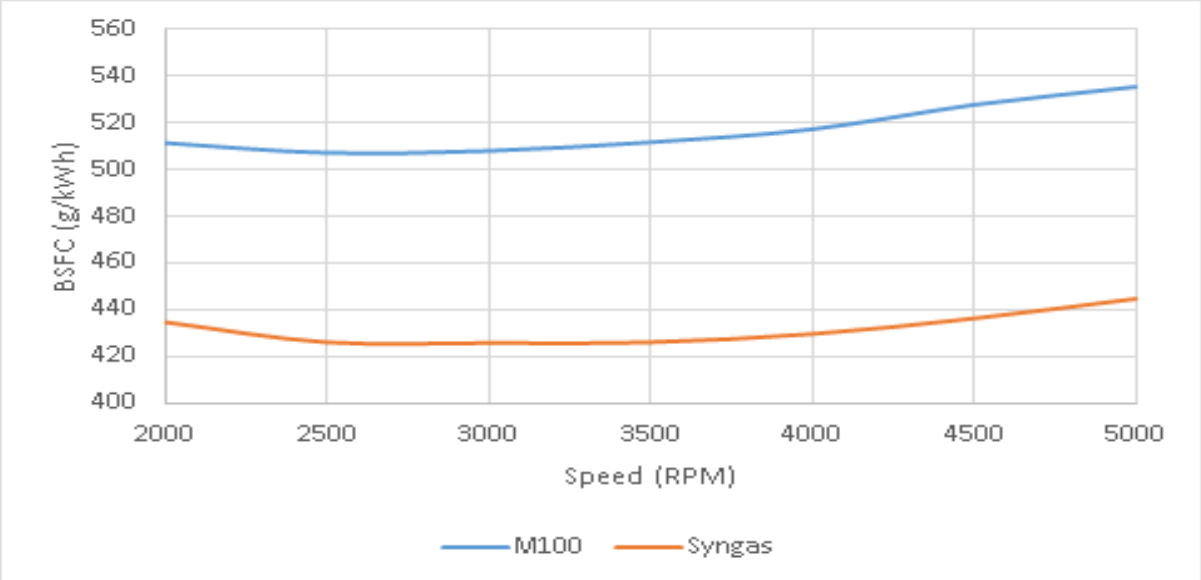

Figure 6.1: Comparison of BSFC of engine (CR=10.5) fueled with methanol and engine (CR=12.5) fueled with syngas

A mean difference of about 20 % is observed between BSFC of two fuels at different compression ratio. A transient VCR engine with methanol as fuel and heat recovery agent provides scope for future research.

Design of M-TCR

In the present study only an energy balance and mass balance of M-TCR is provided. However, it is important to be aware that this can be used as a first step in the evaluation of a concept. There are many other complex mechanisms involved in the M-TCR. For example, heat transfer between the exhaust gases and catalyst should be considered. Added to this, the thermal conductivity of the M-TCR matrix must also be considered.

An important assumption is single step reaction in M-TCR. Evaluation of this assumption by including chemical kinetics of the reaction and its intermediates provides scope for future research.

The catalyst used in M-TCR is sensitive to temperature and the reaction is only complete at about 600 K for a mass flow rate of 1.3 g/s of methanol. With increase in mass flow rate of the fuel, the temperature for 100% conversion further increases. Recently, Beller and his colleagues have discovered a soluble ruthenium-based catalyst that can efficiently turn methanol into hydrogen at a mere 65–95 ^{0}C, and at ambient pressure [87]. Use of such catalysts will provide higher conversion ratios at lower temperature and reduce energy consumption by a great extent. Fig. 6.2 shows the comparison of mean BSFC in different scenarios.

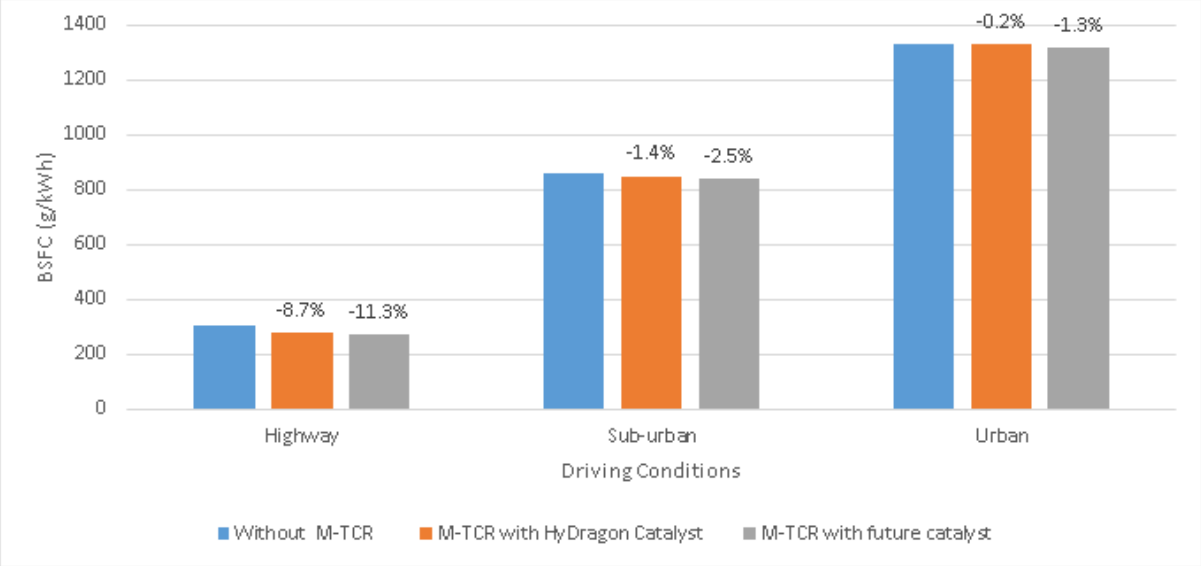

Figure 6.2: Comparison of BSFC without and with M-TCR and different catalysts in three driving conditions (The decrease in BSFC is shown on the respective bars)

However, the % decrease in BSFC is lower than expected due to large amount of fluctuations

in the engine conditions. Therefore, the idle and fuel cut-off condition data are eliminated and the three systems are compared for three driving conditions. The results are shown in Fig. 6.3.

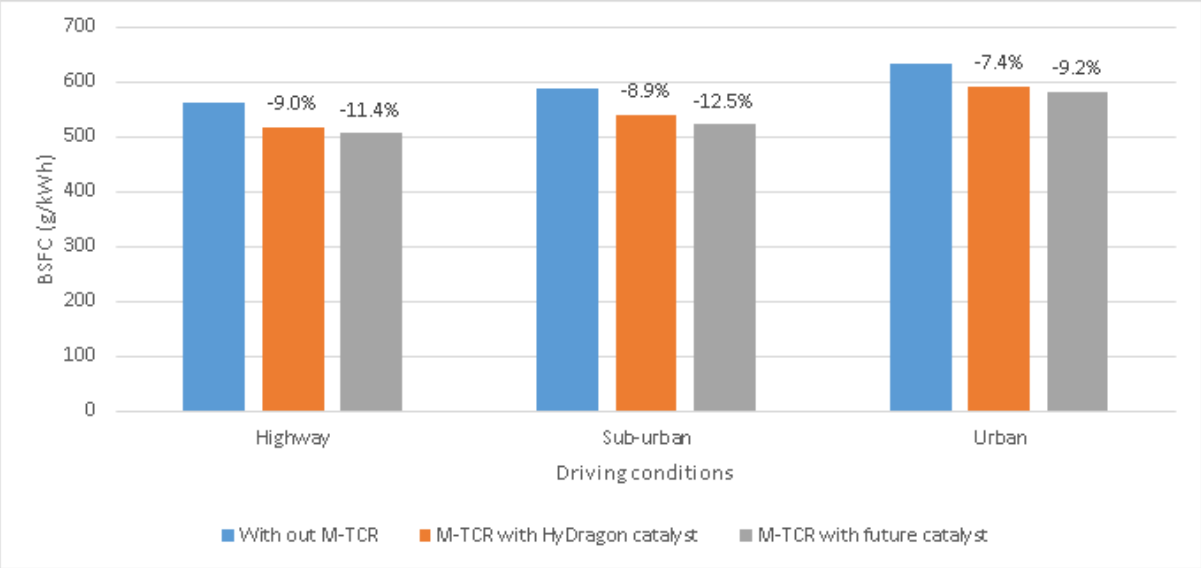

Figure 6.3: Comparison of mean BSFC eliminating the idle and fuel cut-off data for three driving conditions (The decrease in BSFC is shown on the respective bars)

To confirm the results obtained, it was decided to run simulation for a 65 km stretch consisting of various driving conditions. The results are shown in Table 6.2.

Table 6.2: Results obtained for a 65 km stretch with various driving conditions with engine under load

System	mean BSFC (g/kWh)	mean conversion ratio (%)
Without M-TCR	588.9	0
With M-TCR (HyDragon catalyst)	542.8	63.1
With M-TCR (Future catalyst)	529.5	100

From the above table, it is clear that the fluctuations in load and vehicle speed in different driving conditions affects the performance of M-TCR system. The improvement in the system even with a catalyst providing 100% conversion is smaller when the engine changes RPM and load frequently. However, when the idle and fuel cut-off data is eliminated, the system efficiency improves drastically providing a decrease in BSFC by about 11.5 % when there is 100% conversion from methanol to syngas. Hence, a system with lesser variations in speed and load increases the overall efficiency of the system. M-TCR system will be more beneficial in a hybrid vehicle where the ICE is used to drive the generator which charges the battery (series hybrid) [88]. This system can also be used as range extender in an electric vehicle with an arrangement similar to a series hybrid with a smaller capacity portable ICE with generator. The range of a typical all electric vehicle is typically from 100 to 200 km [89]. This is one of the main drawbacks of all electric vehicles. Adding a portable range extender with a sustainable and cleaner fuel like methanol can be instrumental for policy makers championing for electric vehicles to decarbonize the automotive sector. A turbo-generator fueled with methanol and dissociated

methanol can be more suitable for the range extender and hence, use of micro-turbine instead of ICE requires a dedicated research and is discussed in the next section.

Use of micro-turbine as prime mover

With emergence of the hybrid technology, micro turbines can be used as a prime mover in vehicles. Micro-turbines are versatile technical solutions for the production of electrical and thermal power. This term is applied to a new group of small gas turbines being used to provide on-site power and becoming an attractive option to feed the load of small users.

Most microturbines with a power range from 20 kW to 250 kW are based on technologies that were originally developed for the use in auxiliary power systems, aircrafts or automotive turbochargers.

The following are the advantages of micro-turbines [90]:

1. Simple, compact systems - directly connected to high-speed turbo generators
2. Low emissions with multi-fuel capability
3. Low investment costs
4. Reduced maintenance costs

Walmart has already showcased this technology in their trucks [91]. However, the fuel used is diesel. Methanol having a carbon to hydrogen ratio of 0.25 compared to 0.47 of diesel can be a potential fuel to such a system.

Although in general, all commercially available microturbine systems have the potential to be operated with liquid fuels, currently only few microturbines does exist which is specified by the producer for the use of liquid fuels. Several research and demonstration units investigate the technical and emission properties of liquid fuel systems. Two Turbec T100 units are operated on methanol (produced from natural gas) by the Norwegian oil and gas company Statoil ASA. This demonstration project is implemented in the framework of the EC co-funded project 'Optimised Microturbine Energy Systems - OMES', and its main aim is to introduce methanol (as innovative energy carrier) to the fuel market for distributed electricity and heat production [92]. According to the tests, methanol fired microturbines showed comparable results with gas turbines. Hence, it can be concluded that methanol fired microturbines are competitive in the present day scenario.

McDonald and Rodgers have shown that micro turbines can be the source of power in 21st century [93]. Researchers at ICR Tec have studied the use of gas turbines in automotive applications [94]. The microturbines have shown higher efficiencies than existing normal diesel engine. Advanced Gas Turbine for Automobile (AGATA) project of European Union and

Automotive ceramic gas turbine development program of Petroleum Energy Center in Japan have shown the potential of gas turbine in automotive sector [95][96].

Added to this, in a microturbine, the waste heat is concentrated in the exhaust and hence, can be easily utilized for the decomposition of methanol to boost the heat of combustion using M-TCR. The remaining waste heat can be utilized for space heating of the vehicle.

Experimental work

Due to cost and time consuming nature of experimental studies, high performance computing and advances in numerical methods have bolstered the computational studies in the past decade. However, numerical results are always approximate due to truncation errors and they have to be validated by performing experiments. For example in the present study, AVL Boost is used as a computational tool to simulate the engine. The Wiebe function is used for approximating the combustion process. There are two constants, namely the efficiency factor and shape factor which are highly dependent on various properties of the fuel like laminar flame speed. These constants were not changed during the study for different blends. It is a known fact that this plays an important role in analysing the variation of pressure with crank angle and heat release rate. It is important to take this fact in to consideration when analyzing the combustion process of different blends. By performing experiments and obtaining heat release rate curve once for each blends will lead to obtain precise results. It was also seen in previous studies that AVL Boost overestimates HC emissions at higher speeds [47]. AVL Boost theory manual acknowledges this fact as HC emissions is diffciult to predict [55]. Perhaps, few experiments can be helpful in obtaining the trend. Therefore, experimental studies provides enormous scope for future research in this domain.

M-TCR control system

It is clearly seen from the maps that peak torque decreases with increase in syngas concentration. However, when the torque demand is higher than the peak torque provided by that blend at specific engine speed (RPM), there is requirement of a M-TCR control system which reduces the conversion ratio and regulates the concentration of syngas in the blend. This provides a robust system which can be implemented for any driving condition. There is a plethora of research opportunities in this sector.

Lean burn methanol engine with M-TCR

Thermal efficiency of an engine increases with running the engine under lean burn conditions [97] [98]. Recently, Wu et al. compared the indicated thermal efficiency (ITE) of methanol and gasoline at three different excess air ratio [99]. They obtained a peak ITE of 24.7 % at λ=1.4. It was also seen that the rise in COV_{imep} was lower for methanol compared to gasoline

with increase in excess air ratio. Hence, a lean burn methanol engine with M-TCR provides an immense possibility of research. With the increase in conversion ratio of methanol to syngas, the concetration of hydrogen in the blend increases. Hydrogen is well known for its wider flammability limits and faster laminar flame speed. This increases the prospect of lean burn methanol engines with M-TCR. In order to check the potential of lean burn methanol engine, a simulation is carried out with M100 as fuel at λ =1 and λ =1.25.

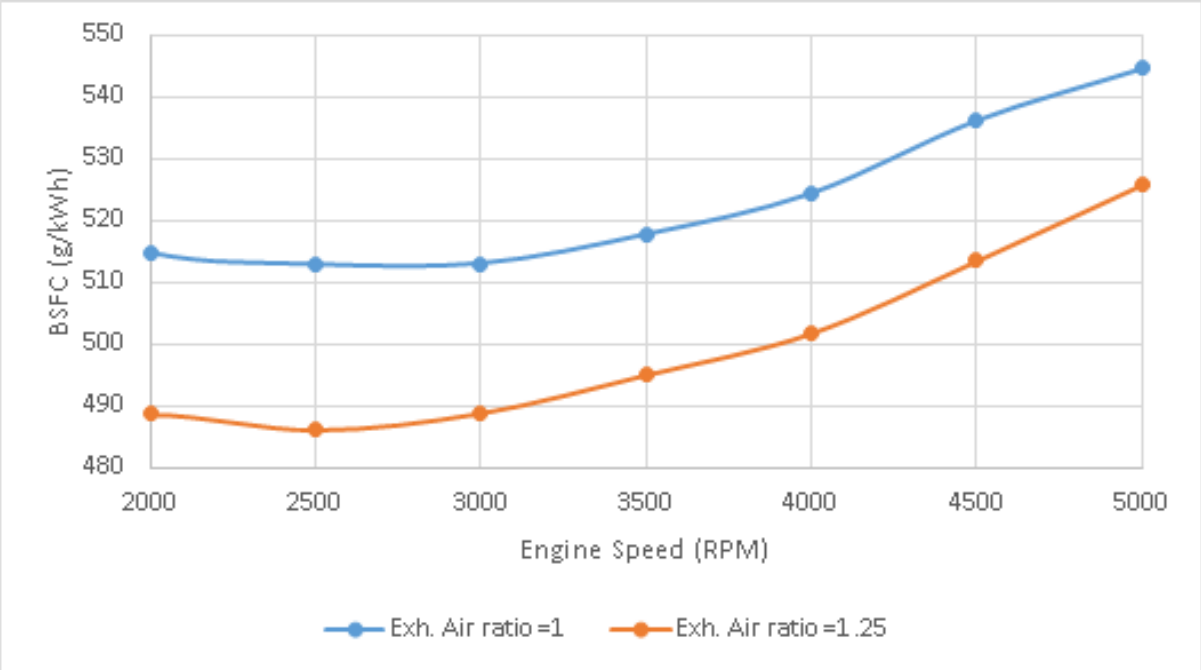

Figure 6.4: BSFC with M100 as fuel at λ =1 and λ =1.25.

There is about 5 % decrease in BSFC. With use of M-TCR, this could decrease further and provides possibility of future research in this area.

Engine Start-Stop system

In automobiles, a start-stop system or stop-start system automatically shuts down and restarts the internal combustion engine to reduce the amount of time the engine spends idling, thereby reducing fuel consumption and emissions. This is advantageous in urban driving conditions. This system is not implemented in the present study and the behaviour of a vehicle with M-TCR equipped with start-stop system can provide scope for future research.

After discussing the scope for future research, conclusion will be drawn from the present study in the next chapter.

7 Conclusions

Methanol has a unique property of thermo chemical recuperation. The present study exploits this property using the exhaust waste heat from an internal combustion engine for the endothermic reaction and evaluates its feasibility and utility in real world applications.

The objectives of the thesis are:

1. To evaluate the feasibility of the proposed concept by performing simulations using various tools
2. To check the utility of the proposed concept by testing it under different driving conditions.

An engine is simulated on AVL Boost and engine maps are obtained. An M-TCR model is built on MATLAB and data acquired from these models are integrated using powertain integrator. Data from engine duty cycles obtained from real world vehicle driving are provided to powertrain integrator and the results are obtained for three driving conditions. This enables us to check the feasibility and utility of the proposed concept.

The following conclusions can be made from the present investigation:

- There is sufficient heat in the exhaust to convert methanol into a mixture of two moles of hydrogen and one mole carbon monoxide (a syngas). This syngas has about 20 % more energy content per unit mass compared to pure methanol.
- Eventhough the syngas has higher energy content, it displaces some amount of intake air and hence the power output is lower per unit volume of charge compared to pure methanol. However, the amount of fuel required to produce unit energy is lower for syngas compared to methanol.
- Due to the limitation on the amount of heat that can be recovered before the catalytic converter, the design of the whole system has a prominent role in increasing the overall efficiency of the system. A system with methanol pre-vaporizer increases overall efficiency due to higher conversion ratios.
- For a given load, BSFC and HC emissions are lower for M0 compared to M100. But, the CO and NOx emissions show the opposite trend. Similarly, for a given speed, BSCO and BSNOx are higher for M0 than M100 and BSHC is lower for M0 than M100.
- The simulations have been performed for three driving conditions (Highway, Sub-urban and Urban). The average BSFC is lower for highway conditions compared to the other two conditions due to the absence of idling and half of the time spent on fuel cut-off mode.

Due to lower fluctuations in average M-TCR matrix temperature, the conversion ratio is higher in this driving condition compared to other two conditions. It is also discovered that using a exhaust gas bypass during idling and fuel cut-off conditions prevents the cooling of M-TCR matrix (exhaust gas temperature is lower than the matrix temperature).

- The overall energy efficiency increases with the use of M-TCR system. Due to the lower amount of fuel burnt, CO_2 emissions are lower. However, with the M-TCR system NOx and CO emissions increase. Hence, a catalytic converter is essential to meet the stringent emission reduction norms. Another way to circumvent this issue is to use ultra lean mixtures in the engine. The presence of hydrogen in the fuel after conversion provides wider flammability range and may even support qualitative governing in the future.
- Scope for future research is also provided. This helps peers to align themselves with one of the many available directions to optimize the system discussed in the present study.

Summarizing, the proposed concept of onboard M-TCR and its utility has shown feasibility in an automotive vehicle. There is immense scope for future research in this domain and a brief overview of this scope was provided earlier.

Bibliography

[1] "BP Statistical review of world energy," Accessed date: 2016-04-25.

[2] "MIT Energy Initiative Symposium," Acessed Date: 2016-04-21.

[3] E. Independence, "Security act (eisa)," in *110th Congress, 1st session*, pp. 110–140, 2007.

[4] E. UNION, "Directive 2009/28/ec of the european parliament and of the council of 23 april 2009 on the promotion of the use of energy from renewable sources and amending and subsequently repealing directives 2001/77/ec and 2003/30/ec," 2009.

[5] R. J. Pearson, J. W. Turner, A. Bell, S. De Goede, C. Woolard, and M. H. Davy, "Iso-stoichiometric fuel blends: characterisation of physicochemical properties for mixtures of gasoline, ethanol, methanol and water," *Proceedings of the Institution of Mechanical Engineers, Part D: Journal of automobile engineering*, p. 0954407014529424, 2014.

[6] I. E. Agency, "World energy outlook 2015," *International Energy Agency*, vol. 1, 2015.

[7] G. A. Olah, A. Goeppert, and G. S. Prakash, *Beyond oil and gas: the methanol economy*. John Wiley & Sons, 2011.

[8] G. A. Olah, A. Goeppert, and G. S. Prakash, "Chemical recycling of carbon dioxide to methanol and dimethyl ether: from greenhouse gas to renewable, environmentally carbon neutral fuels and synthetic hydrocarbons," *The Journal of organic chemistry*, vol. 74, no. 2, pp. 487–498, 2008.

[9] R. Pearson, J. Turner, and A. Peck, "Gasoline-ethanol-methanol tri-fuel vehicle development and its role in expediting sustainable organic fuels for transport," in *IMechE Low Carbon Vehicles Conference, 2009*, University of Bath, 2009.

[10] F. Studt, I. Sharafutdinov, F. Abild-Pedersen, C. F. Elkjær, J. S. Hummelshøj, S. Dahl, I. Chorkendorff, and J. K. Nørskov, "Discovery of a ni-ga catalyst for carbon dioxide reduction to methanol," *Nat. Chem*, vol. 6, no. 4, pp. 320–324, 2014.

[11] J. C. Brown and E. Gulari, "Hydrogen production from methanol decomposition over pt/al 2 o 3 and ceria promoted pt/al 2 o 3 catalysts," *Catalysis Communications*, vol. 5, no. 8, pp. 431–436, 2004.

[12] M. J. Nuvan, "Energy audit: cost-effective solutions for the industry in the era of energy crisis (part-1)," *ChE Thoughts*, vol. 2, no. 2, pp. 13–18, 2011.

[13] J. C. Conklin and J. P. Szybist, "A highly efficient six-stroke internal combustion engine cycle with water injection for in-cylinder exhaust heat recovery," *Energy*, vol. 35, no. 4, pp. 1658–1664, 2010.

[14] G. J. Snyder, "Small thermoelectric generators," *The Electrochemical Society Interface*, vol. 17, no. 3, p. 54, 2008.

[15] J. Yang, "Potential applications of thermoelectric waste heat recovery in the automotive industry," in *Thermoelectrics, 2005. ICT 2005. 24th International Conference on*, pp. 170–174, IEEE, 2005.

[16] D. Wei, X. Lu, Z. Lu, and J. Gu, "Performance analysis and optimization of organic rankine cycle (orc) for waste heat recovery," *Energy conversion and Management*, vol. 48, no. 4, pp. 1113–1119, 2007.

[17] B. Sternlicht, "Waste energy recovery: an excellent investment opportunity," *Energy Conversion and Management*, vol. 22, no. 4, pp. 361–373, 1982.

[18] P. S. Patel and E. F. Doyle, "Compounding the truck diesel engine with an organic rankine-cycle system," tech. rep., SAE Technical Paper, 1976.

[19] T.-C. Hung, T. Shai, and S. Wang, "A review of organic rankine cycles (orcs) for the recovery of low-grade waste heat," *Energy*, vol. 22, no. 7, pp. 661–667, 1997.

[20] H. Chen, D. Y. Goswami, and E. K. Stefanakos, "A review of thermodynamic cycles and working fluids for the conversion of low-grade heat," *Renewable and sustainable energy reviews*, vol. 14, no. 9, pp. 3059–3067, 2010.

[21] T. E. Briggs, R. M. Wagner, K. D. Edwards, S. Curran, and E. J. Nafziger, "A waste heat recovery system for light duty diesel engines," tech. rep., Oak Ridge National Laboratory (ORNL); National Transportation Research Center, 2010.

[22] R. Valentino, M. J. Hall, and T. Briggs, "Simulation of organic rankine cycle electric power generation from light-duty spark ignition and diesel engine exhaust flows," *SAE International Journal of Engines*, vol. 6, no. 2, pp. 1299–1310, 2013.

[23] B. Alfred, "Charging device for internal combustion engines," Sept. 22 1942. US Patent 2,296,268.

[24] S. Park, T. Matsumoto, and N. Oda, "Numerical analysis of turbocharger response delay mechanism," tech. rep., SAE Technical Paper, 2010.

[25] S. D. Arnold, S. P. Martin, K. Slupski, and V. Kanigowski, "Variable geometry turbocharger," Aug. 7 2001. US Patent 6,269,642.

[26] G. Curiel and U. Linsi, "Two-stage exhaust-gas turbocharger," May 22 1979. US Patent 4,155,684.

[27] E. Musu, R. Rossi, R. Gentili, and R. D. Reitz, "Cfd study of hcpc turbocharged engine," tech. rep., SAE Technical Paper, 2010.

[28] M. Okada and S. Sekiyama, "Turbo compound engine," June 7 1988. US Patent 4,748,812.

[29] B. Gunston, *Development of piston aero engines*. Patrick Stephens Limited, 2006.

[30] V. K. Chakravarthy, C. S. Daw, J. A. Pihl, and J. C. Conklin, "Study of the theoretical potential of thermochemical exhaust heat recuperation for internal combustion engines," *Energy & Fuels*, vol. 24, no. 3, pp. 1529–1537, 2010.

[31] T. Heppenstall, "Advanced gas turbine cycles for power generation: a critical review," *Applied Thermal Engineering*, vol. 18, no. 9, pp. 837–846, 1998.

[32] T. Nakagaki, T. Ogawa, H. Hirata, K. Kawamoto, Y. Ohashi, and K. Tanaka, "Development of chemically recuperated micro gas turbine," *Journal of engineering for gas turbines and power*, vol. 125, no. 1, pp. 391–397, 2003.

[33] I. Yamaguchi, T. Takishita, T. Sakai, T. Ayusawa, and Y. K. Kim, "Development research on dissociated methanol fueled spark ignition engine," tech. rep., SAE Technical Paper, 1985.

[34] L. Pettersson and K. Sjostrom, "Decomposed methanol as a fuel-a review," *Combustion science and technology*, vol. 80, no. 4-6, pp. 265–303, 1991.

[35] J. G. Finegold, "Dissociated methanol vehicle test results," tech. rep., Solar Energy Research Inst., Golden, CO (USA), 1984.

[36] T. G. Adams, "A comparison of engine performance using methanol or dissociated methanol as the fuel," tech. rep., SAE Technical Paper, 1984.

[37] A. Konig, K.-W. Ellinger, and K. Korbel, "Engine operation on partially dissociated methanol," tech. rep., Society of Automotive Engineers, Inc., Warrendale, PA, 1985.

[38] Z. Kodah, H. Soliman, M. A. Qudais, and Z. Jahmany, "Combustion in a spark-ignition engine," *Applied Energy*, vol. 66, no. 3, pp. 237–250, 2000.

[39] G. A. Alla, "Computer simulation of a four stroke spark ignition engine," *Energy conversion and Management*, vol. 43, no. 8, pp. 1043–1061, 2002.

[40] M. A. S. Al-Baghdadi, "A simulation model for a single cylinder four-stroke spark ignition engine fueled with alternative fuels," *Turkish Journal of Engineering and Environmental Sciences*, vol. 30, no. 6, pp. 331–350, 2007.

[41] J. Gatowski, E. N. Balles, K. Chun, F. Nelson, J. Ekchian, and J. B. Heywood, "Heat release analysis of engine pressure data," tech. rep., Society of Automotive Engineers, Inc., Warrendale, PA, 1984.

[42] A. M. Pourkhesalian, A. H. Shamekhi, and F. Salimi, "Alternative fuel and gasoline in an si engine: A comparative study of performance and emissions characteristics," *Fuel*, vol. 89, no. 5, pp. 1056–1063, 2010.

[43] S. Iliev, "A comparison of ethanol and methanol blending with gasoline using a 1-d engine model," *Procedia Engineering*, vol. 100, pp. 1013–1022, 2015.

[44] S. P. Iliev, "Developing of a 1-d combustion model and study of engine performance and exhaust emission using ethanol-gasoline blends," in *Transactions on Engineering Technologies*, pp. 85–98, Springer, 2015.

[45] M. S. Yashwanth, T. Venugopal, and A. Ramesh, "Experimental and simulation studies to determine the effective octane number in an engine fuelled with ethanol and gasoline," *Int. J. Automot. Mech. Eng*, vol. 10, pp. 2057–2069, 2014.

[46] S. Trimbake and D. Malkhede, "Investigations of port dual injection (pdi) strategies in single cylinder si engine fueled with ethanol/gasoline blends," tech. rep., SAE Technical Paper, 2016.

[47] S. S. Nagaraja, V. Ravi, R. Teja, V. Nayak, and G. Kumar, "Performance and emission characteristics of a mpi engine fueled with iso-butanol/gasoline blends," tech. rep., SAE Technical Paper, 2014.

[48] R. J. Farrauto and R. M. Heck, "Catalytic converters: state of the art and perspectives," *Catalysis Today*, vol. 51, no. 3, pp. 351–360, 1999.

[49] J. Vancoillie, J. Demuynck, L. Sileghem, M. Van De Ginste, S. Verhelst, L. Brabant, and L. Van Hoorebeke, "The potential of methanol as a fuel for flex-fuel and dedicated spark-ignition engines," *Applied Energy*, vol. 102, pp. 140–149, 2013.

[50] K. Mazloomi and C. Gomes, "Hydrogen as an energy carrier: prospects and challenges," *Renewable and Sustainable Energy Reviews*, vol. 16, no. 5, pp. 3024–3033, 2012.

[51] J. A. Topinka, M. D. Gerty, J. B. Heywood, and J. C. Keck, "Knock behavior of a lean-burn, h2 and co enhanced, si gasoline engine concept," *SAE SP*, pp. 39–52, 2004.

[52] C. Dong, Q. Zhou, Q. Zhao, Y. Zhang, T. Xu, and S. Hui, "Experimental study on the laminar flame speed of hydrogen/carbon monoxide/air mixtures," *Fuel*, vol. 88, no. 10, pp. 1858–1863, 2009.

[53] J. B. Heywood *et al.*, *Internal combustion engine fundamentals*, vol. 930. Mcgraw-hill New York, 1988.

[54] A. Burcat, "Thermochemical data for combustion calculations," in *Combustion chemistry*, pp. 455–473, Springer, 1984.

[55] A. Boost, "Theory manual," *AVL List Gmbh, Graz-Austria*, 2011.

[56] J. Ghojel, "Review of the development and applications of the wiebe function: a tribute to the contribution of ivan wiebe to engine research," *International Journal of Engine Research*, vol. 11, no. 4, pp. 297–312, 2010.

[57] A. K. Agarwal, H. Karare, and A. Dhar, "Combustion, performance, emissions and particulate characterization of a methanol–gasoline blend (gasohol) fuelled medium duty spark ignition transportation engine," *Fuel Processing Technology*, vol. 121, pp. 16–24, 2014.

[58] G. Woschni, "A universally applicable equation for the instantaneous heat transfer coefficient in the internal combustion engine," tech. rep., SAE Technical paper, 1967.

[59] K. Pattas and G. Häfner, "Stickoxidbildung bei der ottomotorischen verbrennung," *MOTORTECHN. Z.*, vol. 34, no. 12, 1973.

[60] A. Onorati, G. Ferrari, and G. D'Errico, "1d unsteady flows with chemical reactions in the exhaust duct-system of si engines: predictions and experiments," tech. rep., SAE Technical Paper, 2001.

[61] J. C. Hilliard and G. S. Springer, *Fuel Economy: In Road Vehicles Powered by Spark Ignition Engines*. Springer Science & Business Media, 2013.

[62] G. D'Errico, G. Ferrari, A. Onorati, and T. Cerri, "Modeling the pollutant emissions from a si engine," tech. rep., SAE Technical Paper, 2002.

[63] A. Goeke and S. Walcher, "Quasi-steady state: Searching for and utilizing small parameters," in *Recent Trends in Dynamical Systems*, pp. 153–178, Springer, 2013.

[64] Y. Usami, K. Kagawa, M. Kawazoe, Y. Matsumura, H. Sakurai, and M. Haruta, "Catalytic methanol decomposition at low temperatures over palladium supported on metal oxides," *Applied Catalysis A: General*, vol. 171, no. 1, pp. 123–130, 1998.

[65] Y. Matsumura, K. Tanaka, N. Tode, T. Yazawa, and M. Haruta, "Catalytic methanol decomposition to carbon monoxide and hydrogen over nickel supported on silica," *Journal of Molecular Catalysis A: Chemical*, vol. 152, no. 1, pp. 157–165, 2000.

[66] "Private e-mail," Dated: 12-01-2016.

[67] G. Gonçalves, "Energy and environmental monitoring of alternative fuel vehicles," *UNIVERSIDADE TÉCNICA DE LISBOA-Instituto Superior Técnico (IST), Lisboa*, 2009.

[68] I. Finlay, D. Harris, D. Boam, and B. Parks, "Factors influencing combustion chamber wall temperatures in a liquid-cooled, automotive, spark-ignition engine," *Proceedings of the Institution of Mechanical Engineers, Part D: Journal of Automobile Engineering*, vol. 199, no. 3, pp. 207–214, 1985.

[69] M. Brusstar, M. Stuhldreher, D. Swain, and W. Pidgeon, "High efficiency and low emissions from a port-injected engine with neat alcohol fuels," *SAE paper*, no. 2002-01, p. 2743, 2002.

[70] A. Shah, R. Srinivasan, S. D. F. To, and E. P. Columbus, "Performance and emissions of a spark-ignited engine driven generator on biomass based syngas," *Bioresource technology*, vol. 101, no. 12, pp. 4656–4661, 2010.

[71] J. Vancoillie and S. Verhelst, "Modeling the combustion of light alcohols in si engines: a preliminary study," in *FISITA 2010 World Automotive Congress, Budapest, Hungary*, pp. 1–12, 2010.

[72] G. D. Ebersole and F. S. Manning, "Engine performance and exhaust emissions: methanol versus isooctane," *SAE Prog. Technol.;(United States)*, vol. 19, 1980.

[73] O. A. Kutlar, H. Arslan, and A. T. Calik, "Methods to improve efficiency of four stroke, spark ignition engines at part load," *Energy Conversion and Management*, vol. 46, no. 20, pp. 3202–3220, 2005.

[74] C. Bauer and T. Forest, "Effect of hydrogen addition on the performance of methane-fueled vehicles. part i: effect on si engine performance," *International Journal of Hydrogen Energy*, vol. 26, no. 1, pp. 55–70, 2001.

[75] H. Li and G. A. Karim, "Exhaust emissions from an si engine operating on gaseous fuel mixtures containing hydrogen," *International journal of hydrogen energy*, vol. 30, no. 13, pp. 1491–1499, 2005.

[76] K. J. Whitty, H. R. Zhang, and E. G. Eddings, "Emissions from syngas combustion," *Combustion Science and Technology*, vol. 180, no. 6, pp. 1117–1136, 2008.

[77] X. Dai, C. Ji, S. Wang, C. Liang, X. Liu, and B. Ju, "Effect of syngas addition on performance of a spark-ignited gasoline engine at lean conditions," *International journal of hydrogen energy*, vol. 37, no. 19, pp. 14624–14631, 2012.

[78] V. Ganesan, *Internal combustion engines*. McGraw Hill Education (India) Pvt Ltd, 2012.

[79] W. M. Haynes, *CRC handbook of chemistry and physics*. CRC press, 2014.

[80] C. Fenimore, "Formation of nitric oxide in premixed hydrocarbon flames," in *Symposium (International) on Combustion*, vol. 13, pp. 373–380, Elsevier, 1971.

[81] S. Mishra and R. Dahiya, "Adiabatic flame temperature of hydrogen in combination with gaseous fuels," *International journal of hydrogen energy*, vol. 14, no. 11, pp. 839–844, 1989.

[82] S. Nagaraja and G. Przybyla, "Experimental study on performance and emission characteristics of lean burn si engine fuelled with hydrogen methane blends," *Combustion Engines*, vol. 162, no. 3, pp. 556–562, 2015.

[83] R. L. Hoekstra, P. Van Blarigan, and N. Mulligan, "Nox emissions and efficiency of hydrogen, natural gas, and hydrogen/natural gas blended fuels," tech. rep., SAE Technical Paper, 1996.

[84] J. B. Heywood, J. Higgins, P. Watts, and R. Tabaczynski, "Development and use of a cycle simulation to predict si engine efficiency and nox emissions," tech. rep., SAE Technical Paper, 1979.

[85] A. Mohammadi, M. Shioji, Y. Nakai, W. Ishikura, and E. Tabo, "Performance and combustion characteristics of a direct injection si hydrogen engine," *International Journal of Hydrogen Energy*, vol. 32, no. 2, pp. 296–304, 2007.

[86] A. S. Bika, L. Franklin, and D. B. Kittelson, "Engine knock and combustion characteristics of a spark ignition engine operating with varying hydrogen and carbon monoxide proportions," *International journal of hydrogen energy*, vol. 36, no. 8, pp. 5143–5152, 2011.

[87] M. Nielsen, E. Alberico, W. Baumann, H.-J. Drexler, H. Junge, S. Gladiali, and M. Beller, "Low-temperature aqueous-phase methanol dehydrogenation to hydrogen and carbon dioxide," *Nature*, vol. 495, no. 7439, pp. 85–89, 2013.

[88] S. Aoyagi, Y. Hasegawa, T. Yonekura, and H. Abe, "Energy efficiency improvement of series hybrid vehicle," *JSAE review*, vol. 22, no. 3, pp. 259–264, 2001.

[89] "All Electric Vehicles- US DOE."

[90] HILTech, "The use of microturbine generators in hybrid electric vehicles," Accessed Date: 05-05-2016.

[91] "Walmart futuristic trucks," Accessed Date: 05-05-2016.

[92] "OMES Project," Accessed Date: 05-05-2016.

[93] C. F. McDonald and C. Rodgers, "The ubiquitous personal turbine (pt)... a power vision for the 21st century," in *ASME Turbo Expo 2001: Power for Land, Sea, and Air*, pp. V002T04A011–V002T04A011, American Society of Mechanical Engineers, 2001.

[94] D. W. Dewis, "Icr350–a turbine solution for medium and heavy duty vehicles," in *Proc. ASME Turbo Expo*, vol. 2012, pp. 823–832, 2011.

[95] R. Lundberg and M. Ferrato, "Ceramic component development for agata," in *ASME 1999 International Gas Turbine and Aeroengine Congress and Exhibition*, pp. V001T04A005–V001T04A005, American Society of Mechanical Engineers, 1999.

[96] N. Nakazawa, M. Sasaki, T. Nishiyama, M. Iwai, H. Katagiri, and N. Handa, "Status of the automotive ceramic gas turbine development program—seven years' progress," in *ASME 1997 International Gas Turbine and Aeroengine Congress and Exhibition*, pp. V001T04A008–V001T04A008, American Society of Mechanical Engineers, 1997.

[97] X. Wang, H. Zhang, B. Yao, Y. Lei, X. Sun, D. Wang, and Y. Ge, "Experimental study on factors affecting lean combustion limit of si engine fueled with compressed natural gas and hydrogen blends," *Energy*, vol. 38, no. 1, pp. 58–65, 2012.

[98] T. Shudo, Y. Nakajima, and T. Futakuchi, "Thermal efficiency analysis in a hydrogen premixed combustion engine," *JSAE review*, vol. 21, no. 2, pp. 177–182, 2000.

[99] B. Wu, L. Wang, X. Shen, R. Yan, and P. Dong, "Comparison of lean burn characteristics of an si engine fueled with methanol and gasoline under idle condition," *Applied Thermal Engineering*, vol. 95, pp. 264–270, 2016.

[100] R. C. Reid, J. M. Prausnitz, and B. E. Poling, "The properties of gases and liquids," 1987.

[101] "Physical Properties of Pure methanol," Accessed Date: 02-05-2016.

APPENDIX

1. Necessity for pre-vaporizer

The average temperature of the exhaust gas was around 1000 K during constant load tests. As mentioned earlier, the exhaust gas temperature cannot go below 573 K due to the presence of catalytic converter. Hence, the maximum amount of heat recoverable from the exhaust is about 3.605 kW/$g_{methanol}$. However, it is important to consider a finite minimum difference of temperature at pinch point in any heat exchanger. Considering this difference to be 20 K, the maximum heat recoverable reduces to 3.436 kW/$g_{methanol}$ [100].

As shown earlier, the heat of reaction for complete conversion of methanol vapour to syngas is about 2.834 kJ/$g_{methanol}$ and the amount of heat required for phase change process at 64.6 ^{0}C is about 1.103 kJ/$g_{methanol}$ [101]. The sensible heat required to raise the temperature of methanol from ambient tempertaure is neglgible compared to phase change heat. The total heat required if both phase change and reaction occurs in M-TCR will be 3.937 kJ/$g_{methanol}$. Since the amount of heat available in the exhaust gas is lower than this value, methanol conversion ratio will be lower. The conversion ratio can be enhanced by separating the phase change process by pre-vaporizing methanol in the independent phase change heat exchanger. There is significant amount of heat left in the exhaust gas after the catalytic converter and this heat can be utilized to vapourize methanol. This scheme has been illustrated earlier.

2. Procedure for obtaining maps

An SI engine is quantitatively governed using a throttle valve. In order to obtain different engine maps used in the study, all the engine performance and emission parameters were obtained at a fixed throttle position for different engine speeds. This procedure for repeated for ten throttle position shown in Fig. 2.1. The lower operating limit was set at 20 Nm below which a 2.0 L engine is either in idle condition or fuel cut-off condition. In order to obtain the engine parameters at intermediate throttle position, linear interpolation was used and iso-contour lines were plotted. For example, a BSFC map for M0 is shown in Fig. 2.2.

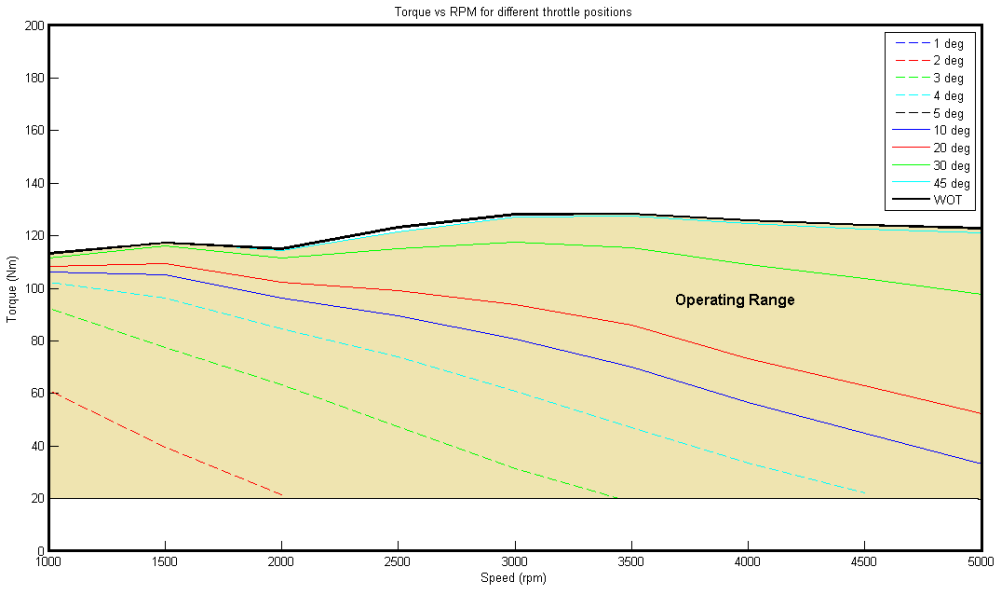

Figure 2.1 Variation of Torque with engine speed for different throttle positions

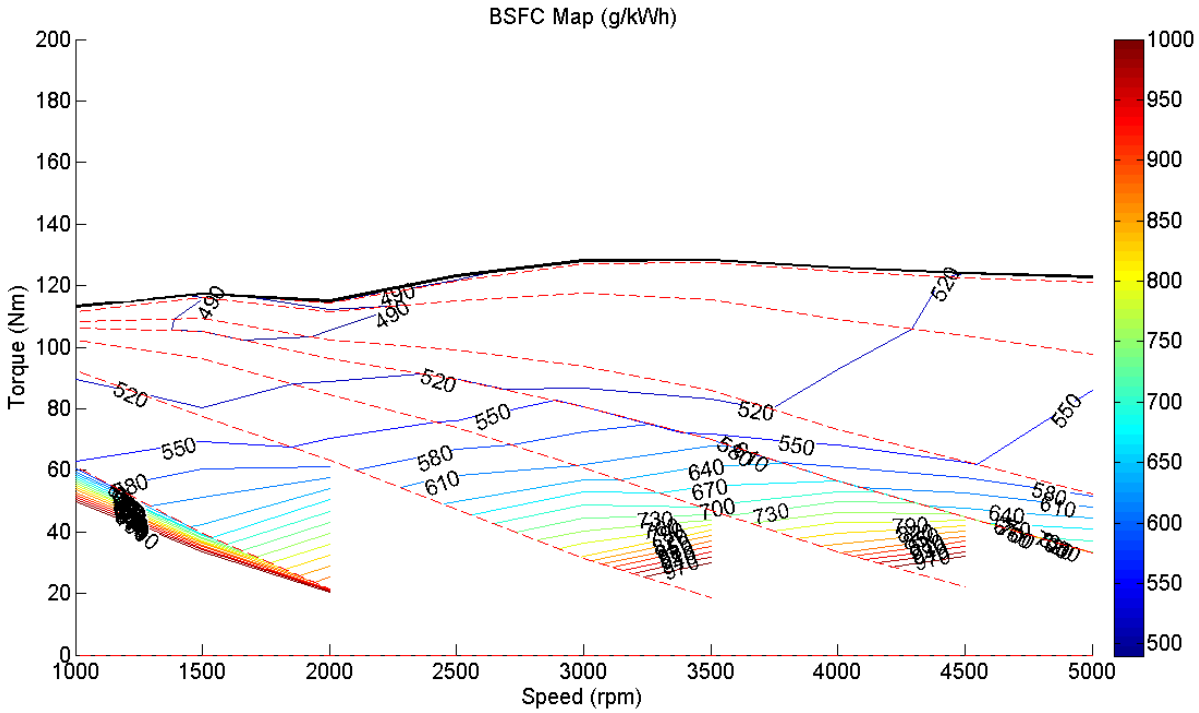

Figure 2.2 BSFC engine map for MO

3. Engine maps for M25 and M75

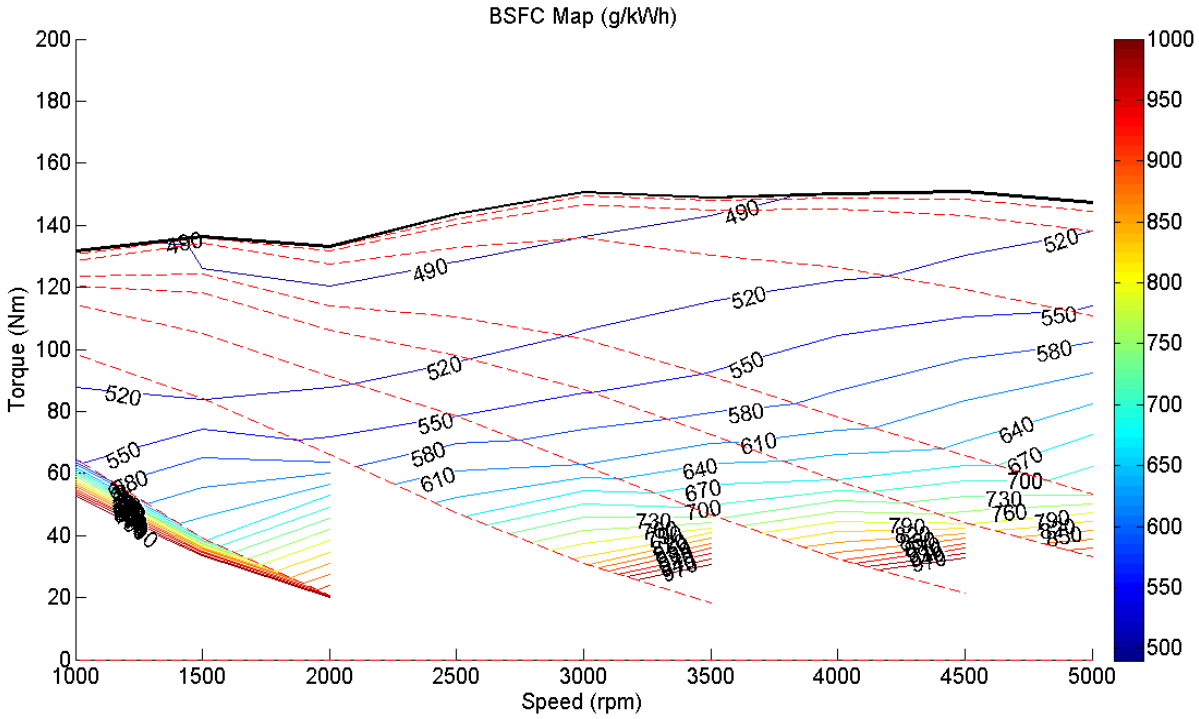

Figure 3.1 BSFC map for M25

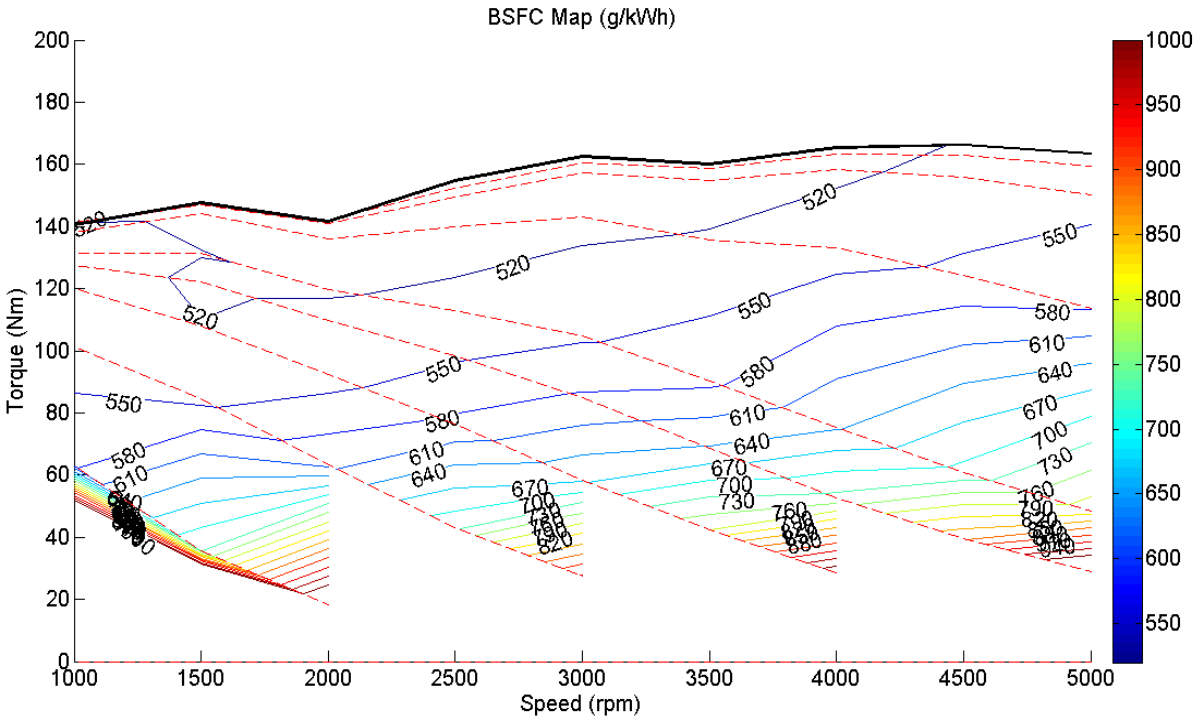

Figure 3.2 BSFC map for M75

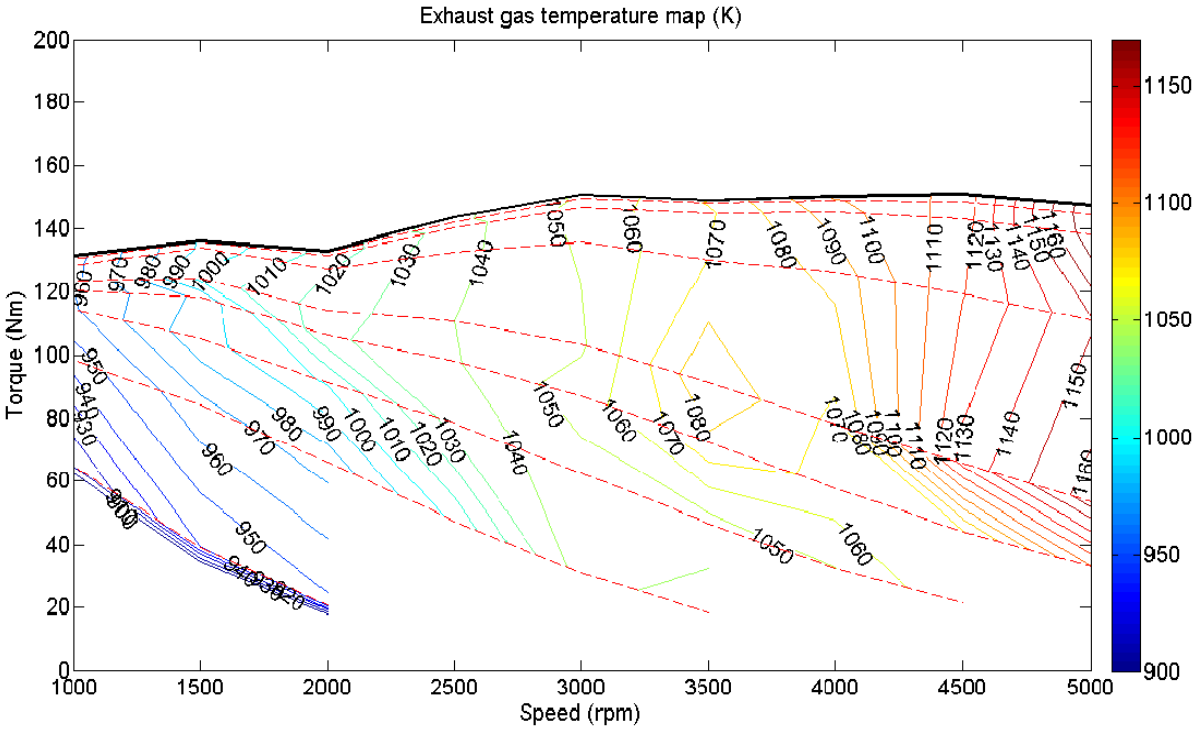

Figure 7.1: Figure 3.3 Exhaust gas temperature map for M25

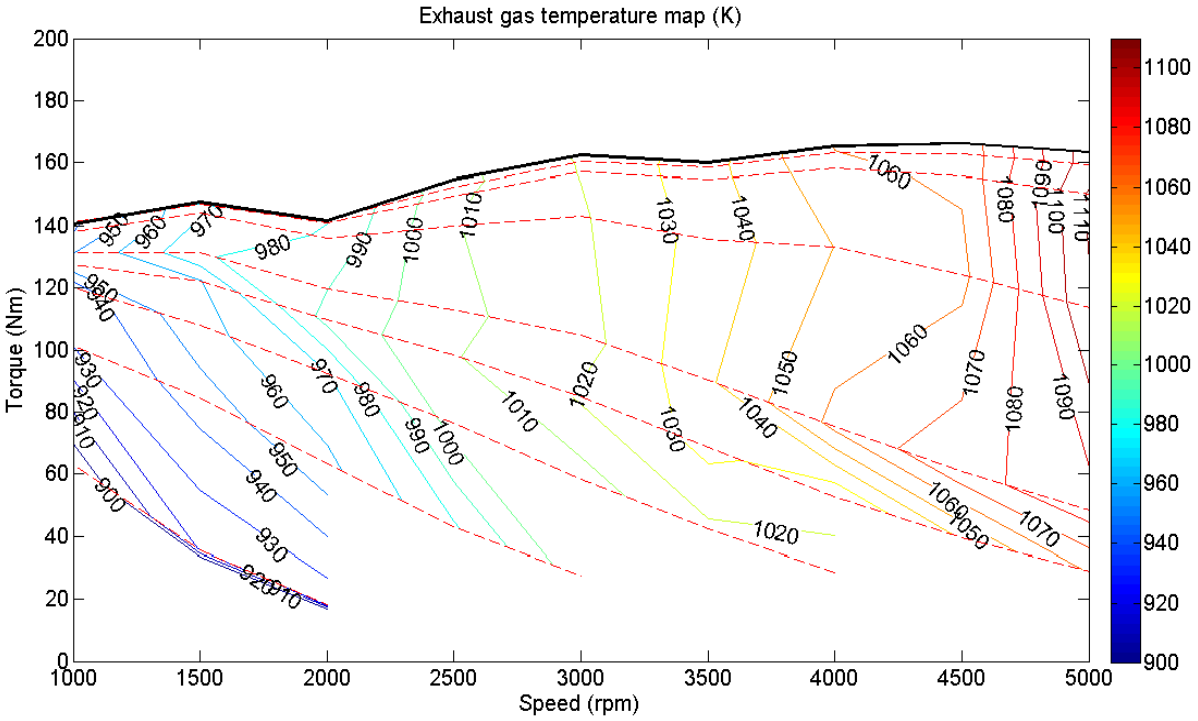

Figure 3.4 Exhaust gas temperature map for M75

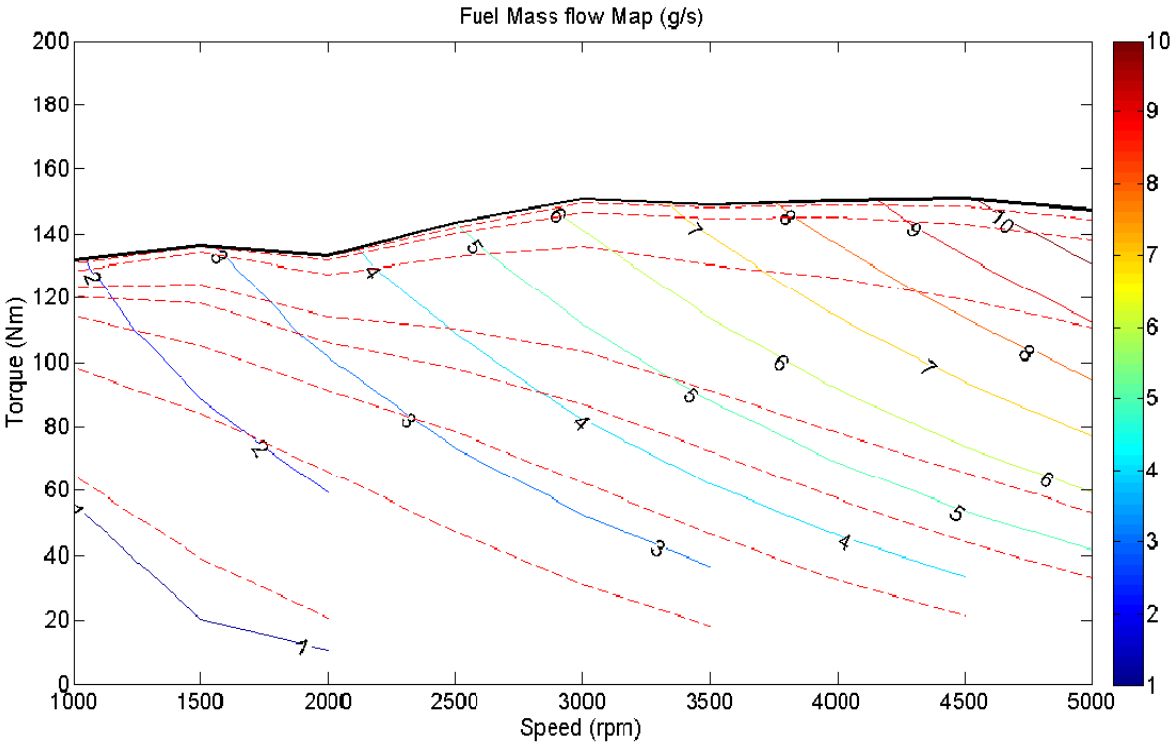

Figure 3.5 Fuel consumption per second for M25 blend

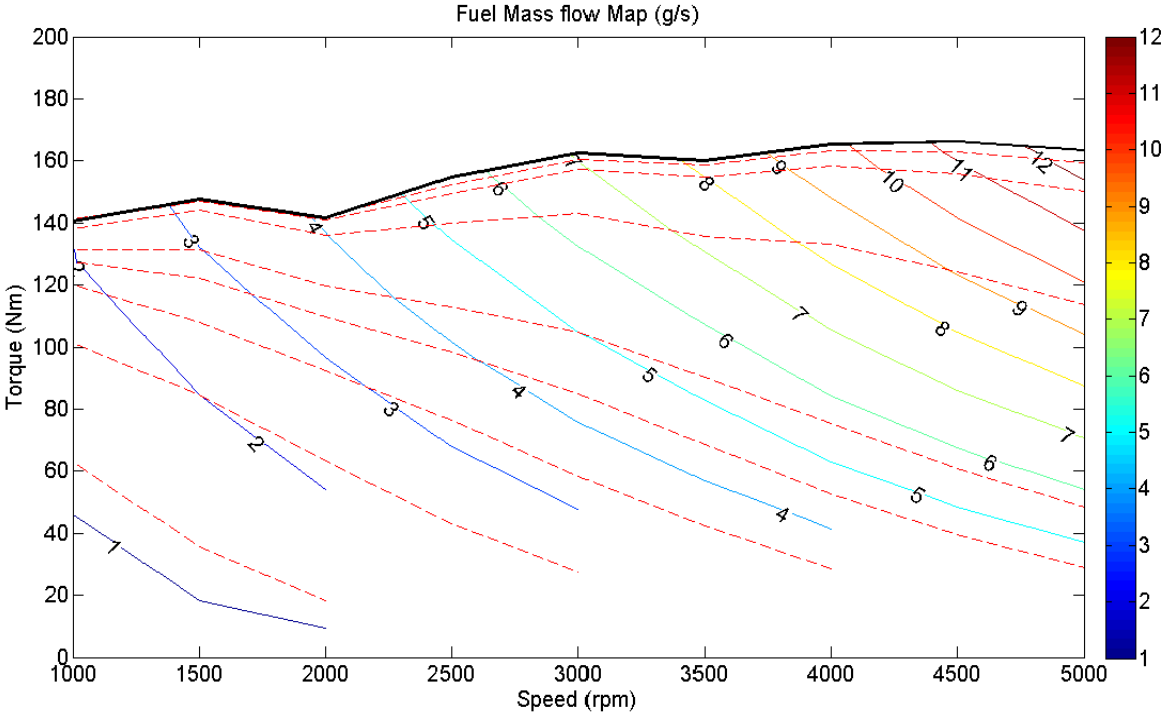

Figure 3.6 Fuel consumption per second for M75 blend

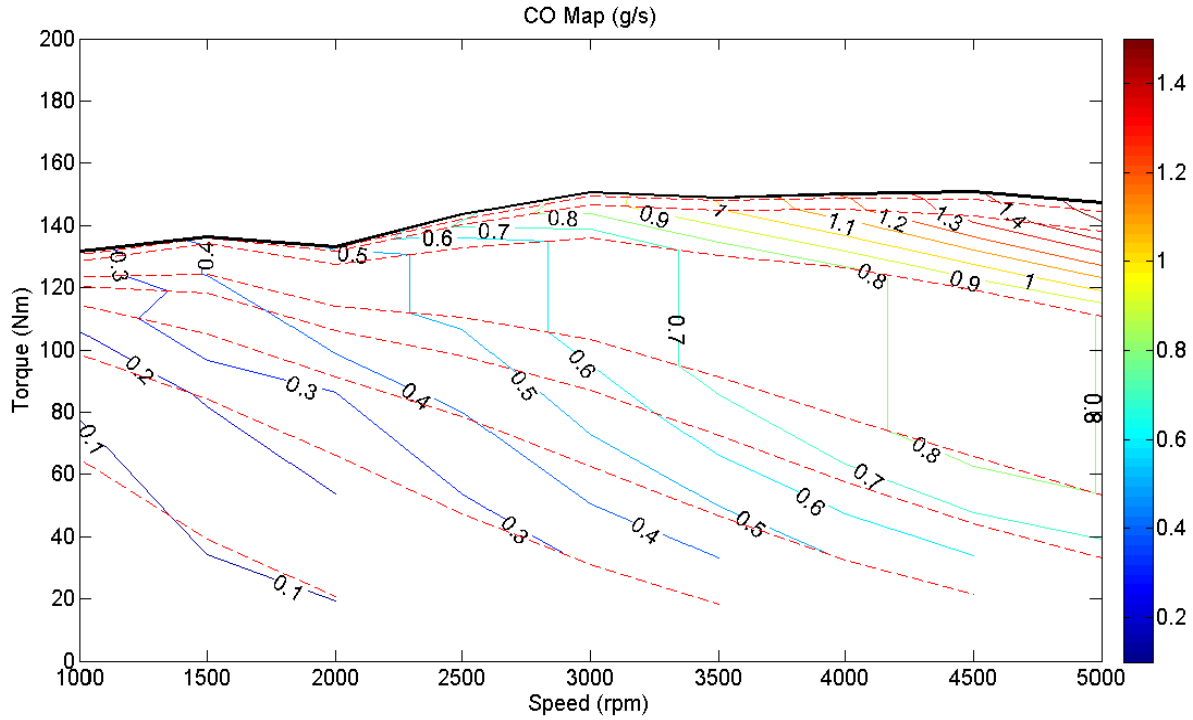

Figure 3.7 CO emission map for M25

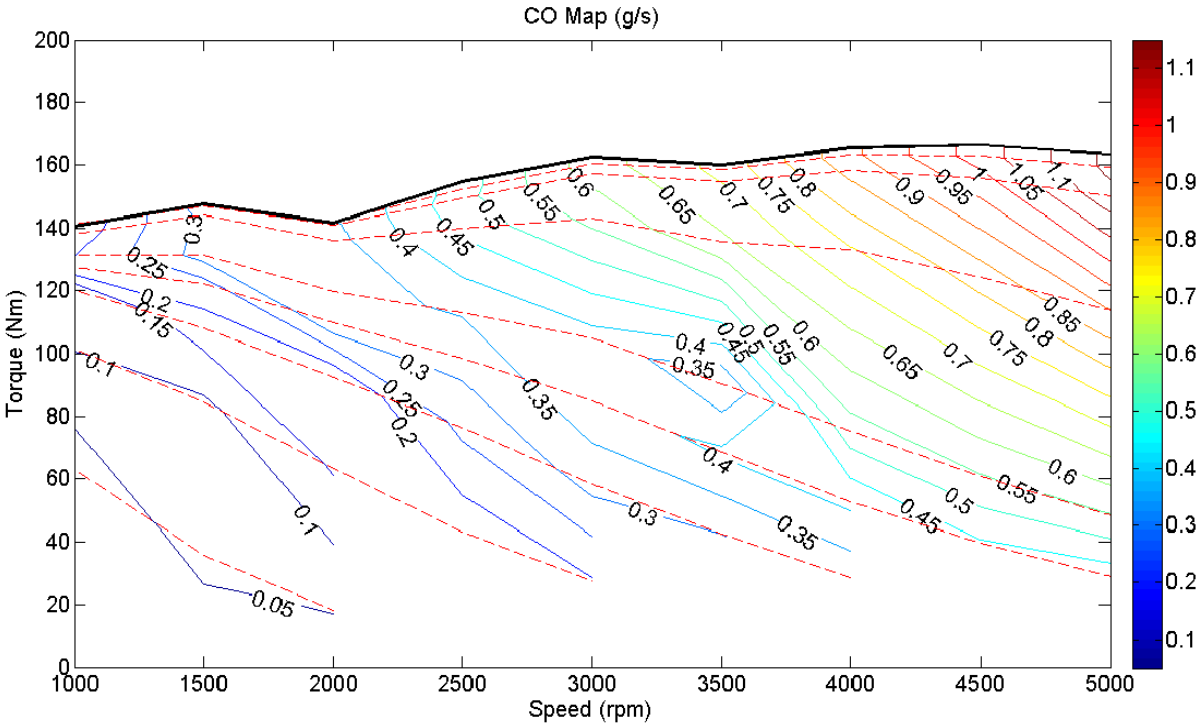

Figure 3.8 CO emission map for M75

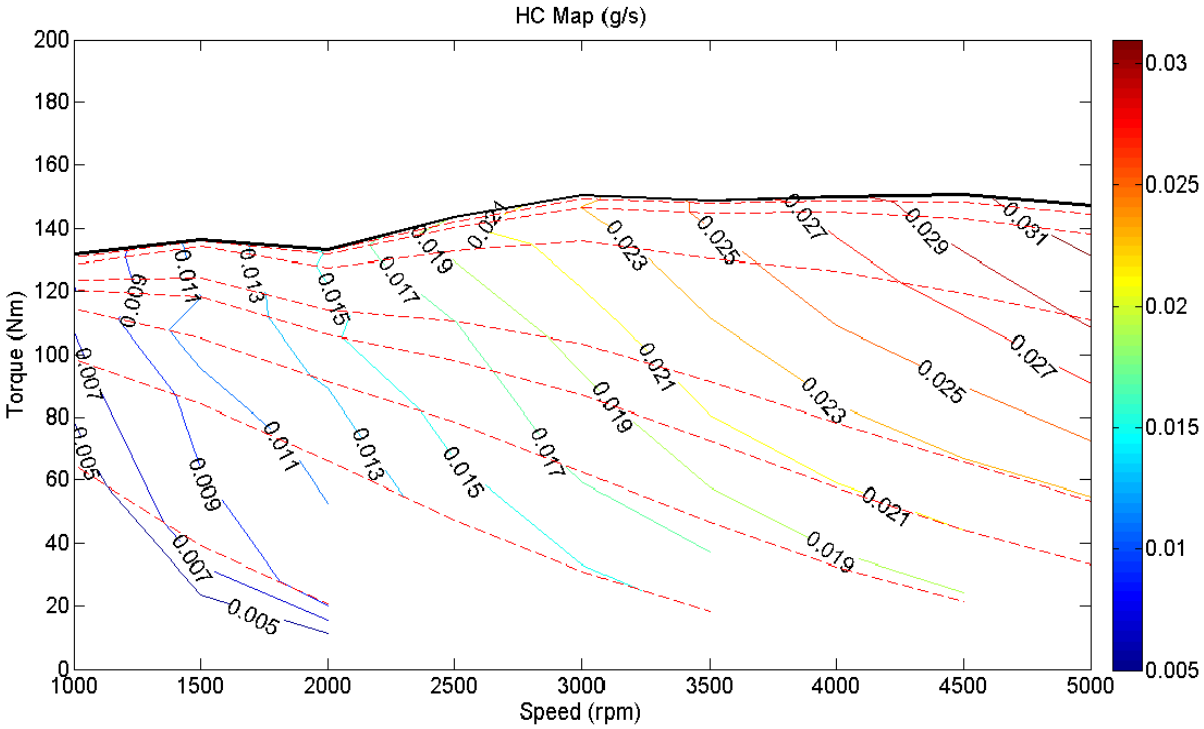

Figure 3.9 HC emission map for M25

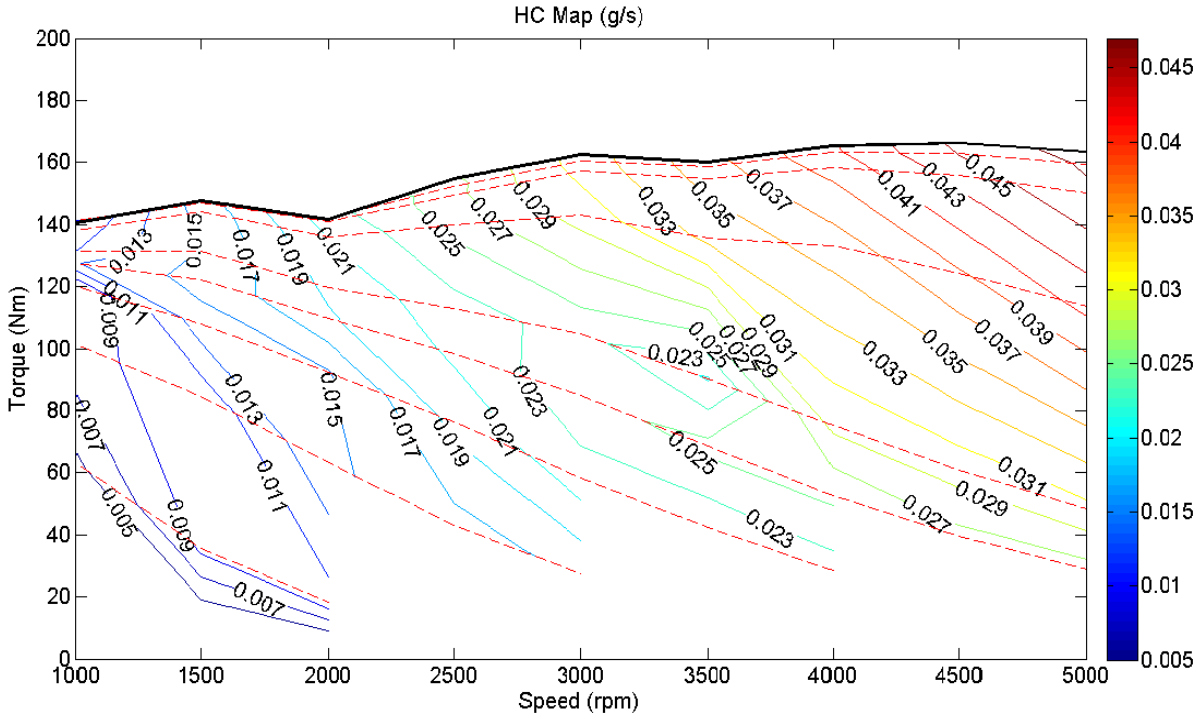

Figure 3.10 HC emission map for M75

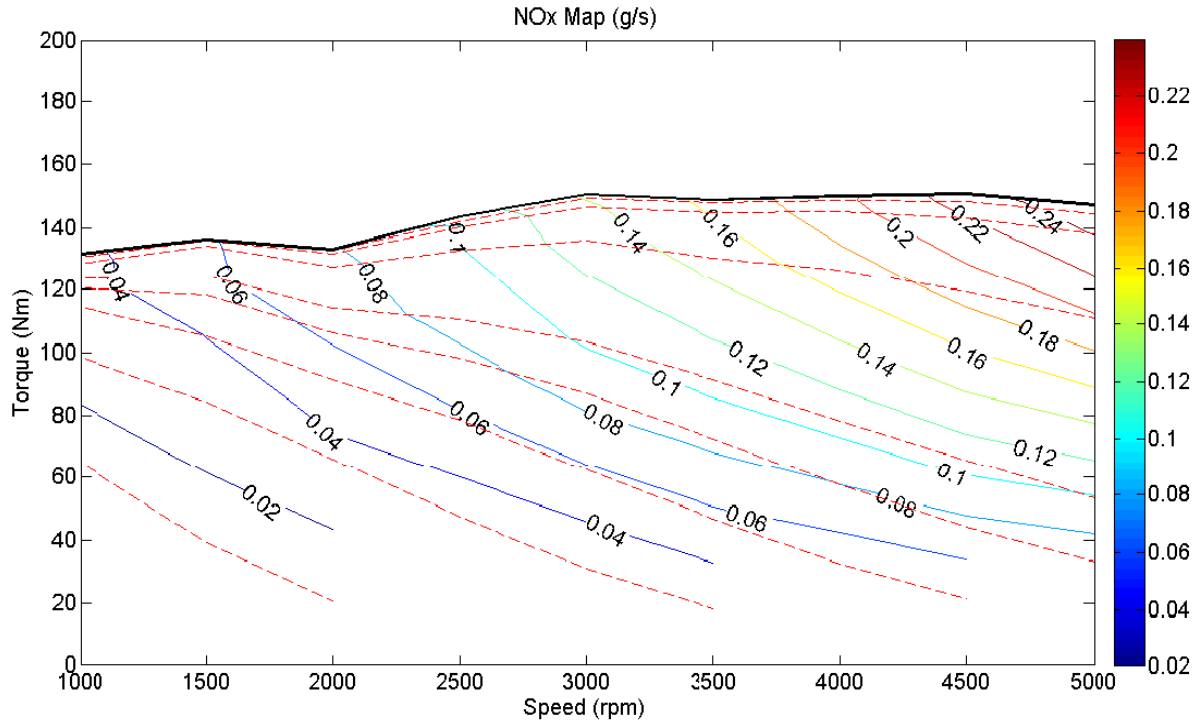

Figure 3.11 NOx emission map for M25

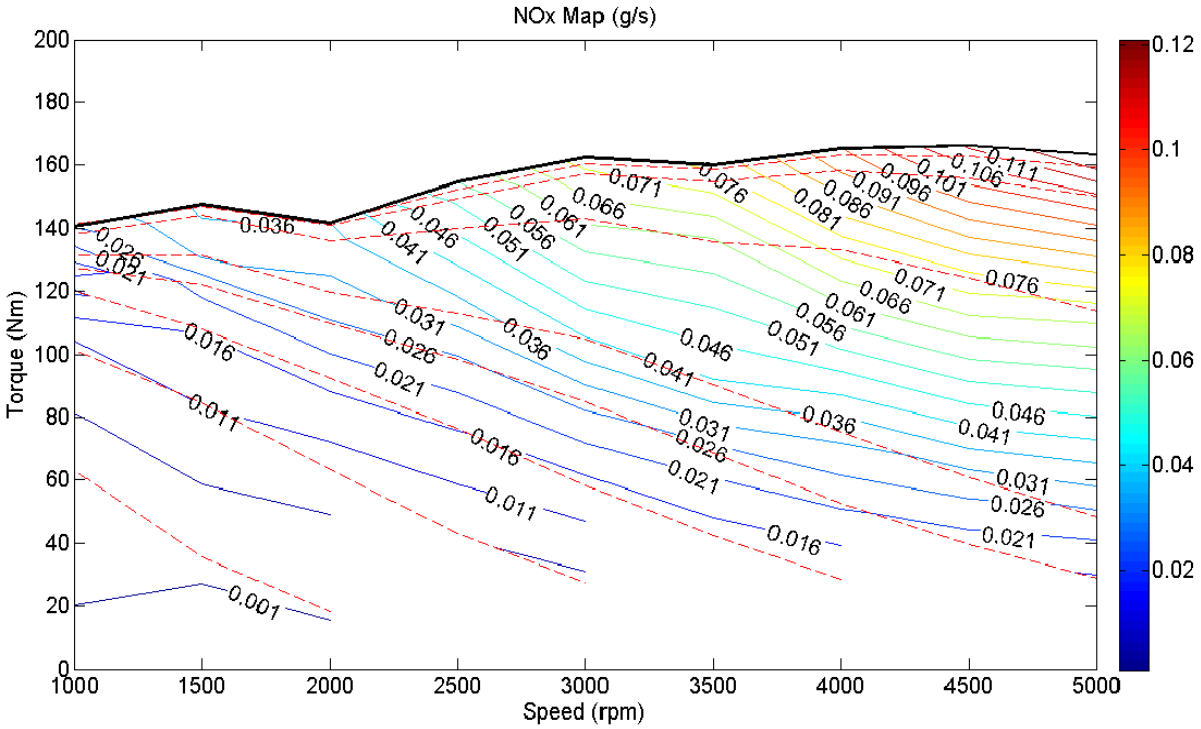

Figure 3.12 NOx emission map for M75